AECL EACL

AECL Research EACL Recherche

Engineering and Design Division Design Document

☒ Chalk River Laboratories
Chalk River Ontario
Canada K0J 1J0

☐ Whiteshell Laboratories
Pinawa, Manitoba
Canada R0E 1L0

DOCUMENT TITLE Safety Analysis Report

PROJECT/JOB TITLE Irradiated Material Transportation Packaging

DOCUMENT TYPE Technical Note

Prepared By	R Lesco for W.R. Taylor	Date	94/04/08
Reviewed By	R Lesco R. Lesco	Date	94/04/08
Approved By	E.W. Butterworth E.W. Butterworth	Date	94 4.15
Accepted By		Date	
Accepted By		Date	

(Signatories for Rev. 0 only)

JUN 16 1998
ENGINEERING AND DESIGN

Design Job No. 13318

Document No. A-13318-TN-5

Revision No. 1

Alternate Document No.

CRL-3554-1-Rev.2

AECL EACL

AECL Research EACL Recherche

Document Status and Revision History

TITLE: Irradiated Material Transportation Packaging - Safety Analysis Report	Job No. 13318 Document No. A-13318-TN-5 Sheet No. 1 of

Rev. No. / Date	Revision History and ECN reference	Prepared / Reviewed	Approved / Accepted
P0	Section 6, Appendices A & B revised	R.J. Lesco	N/A
94.3.30		N/A	N/A
Rev. 1	Insert No. 3 added to Configuration C	S. Gowans	F.W. Bateman
95.4.7			

Iss. No.	Rev. No.	DTS No.	Date	ISSUE/STATUS	By
1	P0	57	93-08-12	Preliminary: Issued for Review	RL
2	0	77	94.3.30	Approved: Issued for Information	RJL
3	1	87	95.4.7		SG

AECL EACL

AECL Research EACL Recherche

Document Status and Revision History

TITLE: Irradiated Material Transportation Packaging - Safety Analysis Report		Job No. 13318 Document No. A-13318-TN-5 Sheet No. 1 of	
Rev. No. Date	Revision History and ECN reference	Prepared Reviewed	Approved Accepted
P0	Section 6, Appendices A & B revised	R.J. Lesco	N/A
94.3.30		N/A	N/A
Rev. 1	Insert No. 3 added to Configuration C	S. Gowans	F.W. Butterworth
95.4.7			

Iss. No.	Rev. No.	DTS No.	Date	ISSUE/STATUS	By
1	P0	57	93-08-12	Preliminary: Issued for Review	R
2	0	77	94.3.30	Approved: Issued for Information	RJL
3	1	87	95.4.7		SG

TABLE OF CONTENTS

		Page
1.0	INTRODUCTION	1-1
2.0	QUALITY ASSURANCE	2-1
2.1	General	2-1
2.2	Design	2-1
2.3	Manufacturing	2-2
2.4	Qualification Testing	2-2
2.5	Operation and Maintenance	2-2
3.0	RADIOACTIVE MATERIAL DESCRIPTION	3-1
3.1	General	3-1
3.2	Irradiated CANDU Natural Uranium Fuel	3-1
3.3	Irradiated Power Reactor Channel Components	3-2
3.4	Irradiated Test Specimens	3-2
4.0	PACKAGING DESCRIPTION	4-1
4.1	General	4-1
4.2	Main Flask Body	4-2
4.3	Lead Shield Insert	4-3
4.4	Drawer	4-3
4.5	Shielding Plugs	4-4
4.6	Shielding Inserts No. 2 & No. 3	4-4
4.7	Closure Flanges	4-4
4.8	Impact Limiters	4-5
4.9	Lifting Assembly	4-5
4.10	Support Frame	4-5
5.0	SHIPMENT DESCRIPTION	5-1
6.0	STRUCTURAL EVALUATION	6-1
6.1	Introduction	6-1
6.2	Packaging Component Masses and Material Properties	6-2
6.3	Component Evaluation	6-3
6.3.1	Impact Limiter	6-3
6.3.1.1	Design Criteria	6-3
6.3.1.2	Calculations	6-4
6.3.1.3	Prototype Testing	6-4
6.3.1.4	Evaluation	6-4
6.3.2	Main Flask Body	6-4
6.3.2.1	Design Criteria	6-4
6.3.2.2	Prototype Testing	6-5
6.3.2.3	Evaluation	6-5
6.3.3	Front and Rear Closures	6-5
6.3.3.1	Design Criteria	6-5
6.3.3.2	Calculations	6-6
6.3.3.3	Prototype Testing	6-8
6.3.3.4	Evaluation	6-8

6.3.4	Valve Cover Plate Closure	6-8
6.3.4.1	Design Criteria	6-8
6.3.4.2	Prototype Testing	6-8
6.4.4.3	Evaluation	6-8
6.3.5	Rear Cover Plate Closure	6-9
6.3.5.1	Design Criteria	6-9
6.3.5.2	Calculations	6-9
6.3.5.3	Prototype Testing	6-10
6.3.5.4	Evaluation	6-10
6.3.6	Lead Shield Insert	6-10
6.3.6.1	Design Criteria	6-10
6.3.6.2	Calculations	6-11
6.3.6.3	Prototype Testing	6-11
6.3.6.4	Evaluation	6-11
6.3.7	Trunnions	6-11
6.3.7.1	Design Criteria - Tie Downs	6-11
6.3.7.2	Calculations - Tie Downs	6-12
6.3.7.3	Evaluation - Tie Downs	6-13
6.3.7.4	Design Criteria - Lifting	6-13
6.3.7.5	Calculations - Lifting	6-13
6.3.7.6	Evaluation - Lifting	6-13
6.3.8	Lifting Bar	6-13
6.3.8.1	Design Criteria	6-13
6.3.8.2	Calculation	6-14
6.3.8.3	Evaluation	6-14
6.3.9	Safety Hoist Rings	6-14
6.3.9.1	Design Criteria	6-14
6.3.9.2	Evaluation	6-14
6.3.10	Air/Rail Shipping Frame	6-15
6.3.10.1	Design Criteria	6-15
6.3.10.2	Calculations	6-15
6.3.10.3	Evaluation	6-15
7.0	THERMAL EVALUATION	7-1
7.1	General	7-1
7.2	Radioactive Decay Heat Generation	7-1
7.3	Package Thermal Design	7-2
7.4	Normal Conditions of Transport	7-3
7.4.1	Regulatory Criteria	7-3
7.4.2	Thermal Analysis and Results	7-4
7.4.3	Evaluation of Results	7-5

7.5	Accident Conditions of Transport	7-8
7.5.1	General	7-8
7.5.2	Fire Test	7-8
7.5.3	Prototype Package	7-9
7.5.4	Fire Test Results	7-9
7.5.5	Discussion of Results	7-10
8.0	CONTAINMENT EVALUATION	8-1
8.1	General	8-1
8.2	Potential Release Scenarios and Considerations	8-1
8.3	Helium Leakage Test Results on Prototype Package	8-3
9.0	SHIELDING EVALUATION	9-1
9.1	Summary	9-1
9.2	Shielding Description	9-1
9.3	Source Specification	9-1
9.3.1	Gamma Source	9-3
9.3.2	Neutron Source	9-5
9.4	Shield Model Description	9-6
9.4.1	Normal Conditions of Transport	9-6
9.4.2	Accident Conditions of Transport	9-7
9.5	Material Densities	9-7
9.6	Gamma Shielding Evaluation	9-8
9.7	Neutron Shielding Evaluation	9-9
9.8	Alternative Shielding Evaluation	9-11
9.8.1	Axial Shielding Plugs	9-11
9.8.2	Shield Insert No. 2	9-11
9.8.3	Shield Insert No. 3	9-12
10.0	ASSESSMENT OF COMPLIANCE	10-1
11.0	REFERENCES	11-1
	APPENDICES	
A	Structural Analyses	A-1
A.1	General	A-1
A.2	Impact Analysis	A-1
A.2.1	Impact Limiter Load-Deflection Characteristics	A-1
A.2.2	Accelerations	A-4
A.3	Package Containment Component Analyses	A-5
A.3.1	Design Criteria	A-5
A.3.2	Closure Flanges	A-5
A.3.2.1	Under Impact Conditions	A-5
A.3.2.2	Under Internal Gas or Vapour Pressure	A-9
A.3.2.2.1	Front and Rear Closure Flanges	A-9
A.3.2.2.2	Rear Cover Plate	A-10
A.3.2.3	Combined Loadings	A-11
A.3.2.3.1	Front and Rear Closure Flanges	A-11
A.3.2.3.2	Rear Cover Plate	A-11
A.3.2.4	Stress Intensities	A-11
A.3.3	Flange Cap Screws	A-13
A.3.3.1	Under Impact Conditions	A-13
A.3.3.2	Under Internal Gas or Vapour Pressure	A-13

A.3.3.2.1	Front and Rear Closure Flange Cap Screws	A-14
A.3.3.2.2	Rear Cover Plate Cap Screws	A-14
A.3.3.3	Combined Loadings	A-15
A.3.3.3.1	Front and Rear Closure Flange Cap Screws	A-15
A.3.3.3.2	Rear Cover Plate Cap Screws	A-16
A.3.4	Lead Shield Insert	A-17
A.3.4.1	Cap Screws	A-17
A.3.4.2	Flange-to-Shell Welds	A-18
A.4	Prototype Package Testing	A-19
A.4.1	Introduction	A-19
A.4.2	Prototype Test Specimen	A-20
A.4.3	Test Procedures	A-21
A.4.4	Acceptance/Rejection Test Criteria	A-22
A.4.5	Prototype Test Results	A-23
A.4.6	Discussion	A-25
A.4.6.1	Impact Limiters	A-25
A.4.6.2	Front Flange	A-25
A.4.6.3	Rear Flange	A-25
A.4.6.4	Valve Cover Plate	A-25
A.4.6.5	Rear Cover Plate	A-26
A.4.6.6	Lead Shield Insert	A-26
A.4.6.7	Drawer Locking Cap Screw	A-26
A.4.6.8	Simulated Fuel Bundle	A-26
A.5	Package Handling and Tiedown Component Analyses	A-26
A.5.1	Tie Down Analysis	A-26
A.5.1.1	Road and Sea Transportation	A-26
A.5.1.1.1	Component Analysis	A-29
A.5.1.2	Rail and Air Transportation	A-33
A.5.1.1.2	Component Analysis	A-40
A.5.2	Lifting Analysis	A-50
A.5.2.1	Trunnion Component Analysis	A-50
A.5.2.2	Safety Hoist Rings	A-53
A.5.2.3	Lifting Bar	A-53
A.6	External Pressure Analysis	A-55
A.6.1	Main Flask Body	A-55
A.6.2	Rear Cover Plate	A-56
A.6.3	Valve Cover Plate	A-56
A.6.4	Rear Flange	A-57
A.6.5	Front Flange	A-57
A.7	References	A-57

B	Thermal Analyses	B-1
B.1	Normal Conditions of Transport	B-1
B.2	Accident Conditions of Transport	B-5
B.3	References	B-8
C	Containment Analyses	C-1
C.1	Introduction	C-1
C.2	Containment Analysis for Tube Sections and Test Specimens	C-2
C.2.1	Calculation	C-2
C.2.2	Discussion	C-6
C.3	Containment Analysis for Irradiated Fuel	C-6
C.3.1	Calculation	C-6
C.3.1.1	Zirconium Alloy Fuel Sheaths	C-7
C.3.1.2	Crud	C-7
C.3.1.3	Irradiated Uranium	C-8
C.4	Discussion	C-15
C.5	Conclusions	C-16

1.0 INTRODUCTION

A packaging has been designed for the transport of either a single irradiated CANDU natural uranium fuel bundle or irradiated CANDU natural uranium fuel elements or irradiated power reactor channel components or irradiated test specimens. This multipurpose use packaging has a mass of approximately 6 Mg and is illustrated in Figure 1.1.

Gamma radiation shielding is provided by thick stainless steel sections and a lead filled insert. No neutron shielding material is required. Different internal packaging components can be used to suit the different radioactive contents. During transportation, each end of the package is fitted with an impact limiter and the package is secured to a support frame. At the shipping destinations the package may be loaded or unloaded in a storage pool or at a hot cell, either in the vertical or horizontal orientations.

The maximum activity and maximum radioactive decay heat for the contents are 2000 TBq (54000 Curies) and 160 watts respectively. The radioactive contents are Type B quantities.

Shipments may be made to destinations in Canada and elsewhere. The possible transport modes include road, rail, ship and air. The Transport Index may be as high as 10 for non-exclusive use shipments.

In accordance with Canadian and International Atomic Agency transportation regulations, References 1 and 2*, the package design and shipments must satisfy Type B(U) requirements. This safety analysis report descibes the allowable radioactive contents, the packaging design and shipments. Analytical and prototype package testing methods were used to evaluate the performance of the radiation shielding features and the containment system of the package during transportation. The evaluation demonstrates that the package design and shipments satisfy Type B(U) requirements and so, certification of the package by the Atomic Energy Control Board is requested.

*References are listed in Section 11.

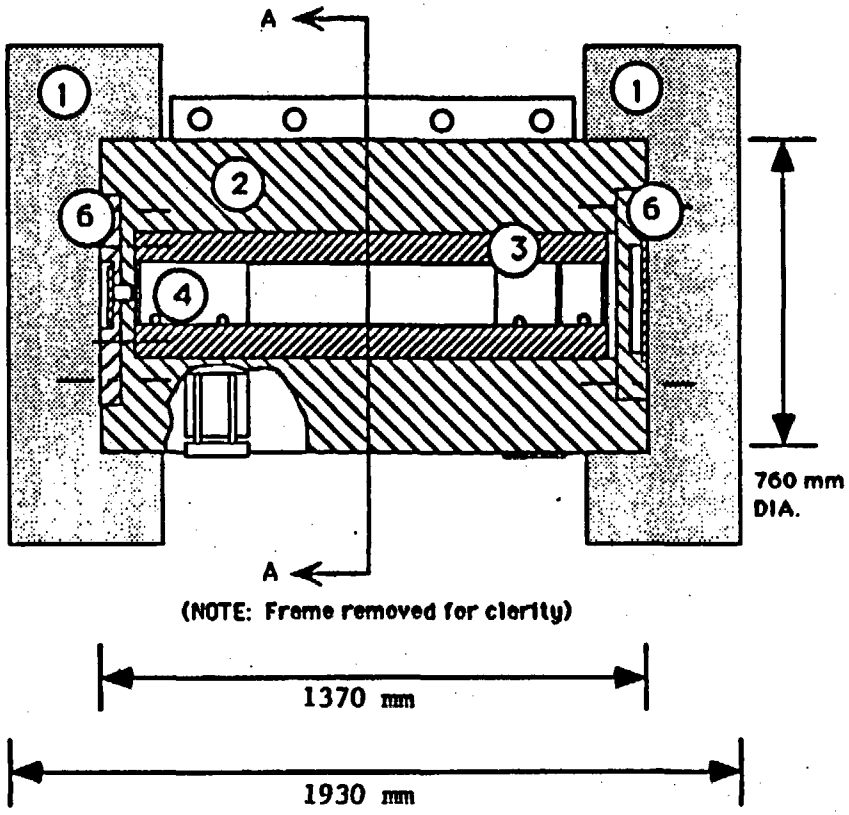

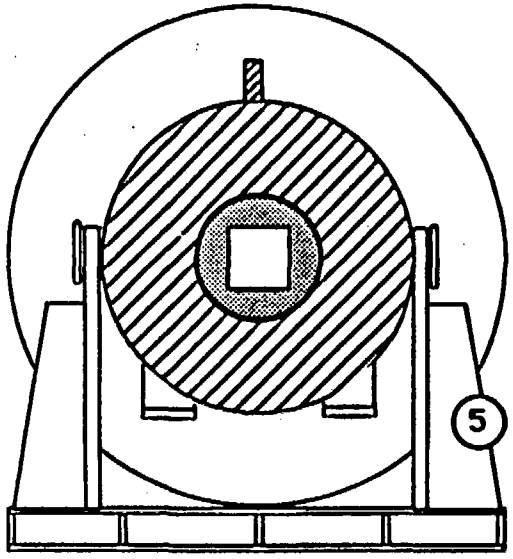

SECTION A-A

1. IMPACT LIMITER
2. MAIN FLASK BODY
3. SHIELD INSERT
4. REMOVABLE DRAWER
5. SUPPORT FRAME
6. SEALING FLANGES

PACKAGE MASS: 5550 kg including support frame
5215 kg excluding support frame

THIS PACKAGE CONFORMS TO TYPE B(U) OF IAEA SAFETY SERIES NO. 6
AECB CERTIFICATE NO. CDN/2061/B(U)-85

IRRADIATED MATERIAL TRANSPORTATION PACKAGING

TITLE
Irradiated Material Transportation
Packaging Illustration

SCALE
Not-to-scale

SUBMITTED R. Cox DATE 93/08/03
APPD F.W. Rutherford DATE 93.8.4
DRFN R. Cox DATE 93/08/03
CHKD. DATE

CHALK RIVER
NUCLEAR LABORATORIES

ATOMIC ENERGY OF CANADA
LIMITED
CHALK RIVER ONTARIO, CANADA

BLDG. NO. N/A
CODE
CLASS

A-5580-106
REV. NO. 01

2.0 QUALITY ASSURANCE

2.1 General

The overall quality assurance program requirements are defined in AECL-Research document "Irradiated Material Transportation Packaging Quality Assurance Plan", Reference 3.

The purpose of the quality plan is to describe the essential activities to be performed in order to provide the assurance that the technical, operational, safety and regulatory requirements are met.

The scope of the quality assurance plan applies to all the activities leading to the development, licensing and use of the Irradiated Material Transportation Package. In particular, it covers the design, manufacture, testing, commissioning, operation, maintenance and decommissioning of the package.

The contents of the quality plan include the following:

- Project Organization, Responsibilities and Control
- Performance Function
  - Design
  - Manufacturing
  - Qualification Testing
  - Commissioning
  - Licensing
  - Operation
  - Decommissioning
- Quality Documents and Records
- Completion Assurance

2.2 Design

The design activities for the package complied with applicable requirements of CSA CAN3-Z299.2-85, Reference 4 within the generic design quality assurance program as described in AECL-Research Engineering and Design Division "Design Quality Assurance Manual", Reference 5 and corresponding Divisional Working Procedures, Reference 6.

Currently the Design Quality Assurance Manual is intended to satisfy the requirements of CSA CAN3-N286.2-86 (Reference 7). In meeting applicable elements of this standard, this program also satisfies the design quality assurance elements/requirements of CSA CAN3-Z299 Series, ISO 9000 Series, CSA B51, CSA CAN3-N285.0 (and related ASME Code Quality Assurance Requirements), and NATO AQAP Series.

2.3 Manufacturing

The requirements for manufacturing are defined in AECL-Research Technical Specification A-13318-SP-1, Reference 8. The manufacturer is required to have in place a quality program which satisfies the requirements of CSA CAN3-Z299.2-85.

The quality assurance activities applied to the fabrication of the containment components must satisfy the requirements of CSA CAN3-Z299.2-85. Notwithstanding, the containment components, the applicable quality program for sub-contracted products and services are required to satisfy the requirements of CSA CAN3-Z299.3-85, Reference 9.

The quality assurance activities associated with fabrication of the test prototype (Serial No. 2061-01) and subsequent refurbishment complied with requirements NATO-AQAP-1, Reference 10.

2.4 Qualification Testing

The requirements for qualification testing of the prototype were defined in AECL-Research Test Specification A-13318-SP-2, Reference 11. The activities associated with qualification testing satisfied the quality requirements of CSA CAN3-N286.2, Appendix D, (Reference 7).

2.5 Operation and Maintenance

Operating Procedures, Reference 12 have been established for the control, use and maintenance of the package. Maintenance and service records will also be established as defined on the operating procedures. Currently AECL-Research is embarking on a quality program to satisfy the requirements of CSA N286.0, Reference 13. For operations, a program will be developed to meet the quality requirements of CSA N286.5, Reference 14.

3.0 RADIOACTIVE MATERIAL DESCRIPTION

3.1 General

The packaging has been designed for the transportation of Type B quantities of various radioactive materials that can be categorized under one of the following general groups:

a) irradiated CANDU natural uranium fuel bundles or elements with a maximum permissible activity of 2,000 TBq (54,000 Curies) and a maximum permissible radioactive decay heat of 160 watts at the time of shipment;

b) irradiated power reactor channel tube sections with a maximum permissible activity of 3,000 A_2 or 1,100 TBq (30,000 Curies), whichever is less, and a maximum permissible radioactive decay heat of 160 watts at the time of shipment; and

c) irradiated test specimens with a maximum permissible activity of 3,000 A_2 or 1,100 TBq (30,000 Curies), whichever is less, and a maximum permissible radioactive decay heat of 160 watts at the time of shipment.

These materials are described below in more detail.

3.2 Irradiated CANDU Natural Uranium Fuel

Shipments of CANDU fuel may occur as, either,

a) one 28-element fuel bundle assembly or up to 28 fuel elements that make up such an assembly with a nominal element diameter is 15.2 mm and the nominal length is 492 mm, or,

b) one 37-element fuel bundle assembly or up to 37 fuel elements that the make up such an assembly with a nominal element diameter is 13.9 mm and nominal length is 492 mm, or,

c) any combination of elements that make up the assemblies described in a) and b) up to 20 kg of initial uranium.

For any of these possibilities, the burn-up shall not exceed 1150 GJ/kg of initial uranium and the minimum storage time before shipment shall be 180 days.

Because the shipment of CANDU fuel in this packaging will be for research and development purposes, it is possible that some shipments will include defected fuel elements or bundles. In these cases, the fuel may be shipped with a cover gas if the fuel temperature exceeds 200°C to prevent oxidation.

Figures 3.1 and 3.2 shows the designs of the bundle assemblies and Tables 3.1 and 3.2 give the relevant design data, as extracted from Reference 15.

The above materials are classified as Type B quantities and not Fissile because the fuel elements used natural uranium prior to irradiation.

3.3 Irradiated Power Reactor Channel Components

These sections will originate from CANDU power reactors and shipments may consist of,

a) pressure tube sections in which the predominant radionuclides will be Zr-95 and Nb-95 and the typical total activity will be approximately 35 TBq (900 curies/kg) of component,

b) calandria tube sections in which the predominant radionuclides will be Zr-95 and Nb-95 and the typical total activity will be approximately 55 TBq (1470 curies/kg) of component,

c) end fitting sections in which the predominant radionuclides will be Co-60, and Cr-51 and the typical activity will be approximately 2.6 TBq/kg (70 curies/kg) of component, and

d) garter springs in which the predominant radionuclide will be Co-60, Cr-51 and Ta-182 and the typical activity will be approximately 1500 TBq/kg (40,000 curies/kg) of component.

The activities given above have been extracted from Reference 16.

3.4 Irradiated Test Specimens

Because this packaging will be used to transport specimens for research and development purposes, it is not possible to list all of the test specimens in detail. Those that are given below are typical.

(1) Bruce carrier bundle irradiation, Bruce 'B' G.S.

- Zirconium specimens (Zr-95, Nb-95), 120 TBq (3,200 Curies)

(2) Irradiations in the ATR, Idaho Falls, USA

- Zirconium specimens (Zr-95, Nb-95), 40 TBq (1,100 Curies)
- Hafnium specimens (Hf-175, Hf-181), 110 TBq (3,000 Curies)

(3) Irradiations in the ORIRIS Reactor, CEN, Saclay France

- Zirconium specimens (Zr-95, Nb-95), 20 TBq (540 Curies)

(4) Irradiations in the HFR, CEL Reactor, Petton, Netherlands

- Zirconium specimens (Zr-95, Nb-95) 30 TBq (800 Curies).

Because there is some uncertainty about all the possible test specimens that could be transported in this packaging it will be necessary to assess each shipment on a case-by-case basis to ensure that the total maximum activity does not exceed 3000 A_2 or 1,100 TBq (30,000 Curies), whichever is less <u>and</u> to ensure that the total radioactive decay heat does not exceed 160 watts at the time of shipment <u>and</u> to ensure that the regulatory radiation levels will not be exceeded.

4.0 PACKAGING DESCRIPTION

4.1 General

The packaging is shown on the following drawings:

E-5580-A-32	Assembly, Shipping Flask
E-5580-A-33	Assembly, Shipping Drawer
E-5580-A-36	Assembly, Shipping Flask with Shield Plugs and Basket
E-5580-A-37	Assembly, Shipping Flask with Shielded Insert No. 2
E-5580-A-39	Assembly, Shipping Flask with Shielded Insert No. 3
E-5580-SA-12	Sub-Assembly and Details, Shield Insert
E-5580-SA-13	Sub-Assembly Frame and Package
E-5580-SA-18	Sub-Assembly and Details, Shield Insert No. 3
E-5580-77	Details, Shipping Drawer
E-5580-78	Details, Flask Body
D-5580-79	Details, Main Closure
D-5580-80	Details, Valve Cover Plate
D-5580-81	Details, Rear Closure
C-5580-82	Details, Rear Cover Plate
E-5580-84	Details, Impact Limiter
D-5580-86	Details, Lifting Trunnions and Shear Discs
E-5580-87	Details, Shipping Frame
B-5580-88	Details, Label
D-5580-104	Details, Shielding Plugs
E-5580-105	Details, Basket and Support Stand
D-5580-110	Details, Shielding Plug No. 2
D-5580-111	Details, Shipping Basket No. 2
E-5580-113	Details, Air/Rail Shipping Frame

Figure 4.1 illustrates the following major components of the packaging:

- main flask body, 4000 kg
- lead shield insert, 670 kg
- drawer, 115 kg
- sealing flanges, 175 kg
- impact limiters, 255 kg
- support frame, 335 kg.

Minor components such as shipping cans and simple fixtures for supporting the different radioactive materials in the package cavity are not illustrated in Figure 4.1.

The packaging has been designed for multipurpose use and so there could be three possible configurations within the main flask body. These configurations do not involve changes to the package containment system which is bounded by the main flask body and the two closure flanges which are secured to the ends of the main flask body.

Figure 4.2 illustrates the three configurations.

Configuration A includes all the major components listed above and provides the maximum amount of gamma radiation shielding but the minimum cavity space. This configuration will be used for irradiated fuel shipments, irradiated power reactor channel tube sections or irradiated test specimens.

Configuration B differs from Configuration A in that the drawer has been removed. This configuration increases the package cavity length at the expense of reduced gamma radiation shielding in the axial direction of the packaging. This configuration will be used for the shipment of irradiated test specimens or irradiated power reactor channel tube sections.

In cases where the package does not provide adequate gamma radiation shielding in the axial direction, separate shield plugs will be added as appropriate.

Configuration C contains a integral lead shield insert complete with a separate shield plug which maximizes the package cavity size. This configuration will be used to ship irradiated test specimens or irradiated power reactor channel components.

For Configuration A, the packaging has a mass of approximately 5,550 kg (12,235 lb) when the support frame is included and a mass of 5,215 kg (11,485 lb) when the frame is excluded.

The main flask body and the lead shield insert provide gamma radiation shielding. Neutron shielding is not required for irradiated CANDU natural uranium fuel.

There are no neutron absorbers or poisons within the packaging because these items are not required to ensure criticality safety for irradiated CANDU natural uranium fuel.

The packaging can be loaded and unloaded in either the horizontal or vertical orientation. In the horizontal orientation, the packaging centre of gravity coincides with the mid plane of the packaging. In the vertical orientation, the packaging centre of gravity coincides with the packaging cavity axis. The packaging can be loaded and unloaded either underwater in a storage pool or dry at a hot cell. The package is transported with a dry cavity and in the horizontal orientation.

4.2 Main Flask Body

The main flask body, is a monolithic stainless steel forging (Type 304) with 225 mm (8.625 in.) thick walls. The main body has a 760 mm (30 in.) outer diameter and is 1370 mm (54 in.) long. The flask body cavity is 320 mm (12.625 in.) in diameter and is 1170 mm (46 in.) long.

The main body provides gamma shielding and containment of the radioactive contents and structural support for the internal components such as the shield insert and drawer.

An austenitic stainless steel forging is specified because the material exhibits good impact properties at -40°C (regulatory requirement). Because 300 series stainless steel have a face-cubic-centre structure, it does not exhibit a ductile-to-brittle transition temperature. Unlike lead, steel will also withstand the regulatory thermal test of 800°C for 30 minutes.

The outside surface is smooth to facilitate decontamination and minimize "weeping" of fixed radioactive contaminants during transportation.

4.3 Lead Shield Insert

The shield insert which houses the drawer (or axial shielding plugs) provides additional radial gamma shielding for the radioactive payload. The insert is 1168 mm (46 in.) long and has an outer diameter of 320 mm (12.625 in.) and has a mass of approximately 670 kg (1475 lb). The insert is secured to the main body by eight cap screws. Two 13 mm (0.5 in.) tapped holes are provided to allow installation and removal of the insert. The interface between the insert and flask body is sealed with two O-rings to prevent contamination between the two components.

The insert is fabricated from poured lead and clad in stainless steel. The use of lead decreases the package mass to below 6 Mg while maintaining the radiation shielding capability of the package. The main flask body will provide thermal protection for the shield insert to prevent melting of the lead in the regulatory thermal test. The stainless steel cladding provides structural support for the lead and facilitates decontamination.

The use of a removable insert offers the following advantages.

1. The packaging cavity can be increased to approximately 300 mm (12 in.) in diameter. This increases the versatility of the package provided that there is sufficient shielding for the radioactive payload.

2. The insert can be removed from the main flask body to facilitate decontamination of the main flask body cavity.

3. The fabrication of the main flask body is simplified.

4.4 Drawer

The drawer provides axial gamma shielding for the radioactive payload. The drawer is 152 mm (6 in.) square and 1168 mm (46 in.) long and has a mass of 115 kg (250 lb.). The drawer cavity is 143 mm (5.625 in.) square and 660 mm (24 in.) long. The drawer is fabricated from austenitic stainless steel (Type 304 SS) with 280 mm (11 in.) of steel shielding at each end.

During transportation, the drawer is secured to the main flask body by a 25 mm (1 in.) cap screw.

Rollers are provided to facilitate dry horizontal loading/unloading at a hot cell. The drawer was specifically designed to mate with hot cells at Whiteshell and Chalk River Laboratories. A push rod threaded into the drawer end can be used to push and pull the drawer out and into the package. The front end of the drawer has a removable shield plug to allow vertical loading/unloading in a storage pool.

4.5 Shielding Plugs

In cases where the drawer is not installed, the shielding plug can be used at each end of the shield insert to provide the required axial gamma shielding. Each plug is 152 mm (6 in.) square and 178 mm (7 in.) long and has a mass of 45 kg (100 lb.). Each plug is fabricated from poured lead and clad in stainless steel.

One shield plug (rear) is secured to the main flask body by a 25 mm (1 in.) cap screw. The other shield plug is secured to the front main closure.

Using the shielding plugs will increase the payload cavity length of the shield insert to 813 mm (32 in.).

4.6 Shield Inserts No. 2 and No. 3

If the drawer together with the square shield insert is not used, it can be replaced with shield insert No. 2 or No. 3 as shown in drawing E-5580-SA-16 or E-5580-SA-18. These inserts provide the necessary axial gamma shielding and supplement the radial gamma shielding of the main flask body. The inserts are fabricated from poured lead and clad in stainless steel. At one end of the insert is a removable lead plug for vertical (top) loading/unloading of the package. The inserts are 46" (1168 mm) long and have an outer diameter of 12-5/8" (320 mm). Insert No. 2 weighs approximately 1565 lbs (711 kg) with the removable end plug and has an internal cavity length of 32" (813 mm) and a cavity diameter of 7" (178 mm).

Insert No. 3 weighs approximately 1040 lb (470 kg) with removable end plug and has an internal cavity length of 30½" (775 mm) and a cavity diameter of 10½" (267 mm).

The insert is secured to the main body by eight cap screws. Two 1/2" (13 mm) tapped holes are provided to allow installation and removal of the insert. The interface between the insert and flask body is sealed with two O-rings to prevent contamination between the two components.

4.7 Closure Flanges

The main body is sealed with two main flanges. Each stainless steel flange (Type 304 SS) is secured to the flask body with eight 25 mm (1 in.) diameter Nitronic 60 cap screws. The use of Nitronic 60 cap screws prevent galling of the main flask body.

For containment each flange is sealed with two O-rings. The inner seal O-ring material is ethylene propylene which is suitable for low temperature environment, that is -40°C. The outer O-ring material is fluorocarbon which has high thermal resistance which will be effective in fire accidents. A test port is provided through the flange between the O-rings so that leakage tests can be completed on the seals.

The front flange houses a bellow-sealed valve. This valve is used to vent the drawer cavity prior to unloading any radioactive material. A cover plate together with an O-ring seals the valve cavity. A test port in the cover plate will allow leakage testing of the valve.

The back flange contains a 65 mm (2.56 in.) diameter through hole. This allows access to the drawer without removing the main flange. Tapped holes are provided in the back flange to allow the installation of push-rod cranking mechanisms. This access hole is sealed with a double O-ring cover plate.

4.8 Impact Limiters

The impact limiters are designed to provide impact protection for the packaging. The impact limiters are made of balsa wood, redwood and thermal insulation and are encased in stainless steel sheet (Type 304 SS). The limiters are secured to each end of the flask body by eight 25 mm (1 in.) diameter Nitronic 60 cap screws.

Wood is used because it has excellent impact absorbing properties and low thermal conductivity. The wood grain is oriented to provide the greatest amount of energy absorption on impact.

The thermal insulation (Marinite P) is a non-asbestos board material formed from calcium silicate with inert fillers and reinforcing agents. This insulation provides additional thermal protection to the package due to secondary burning of the wood in the event of a fire accident.

4.9 Lifting Assembly

A lifting bar and four trunnions are provided for lifting and handling the package. The trunnions will also allow the package to be tied down to the support frame. Four safety hoist rings are provided for tying down the package to the conveyance.

4.10 Support Frame

The support frame allows the package to be supported on the conveyance.

For air or rail transport, a shipping frame shown on drawing E-5580-113 is available for supporting the package on the conveyance.

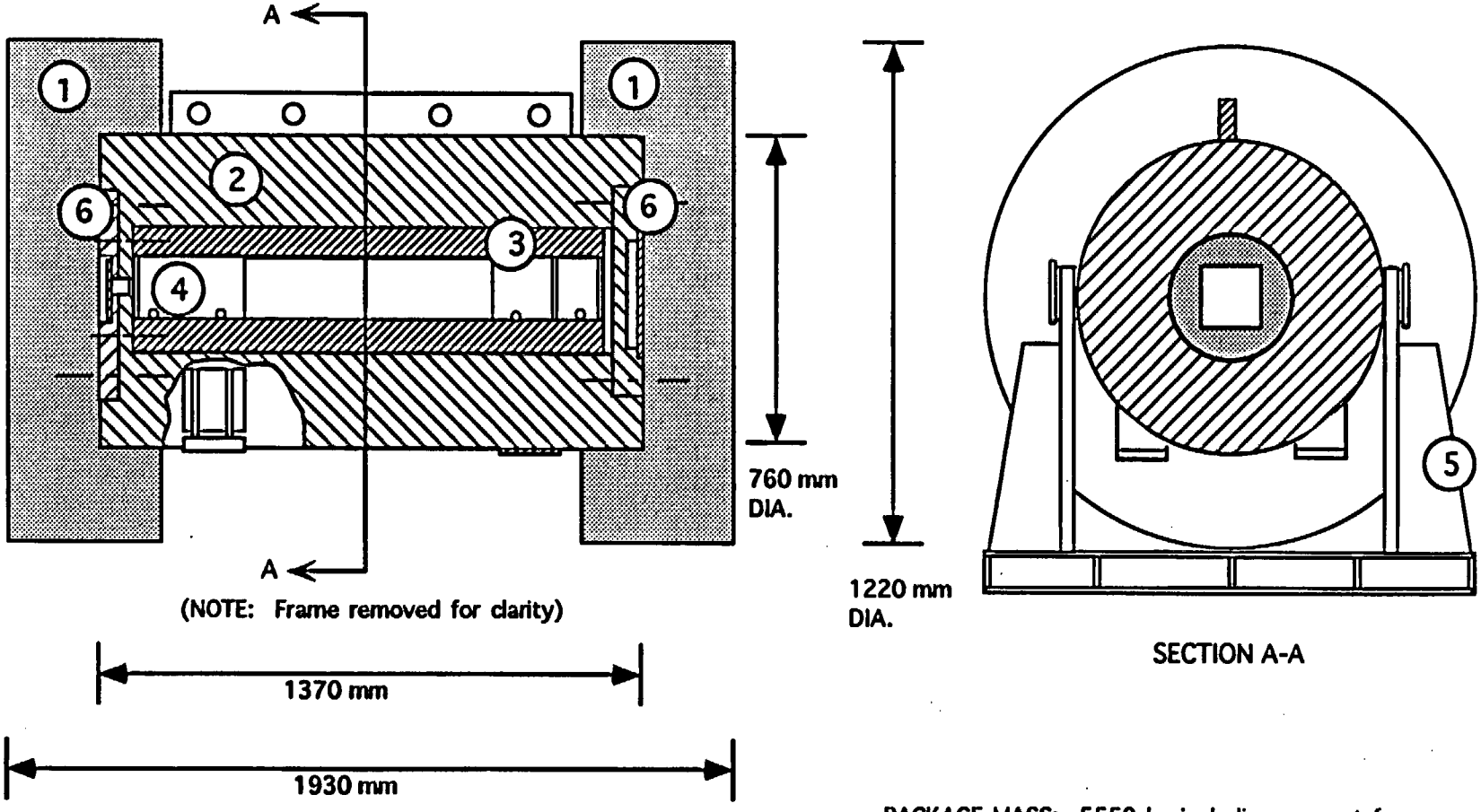

PACKAGE MASS: 5550 kg including support frame
5215 kg excluding support frame

1. IMPACT LIMITER
2. MAIN FLASK BODY
3. SHIELD INSERT
4. REMOVABLE DRAWER
5. SUPPORT FRAME
6. SEALING FLANGES

Figure 4.1 Irradiated Material Transportation Packaging

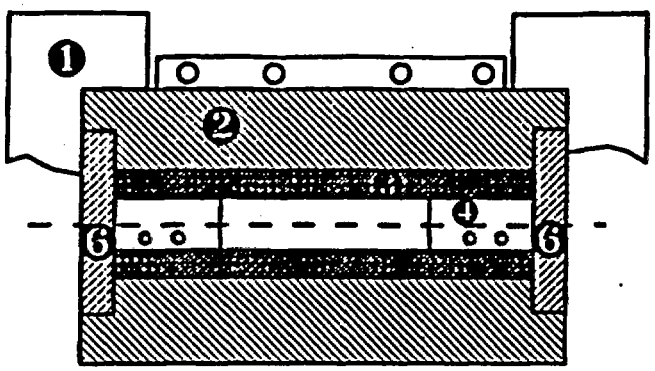

CONFIGURATION A
1. Impact Limiters
2. Main Flask Body
3. Shield Insert
4. Drawer
5. Support Frame (not shown)
6. Sealing Flanges

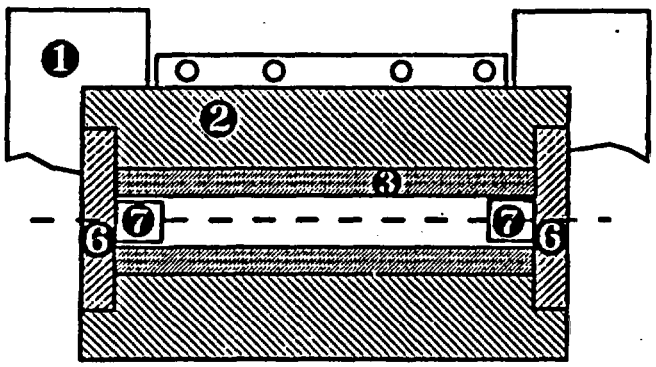

CONFIGURATION B
1. Impact Limiters
2. Main Flask Body
3. Shield Insert
4. --------
5. Support Frame (not shown)
6. Sealing Flanges
7. Shield Plugs

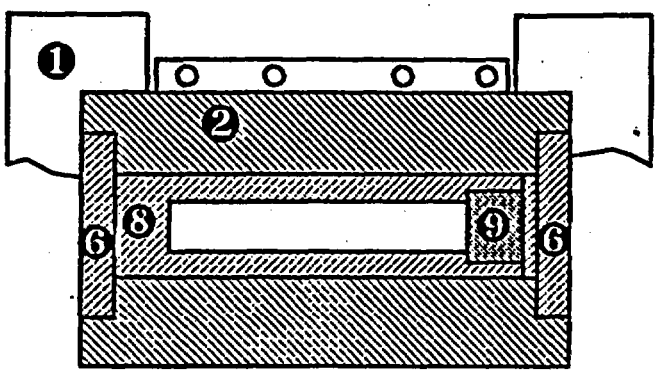

CONFIGURATION C
1. Impact Limiters
2. Main Flask Body
3. ---------
4. ---------
5. Support Frame (not shown)
6. Sealing Flanges
8. Shield Insert No. 2 or No. 3
9. Removable Shield Plug

FIGURE 4.2 PACKAGING CONFIGURATIONS

5.0 SHIPMENT DESCRIPTION

Shipments of the different radioactive materials will not be limited to Canada.

Most shipments will be by road but, transport is not limited to this mode. Some shipments, such as those between Canada and another country may involve more than one transport mode. The possible transport modes include road, rail, air or sea.

Shipment need not be by exclusive use vehicles although most shipments in Canada will be with dedicated vehicles.

The possible radioactive materials that may be transported in this package fall outside of Categories I, II and III of Reference 17 and so prudent management practices will be applied for the physical protection of these materials during transit.

Irradiated fuel shipments will occur routinely in Canada. There may be a need to transport irradiated fuel between a country which operates a CANDU reactor and Canada but such shipments will be infrequent.

Irradiated power reactor channel components and irradiated test specimens will be transported routinely within Canada and between Canada and other countries.

It is also possible that the package may be used to transport any of the authorized radioactive contents by a country other than Canada.

Vehicles will be placarded and packages will be labelled in accordance with the appropriate national and international requirements.

Radiation levels and non-fixed radioactive contamination levels on the outer package surfaces shall comply with the appropriate national and international requirements.

6.0 STRUCTURAL EVALUATION

6.1 Introduction

With reference to drawing E-5580-A-32, the packaging components that need to be evaluated with respect to radiation shielding or containment of the radioactive contents consist of:

a) the impact limiters,
b) the main flask body,
c) the front and rear closure flanges, including cap screws and O-ring seals,
d) the valve cover plate, including cap screws and O-ring seals,
e) the rear cover plate, including cap screws and O-ring seals, and
f) the lead shield insert cap screws and welds.

The packaging components that need to be evaluated with respect to package tie downs and handling consist of:

a) the trunnions,
b) the lifting bar,
c) the safety hoist rings, and
d) air/rail shipping frame.

The components have been evaluated by calculation methods, by prototype packaging testing methods or a combination of these methods. In general, where both calculation and prototype testing methods are used, the general procedure is as follows:

a) simplified calculations were used to establish a relationship between an acceptable impact limiter design and acceptable 'g' load values for the package as a whole;

b) calculations were used to establish the sizes and materials for the critical packaging components, based on derived 'g' load values;

c) prototype package testing was performed to verify the structural integrity of the package;

d) prototype package testing was performed to determine any reduction of the gamma radiation shielding integrity of the package;

e) prototype package testing was performed to verify that the regulatory containment requirements would be satisfied; and

f) prototype package testing was used to inspect the condition of the packaging components, particularly the various cap screws and O-ring seals.

Appendix A of this report supplements this section on Structural Evaluation. Appendix A contains detailed calculations and detailed results of the prototype package testing program (from Reference 28). The pertinent results that are given in Appendix A are summarized in the appropriate subsections below.

6.2 Packaging Component Masses and Material Properties

Table 6.1 lists the mass/weight of the packaging components that will affect the structural evaluation.

TABLE 6.1

COMPONENT MASSES/WEIGHT

Component	Mass, kg	Weight, lb
Main Flask Body	4000	8800
Lead Shield Insert	670	1475
Front Flange	115	250
Rear Flange	60	125
Impact Limiters (2)	255	560
Drawer	115	250
TOTAL	5215	11460

Table 6.2 lists the mechanical properties of these components. The values have been extracted from Appendix I of the ASME Code, Section III, Reference 18.

TABLE 6.2
COMPONENT MATERIAL MECHANICAL PROPERTIES

Component	Material	Su_{min} MPa	Sy_{min} MPa	Sm at 38°C MPa
Main Flask Body	SA-182 F304	515	205	138
Closure Flanges	SA-182 F304, SA-240 Type 304	515	205	138
Closure Capscrews	SA-193 Class 1C B8S	655	345	115
Trunnions	SA-479 XM-19 annealed	690	380	230
Shear Disc	SA-479 XM-19 annealed	690	380	230
Capscrews	SA-564 Type 630 H1100	965	795	322
Lead Shield Insert				
Outer Shell	SA-312 Type 304L	485	170	115
Inner Shell	SA-240 Type 304L	485	170	115
Flanges	SA-240 Type 304	515	205	138
Capscrews	SA-564 Type 630 H1100	965	795	322
Draver				
Sides	SA-240 Type 304L	485	170	115
Ends	SA-479 Type 304	515	205	138
Locking Capscrews	SA-564 Type 630 H1100	965	795	322

6.3 COMPONENT EVALUATION

6.3.1 Impact Limiter

6.3.1.1 Design Criteria

Drawing E-5580-84 shows the impact limiter design. The function of the impact limiter is to reduce the impact loading on the packaging components as a result of the regulatory drop tests for accident conditions of transport. The impact limiters will also provide protection to the package for the normal conditions of transport drop test but this is not a design requirement. They also provide thermal protection in the event of a fire accident. The design criterion for the impact limiters is that they they reduce the deceleration of the package components to acceptable level for a 9 metre drop test, regardless of the package orientation at the time of impact.

6.3.1.2 Calculations

Section A.2 of Appendix A describes the calculation method and results for estimating the deceleration rates and impact limiter deformations that will occur as a result of end, side and oblique drops from 9 metres. Table 6.3 summarizes the results.

6.3.1.3 Prototype Testing

The deformation of the impact limiters and decelerations during testing (from Section A.4) is also shown in Table 6.3. The maximum deformation during the oblique angle drop test is due to the balsa wood crushing. The redwood had crushed approximately 114mm (4.5 inches) during this test.

6.3.1.4 Evaluation

The impact limiters provide adequate protection to the packaging components during the drop tests and provided adequate thermal protection during the fire test.

TABLE 6.3
IMPACT RESULTS

	Calculation		Test	
Case	Deceleration g's	Deformation mm	Deceleration g's	Deformation mm
Flat End Impact	90.2	106.7	180*	75
Horizontal Side Impact	128.8	106.7	95*	100
Oblique (60.9°) Impact	122.1	180.3	94	190

* Derived values

6.3.2 Main Flask Body

6.3.2.1 Design Criteria

The functions of the main flask body are to provide gamma radiation shielding and containment of the radioactive contents for routine, normal an accident conditions of transport. The design criteria for gamma radiation shielding are given in Table 9.1 and the containment criterion is a gas leakage test which shows that the containment system is leaktight as defined in Reference 19, i.e. 1×10^{-8} Pa.m ^{3}/s or less.

6.3.2.2 Prototype Testing

The test results in Section A.4 showed that the main flask body is a very rugged packaging component and that it was virtually unaffected by any of the regulatory tests for either normal or accident conditions of transport. There was no loss of gamma radiation shielding integrity and the main flask body maintained the leak tightness criterion, even after multiple drop tests.

As far as the tests for normal conditions of transport are concerned, the water spray test, which was not conducted, will not affect the package integrity because all the external surfaces are metal. The stacking test was not completed because the packaging is cylindrical in shape and transported with its axis in the horizontal position. The shape and orientation of the package essentially prevents stacking. It is also anticipated that not more than one package will be shipped in one consignment. The penetration test was not completed because the effect would be trivial. The test would cause an indentation of about 1 mm but this will not affect the integrity of the main flask body.

6.3.2.3 Evaluation

The test results show that the main flask body complies with the regulatory requirements. Because the material of the main flask body does not exhibit a nil ductility temperature transition, the performance of this component at an ambient temperature of -40°C would be expected to be the same as that observed in the prototype package test program.

Analyses in Section A.6 shows that the main flask body will maintain its structural integrity when subjected to an external pressure of 150 kPa.

6.3.3 Front and Rear Closures

6.3.3.1 Design Criteria

The closures include the flanges, their cap screws and O-ring seals. The functions of the closures are to provide containment of the radioactive contents and to resist any internal gas or vapour pressures within the package cavity.

The containment criterion is a gas leakage test which shows that the containment system is leaktight as defined in Reference 19, i.e. 1×10^{-8} Pa.m ^{3}/s or less. Where evaluation of the flanges and cap screws under hypothetical accident conditions is assessed by calculation, the evaluation uses the design criteria in Appendix F, Article F-1000, "Rules for Evaluation of Service Loadings with Level D Service Limits", Section III of the ASME Code, Reference 20, in accordance with USNRC Regulatory Guide 7-6, Reference 21.

6.3.3.2 Calculations

For impacts under hypothetical accident conditions a vertical flat end impact will cause the maximum bending stresses in the closure flanges. Section A.3.2.1 of Appendix A describes the calculation methods and results for the front flange. The results can also be used to evaluate the rear flange because both flanges have the same diameter, same sized cap screws and same sized O-ring seals.

For resistance to internal gas or vapour pressure, the following operating conditions were established in Section 7, Thermal Evaluation.

a) Maximum Normal Operating Pressure = 1.5×10^5 Pa at 150°C.

b) Normal Conditions of Transport = 6.1×10^5 Pa at 150°C. This pertains to the unusual situation where some residual moisture remains in the cavity after vacuum-drying.

c) Accident Conditions of Transport = 2.0×10^5 Pa at 265°C.

d) Accident Condition of Transport = 53.7×10^5 Pa at 265°C. This pertains to the unusual situation that some residual moisture remains in the cavity after vacuum-drying.

Section A.3.2.2 and A.3.3.2 of Appendix A give analyses for b) and d).

The internal gas or vapour pressure generates a stress of 9.8 MPa. Table 6.4 summarizes the combined effects of an end impact and the internal pressure. From Table 7.1, the flange temperature is 62°C at the time of impact.

TABLE 6.4
FRONT FLANGE STRESSES - COMBINED END IMPACT AND INTERNAL PRESSURE

Impact MPa	Internal Pressure MPa	Calculated Stress Intensity MPa	Allowable Stress Intensity at 62°C MPa
34.4	9.8	44.2	497

These results show that the design criteria are satisfied.

An additional analysis of the flange but with an internal pressure of 53.7×10^5 Pa shows that the stress intensity would be 86.3 MPa. This pressure could occur as a result of the thermal test and when the quasi-steady state temperature of the flange is about 200°C (see Figure 7.10 in Section 7). The allowable stress intensity at 200°C is 465 MPa and so this design criteria is satisfied.

For impacts under hypothetical accident conditions, the cap screws must be evaluated for side and oblique orientations. For end drop orientations the cap screws are not subjected to tensile loads. Section A.3.3.1 of Appendix A describes the calculation methods and results for the front flange, but these results can also be used to evaluate the rear flange cap screws. Tables 6.5 summarizes the results.

TABLE 6.5
FLANGE CAP SCREW STRESSES - IMPACT

Impact Orientation	Tensile MPa	Shear MPa
Side	0	77.3
Oblique at 60°	66.9	112.8

The internal gas or vapour pressure of 1.5×10^5 Pa generates a tensile of 22 MPa in the cap screws. Table 6.6 summarizes the combined effects of the different impact orientations and the internal pressure as calculated in Section A.3.3.

TABLE 6.6

Impact Orientation	Tensile Stress MPa	Shear Stress MPa	Combined Stress Ratio
Side	22.0	77.3	0.22
Oblique	88.9	38.6	0.16
Design Criteria at 62°C	307	184	1

These results show that the design criteria are satisfied.

An additional analysis assessed the effect of the inertia of the front flange plus the draver and its contents for an end impact. The cap screw tensile stress would be 250.9 MPa which is still below the design criterion.

An additional analysis of the cap screws but with an internal pressure of 53.7 MPa shows that the tensile stress would be 193.5 MPa. The temperature of the capscrews at this time would be about 200°C and the allowable stress intensity would be 204 MPa; therefore, the design criteria is satisfied.

6.3.3.3 Prototype Testing

The test results in Section A.4 showed that the front and rear closures maintained the leak tightness criterion, even after multiple drop tests.

6.3.3.4 Evaluation

The test results show that the flange closures comply with regulatory containment requirements while the calculations show that the flange closures provide adequate strength to resist internal gas and vapour pressures. Because the materials for the flanges, screws and O-ring seals have been selected for cold ambient environments, the performance of these components at an ambient temperature of -40°C would be expected to be the same as that observed in the prototype package test program.

As showed in Section A6, the main flange closures will retain its structural integrity when subjected to an external pressure of 150 kPa.

6.3.4 Valve Cover Plate Closure

6.3.4.1 Design Criteria

The valve cover plate closure includes the plate itself, the cap screws and the O-ring seal. The function of the closure is to protect the bellows sealed valve against impact accidents. The O-ring seal could enhance the containment integrity of the package but the valve cover plate closure is not considered to be part of the containment system.

6.3.4.2 Prototype Testing

The test results in Section A.4 showed that the prototype valve cover plate which is shown on prototype drawing D-5580-96 did not perform satisfactorily as a result of the puncture test. The puncture test caused the plate to bend inwardly towards the valve. This resulted in bent cap screws and a broken valve handle but did not cause any loss of package containment integrity.

6.3.4.3 Evaluation

The valve cover plate has been redesigned as shown on drawing D-5580-80 to eliminate the excessive plate bending. The plate thickness has been increased to 50 mm from 25.4 mm. Counterbores are now provided for the cap screws. Minimum sized cut outs have been incorporated for the valve and its piping. Plate bending will be minimized because, impacts from the puncture test will be distributed more evenly to the front closure flange. This modification will satisfy the design criteria.

As shown in Section A6, the valve cover plate will retain its structural integrity when subjected to an external pressure of 150 kPa.

6.3.5 Rear Cover Plate Closure

6.3.5.1 Design Criteria

The rear cover plate closure includes the plate itself, the cap screws and the O-ring seals. The functions of the closure are to provide containment of the radioactive contents and to resist any internal gas or vapour pressures within the package cavity.

The containment criterion is a gas leakage test which shows that the containment system is leak tight as defined in Reference 19, i.e. 1×10^{-8} Pa.m ^{3}/s or less.

The design criteria for resistance to internal gas or vapour pressures are given in Appendix F, Article F-1000, "Rules for Evaluation of Service Loadings with Level D Service Limits", Section III of the ASME Code, Reference 20.

6.3.5.2 Calculations

For resistance to internal gas or vapour pressures, the following operating conditions were established in Section 7, Thermal Evaluation.

a) Maximum Normal Operating Pressure = 1.5×10^5 Pa at 150°C.

b) Normal Conditions of Transport = 6.1×10^5 Pa at 150°C. This pertains to the unusual situation where some residual moisture remains in the cavity after vacuum drying.

c) Accident Conditions of Transport = 2.0×10^5 Pa at 265°C.

d) Accident Conditions of Transport = 53.7×10^5 Pa at 265°C. This pertains to the unusual situation where some residual moisture remains in the cavity after vacuum drying.

The temperature of the rear cover plate and its cap screws is 62°C for normal conditions of transport and 200°C for accident conditions of transport.

Section A.3.2.2 and A.3.3.2 of Appendix A gives analyses for b) and d). Tables 6.7 and 6.8 summarize the results.

TABLE 6.7
REAR COVER PLATE BENDING STRESSES

Internal Pressure Pa	Calculated Stress MPa	Allowable Stress MPa
6.1×10^5	5.4	497 at 62°C
53.7×10^5	47.5	465 at 200°C

TABLE 6.8
REAR COVER PLATE CAP SCREW STRESSES

Internal Pressure Pa	Calculated Stress MPa	Allowable Stress MPa
6.1×10^5	18.9	274 at 62°C
53.7×10^5	166.5	204 at 200°C

From the above results, the rear cover plate closure satisfies the design criteria.

6.3.5.3 Prototype Testing

The test results in Section A.4 showed that the rear cover plate closure maintained the leak tightness criterion, even after multiple drop tests. However, inspection of the condition of the prototype rear cover plate, which is shown on drawing C-5580-99, showed that some bolt heads had been bent and that, in a number of cases, the bolt torques were reduced to zero.

6.3.5.4 Evaluation

Although the leak tightness criterion was satisfied, the rear cover plate closure has been redesigned as shown on drawing C-5580-82 to eliminate impacts onto the bolt heads. In the prototype test package, the rear cover plate was 12.7 mm thick and the heads of the bolts protruded above the plate. The plate has been thickened to 25.4 mm and it is counterbored so that the bolt heads will no longer be exposed to impacts. The size of the capscrews have been increased to 9.53 mm (3/8") in diameter.

Section A6 also demonstrates by analyses that the rear cover plate will maintain its structural integrity when subjected to an external pressure of 150 kPa.

The calculations show that the rear cover plate closure provides adequate strength to resist internal gas and vapour pressures. Because the materials for the plate, cap screws and O-rings have been selected for cold environments, the performance of these components at an ambient temperature of -40°C would be expected to be the same as that observed in the prototype package test program.

6.3.6 Lead Shield Insert

6.3.6.1 Design Criteria

The integrity of the lead insert must be maintained to prevent additional loads on the front closure flange during package impacts. For the calculations, the evaluation uses the design criteria in Appendix F, Article F-1000, "Rules for Evaluation Service Limits", Section III of the ASME Code, Reference 20, in accordance with USNRC Regulatory Guide 7-6, Reference 21.

6.3.6.2 Calculations

Section A.3.4.1 of Appendix A gives the calculations for the cap screws and Table 6.9 summarizes the results.

TABLE 6.9
SHIELD CAP SCREW STRESSES

Impact Orientation	Tensile MPa	Shear MPa	Combined Stress Ratio
End	450	0	0.443
Oblique at 60°	390	225*	0.641
Stress Design Criteria	676	405	1

* Insert is laterally constrained by the flask body; therefore shear stresses are minimized.

As calculated in Section A.3.4.2, the stress intensity of the welds (172 MPa) under end impact is below the allowable stress intensity (270 MPa).

6.3.6.3 Prototype Testing

The test results in Section A4 showed that, although there was a reduction in the cap screw torques the cap screws did not fail, even after multiple drop tests. Test results also showed that there was not failure of the welds.

6.3.6.4 Evaluation

For the end and oblique drop tests the calculation show that the cap screws will not fail (or yield). The prototype tests confirmed that the cap screws and welds.

6.3.7 Trunnions

6.3.7.1 Design Criteria - Tie Downs

The trunnions include the trunnions themselves, the shear discs and their cap screws.

The design loads are based on IAEA Safety Series No. 37 (Reference 22) as follows:

<u>Road and Sea Transportation</u>

Longitudinal	± 2 g
Lateral	± 2 g
Vertical	3 g down, 2 g up

Rail and Air Transportation

Longitudinal ± 10 g

Lateral ± 2 g

Vertical ± 4 g

The vertical acceleration includes gravity and are actual absolute factors experienced by the package. The loads are assumed to be applied simultaneously. The allowable stress criteria is the yield strength of the component.

6.3.7.2 Calculations - Tie Downs

Section A.5.1 in Appendix A gives the calculations and Tables 6.10 and 6.11 summarizes the results.

TABLE 6.10
TRUNNION COMPONENT STRESSES - TIE DOWNS
FOR ROAD AND SEA TRANSPORTATION

Component	Stresses MPa	
	Calculated	Allowable
Trunnion	151.7	190
Shear Disc	84.5	190
Cap Screw	724.3	795

TABLE 6.11
TRUNNION COMPONENT STRESSES - TIE DOWNS
FOR AIR AND RAIL TRANSPORTATION

Component	Stresses MPa	
	Calculated	Allowable
Trunnion	112.6	190
Shear Disc	55.8	190
Cap Screw	624	795

6.3.7.3 Evaluation - Tie Downs

The calculated results show that the stresses satisfy the design criteria.

6.3.7.4 Design Criteria - Lifting

The trunnions include the trunnions themselves, the shear discs and their cap screws. It is assumed that safety hoist rings are used for lifting as opposed to the trunnions themselves. The design load was 29 kN assuming only two safety hoist rings and trunnions are used for lifting. The design criteria used was one-third of the yield strength.

6.3.7.5 Calculations - Lifting

Section A.5.2 in Appendix A gives the calculations and Table 6.12 summarizes the results.

TABLE 6.12
TRUNNION COMPONENT STRESS INTENSITIES LIFTING

Component	Stress Intensity (MPa)	
	Calculated MPa	Allowable MPa
Trunnion	17.1	63.3
Shear Disc	10.4	63.3
Cap Screw	65.9	265

6.3.7.6 Evaluation - Lifting

The calculated results show that the stress intensities satisfy the design criteria.

6.3.8 Lifting Bar

6.3.8.1 Design Criteria

The function of the lifting bar is to handle the package, usually on site at a hot cell. The design criterion is that the calculated stress intensity should include a factor of safety, at least 5, based on the minimum ultimate tensile strength of the base material.

6.3.8.2 Calculation

Section A.5.2.3 in Appendix A gives the calculations. The calculated stress intensity is 74.4 MPa and the minimum ultimate tensile strength of the Type 304 stainless steel base material is 485 MPa, about seven times the calculated stress intensity.

6.3.8.3 Evaluation

The calculated results show that the stress intensity satisfies the design criterion.

6.3.9 Safety Hoist Rings

6.3.9.1 Design Criteria

The function of the safety hoist rings is to ease handling of the package and provide a tie-down attachment point for the package. The lifting loads and tie-down loads are transmitted through the package trunnions. The design loads for tie-down and lifting are given in Section 6.3.7.1 and 6.3.7.4 respectively. For lifting, an allowable load is based on the rated capacity of the safety hoist ring. For tie-down the allowable load is based on the ultimate strength of the safety hoist ring.

6.3.9.2 Evaluation

Each safety hoist ring has a rated capacity of 66.7 kN (15000 lb) with a factor of safety of 5 on the ultimate strength of 333.6 kN. Using the lifting and tie down loads given in Section A.5 of Appendix A, a comparison with the allowable loads is given in Table 6.20. The calculated force assumed only two safety hoist rings will be used for lifting.

TABLE 6.13
SAFETY HOIST RING LOADS

Load Condition	Load kN	
	Calculated	Allowable
Tie Down		
Road & Sea	273	333.6
Rail and Air	273	333.6
Lifting	29	66.7

The results show that the calculated load satisfies the design criteria.

6.3.10 Air/Rail Shipping Frame

6.3.10.1 Design Criteria

Under chocked conditions, the chocked forces will be transferred through the shipping frame. As stated in Section 6.3.7.1, the tie down loads for rail and air transportation are as follows:

Longitudinal	± 10 g
Lateral	± 2 g
Vertical	± 4 g.

The acceptance criteria was based on the yield strength of the components.

6.3.10.2 Calculations

Detailed calculations are given in Section A.5.1.2.1 in Appendix A. A summary of the results are given in Table 6.14.

TABLE 6.14
AIR/RAIL SHIPPING FRAME STRESSES

Component	Stresses MPa	
	Calculated	Allowable
Trunnion Saddle		
Bending	68.8	125
Bearing	33.5	250
Longitudinal Gusset Weld	78	125
Lateral Gusset Weld	33.7	125
Longitudinal Beam	229.2	300
Lateral Beam	28.4	300

6.3.10.3 Evaluation

The calculated results show that the stress intensity satisfies the design criteria.

7.0 THERMAL EVALUATION

7.1 General

Calculations and full scale prototype tests have been completed to evaluate the effect of various thermal conditions that will be imposed on the package, both for normal and accident conditions of transport. In general, calculational methods were used for normal conditions of transport and full scale prototype test methods were used for accident conditions of transport. This approach was adopted because the structural distortion of the package that results from the different required drop tests can be discounted for normal conditions of transport but not necessarily for accident conditions of transport.

7.2 Radioactive Decay Heat Generation

Both the minimum and maximum radioactive decay heat must be taken into account, the former in combination with a cold environment and the latter in combination with a hot environment. The minimum radioactive decay heat is considered to be zero watts. The maximum radioactive decay heat results from irradiated fuel and is 160 watts.

A single Pickering fuel bundle assembly, which contains 19.86 kg of uranium initially, with a burnup of 1150 GJ/kg of initial uranium, and a storage time before shipment of 180 days has been used in the evaluation. After the irradiated fuel is removed from the reactor, heat is generated from the absorption of the energy released in the radioactive decay of the unstable isotopes in the fuel. Approximately two-thirds of the power generated is in the form of alpha and beta radiation which will be absorbed in the bundle. The remaining one-third of the power is generated in the form of gamma radiation, of which, two-thirds of the energy is absorbed by the bundle. Therefore, about 90% of the total decay energy released actually manifests itself as heat in the fuel bundle. The remaining 10% of the energy is emitted in the form of photons.

From Reference 23, the total decay energy release rates for 180 days cooling and 1150 GJ/kg U burnup are as follows:

Actinide	0.200 W/kg U
Fission Products	7.705 W/kg U
TOTAL	7.905 W/kg U

Therefore, for one Pickering fuel bundle which contains 19.86 kg of uranium, the total energy release rate would be 157 watts. For the purposes of analysis, it has been assumed that all the energy is released in the form of heat, and that it amounts to 160 watts. This decay heat value is considered to represent the upper bound because it has been assumed that the fuel may be subjected to above normal burnup, i.e. above 650 GJ/kg U. Also, the above conditions are considered to be valid for either 28 element or 37 element fuel bundles because, although there may be minor temperature differences within the bundles themselves, the temperature gradients throughout the packaging will be the same.

Finally, the heat generated by a fuel bundle will be considerably greater than the heat generated by either the irradiated power reactor channel tube sections or the irradiated test specimens and consequently, the radioactive decay heat value of 160 watts imposes the most significant thermal conditions on the packaging for all the authorized radioactive contents.

7.3 Package Thermal Design

For routine and normal conditions of transport the design of the packaging components must take into account temperatures that range from -40°C to +70°C and the package must be designed for an ambient temperature range of -40°C to +38°C. For accident conditions of transport the package must be designed for a thermal test of 800°C for 30 minutes.

The packaging components that must be considered are:

a) the outer stainless steel shielding
b) the lead shield insert
c) the wood impact limiters
d) the elastomeric closure seals
e) the valve on the front closure flange, and
f) the closure cap screws.

The outer stainless steel shielding has been designed to accommodate the temperature range of -40°C to 70°C and the thermal test. The stainless steel shielding is an austenitic material that exhibits good impact properties at -40°C because this material has a face-cubic-centred structure that does not exhibit a ductile to brittle transition temperature. At 800°C, the stainless steel is virtually unaffected.

The lead shield insert will readily accommodate the temperature range of -40°C to 70°C because it does not exhibit brittle fracture characteristics at -40°C and its melting temperature is 325°C. Although the lead shield would melt if it were exposed to the thermal test directly, the lead shield insert is adequately protected by the outer stainless steel forging so that its temperature will remain below 325°C as a result of the thermal test.

The wooden impact limiters will readily accommodate the temperature range of -40°C to 70°C. As a result of the 9 metre drop test and the 1 metre puncture test the impact limiter casing may be breeched and the wooden contents will burn as a result of the thermal test. For this package design this possibility is acceptable because the impact limiters are considered to be expendable as a result of the thermal test. However, the combustion of the wooden materials will generate additional heat. In order to minimize the effect of this heat on the steel shielding and its closure systems, thermal insulation (i.e. Marinite P) has been incorporated into the impact limiter design (see drawing E-5580-84).

The main closure flanges use double 'O'-ring elastomeric seals. One 'O'-ring is fabricated from ethylene propylene which has good low temperature properties. The other 'O'-ring is fabricated from fluorocarbon which has excellent high temperature properties. Typical temperature ranges for 10 and 1000 hour exposure times, as quoted by the manufacturer, Reference 24, are as follows:

Ethylene Propylene:	-54°C to 193°C (-65°F to 380°F) for an exposure time of 10 hours
	-54°C to 149°C (-65°F to 300°F) for an exposure time of 1000 hours
Fluorocarbon:	-40°C to 243°C (-40°F to 470°F) for an exposure time of 10 hours
	-40°C to 204°C (-40°F to 400°F) for an exposure time of 1000 hours

Because the degradation of elastomers is time dependent at high temperatures, the temperature range for a 10 hour period is significant for assessment of the package under thermal test conditions.

The front closure flange houses a bellows-sealed valve which, according to the manufacturer, has a temperature range of up to 315°C, Reference 25.

The closure cap screw material has been selected to accommodate the temperature range of -40°C to 70°C and the thermal test. The cap screws are fabricated from Nitronic 60, an austenitic stainless steel material that exhibits good impact properties at -40°C because this material has a face-cubic-centred structure that does not exhibit a ductile to brittle transition temperature. At 800°C, the stainless steel is virtually unaffected.

7.4 Normal Conditions of Transport

7.4.1 Regulatory Criteria

(1) For non-exclusive use shipments or transportation by air, the package surface temperatures shall not exceed 50°C (122°F) for an ambient temperature of 38°C with no account taken for insolation.

(2) For exclusive use shipments, the package surfaces temperatures shall not exceed 85°C (185°F) for an ambient temperature of 38°C with no account taken for insolation.

(3) For an ambient temperature of 38°C and with account taken for insolation, heat generated within the package by the radioactive contents shall not adversely affect the package in such a way that it would fail to meet the applicable requirements for containment and shielding if the package were left unattended for a period of one week.

This requirements is significant in the case of shipments which contain defected fuel because oxidation of UO_2 to U_3O_8 becomes a concern when the fuel sheath temperature reaches 200°C.

(4) The design of the package shall take into account temperatures ranging from -40°C to 70°C for the components of the packaging.

(5) The package shall be designed for an ambient temperature range from -40°C to 38°C. At -40°C, the decay heat shall be assumed to be a minimum and no account shall be taken for insolation. At 38°C, the decay heat shall be assumed to be a maximum and account shall be taken for insolation.

Reference 1 defines insolation as 400 W/m^2, 12 hours per day for cylindrical packages.

7.4.2 Thermal Analysis and Results

Thermal analyses have been completed for,

a) package component temperatures for maximum decay heat and with no account taken for insolation,

b) package component temperatures for maximum decay heat and with account taken for insolation,

c) package outside surface temperature - approach to thermal equilibrium for maximum decay heat with no account taken for insolation, and

d) package component temperatures for zero decay heat and with no account taken for insolation.

This section summarizes the methods used and the results. Reference 26 gives completed details for a) and b) while Appendix B gives complete details for c). The results for d) are self evident.

For items a) and b), the Thermohydraulics Development Branch used the code THERMOS- a code for fuel in air heat transfer analysis, to assess seven cases; three when insolation is excluded and four when insolation is included. The different cases explored the effect of painted and unpainted surfaces on the package component temperatures. The analyses for items a) and b) uses the following general heat balance equation at equilibrium conditions,

$$Q_t \text{ (total)} = Q_c \text{ (convection)} + Q_r \text{ (radiation)} \qquad \text{Eq. 7.1.}$$

These analyses included the following simplifying assumptions:

- there will be no heat losses in the axial direction of an irradiated fuel bundle,
- there will be no heat transferred from the stainless steel shielding to the impact limiters,
- there will be no heat transferred from the stainless steel shielding to the support frame,

Table 7.1 gives the results for items a), b) and d). In addition, Reference 26 points out that the time to reach a safe limit before severe damage due to UO_2 oxidation occurs is 5.2 to 6.0 days when insolation is excluded or 2.5 to 5.4 days when insolation is included. Severe damage due to oxidation is considered to occur for fuel sheath temperatures of 200°C and greater.

Equation 7.1 was also used to determine that a package surface temperature of 50°C requires a decay heat of 262 watts.

For item c) Equation 7.1 was modified to account for transient conditions. Thus,

$$Q_t \text{ (total)} = Q_c \text{ (convection)} + Q_r \text{ (radiation)} + Q_a \text{ (absorbed)} \quad \text{Eq. 7.2}$$

In this analysis, reiterative calculations were completed for time increments of 2, 5 and 10 hours. This analytical approach is not sophisticated but is adequate to address the regulatory requirement which relates to holding packages until equilibrium conditions are approached (paragraph 402c). Table 7.2 summarizes the results and the calculations given in Appendix B show that more than 50 hours will be required for equilibrium to be attained for a decay heat of 160 watts and constant ambient temperature of 38°C.

7.4.3 Evaluation of Results

For a decay heat of 160 watts the package surface temperature has been calculated to be 45.8°C when no account is taken of insolation and the ambient temperature is 38°C. Therefore, the package design complies with regulatory requirements for both exclusive and non-exclusive use shipments. Also, there is quite a margin of safety because the calculations show that the decay heat would have to be 262 watts before the package surface temperature reaches 50°C. If a weather cover were in place, the package surfaces would not be accessible and the surface temperature would be slightly greater than 45.8°C. The surface temperature of the weather cover, which would be accessible, would be slightly less than 45.8°C.

For a decay heat of 160 watts and for an ambient temperature of 38°C and with account taken for insolation, all the packaging component temperatures are acceptable. However, in the case of the fuel elements the calculations show that sheath temperatures will exceed 200°C whether or not insolation is taken into account. This result is important in the case where, at the time of shipment, some or all of the fuel elements <u>are known to be defected</u>. In this case, the release fraction of radionuclides from the radioactive source to the package cavity could increase significantly due to oxidation of the UO_2. However, the elastomeric seals and the package containment system will not be affected by this oxidation; the containment system will remain "leaktight" (see Containment Evaluation, Section 8). So, in the case of known defected fuel shipments, the fuel should be under a cover gas such as argon, not for safety reasons but rather to maintain the integrity of the fuel for experimental or research purposes.

Table 7.1 PACKAGE COMPONENT TEMPERATURES FOR NORMAL CONDITIONS OF TRANSPORT

Temperature Location	Temperature, °C		
	Decay Heat 160 W Insolation Included*	Decay Heat 160 W Insolation Excluded**	Decay Heat 0 W Insolation Excluded
Ambient	38	38	-40
Outside Steel Shield	60.8	45.8	-40
Inside Steel Shield	62.2	47.2	-40
Outside Lead Shield Insert	67.2	52.2	-40
Inside Lead Shield Insert	67.5	52.5	-40
Drawer	88.1	73.6	-40
Shipping Can	148.0	135.4	-40
Outer Fuel Elements (Sheath)	221.4 to 225.9	214.0 to 218.6	N/A
Middle Fuel Elements (Sheath)	236.8 to 240.3	230.0 to 233.6	N/A
Inner Fuel Elements (Sheath)	242.6 to 243.9	235.9 to 237.2	N/A

* Case 5, Reference 26 (unpainted surfaces)
** Case 1, Reference 26 (unpainted surfaces)
N/A means not applicable

TABLE 7.2 PACKAGE OUTSIDE TEMPERATURE APPROACH TO EQUILIBRIUM FOR 160 WATTS

Time After Loading, Hours	Estimated Package Surface Temperature, °C
0	38.0
4	38.6
10	40.1
24	42.6
54	45.0

When the fuel is known to be intact at the time of shipment, it is not necessary to provide a cover gas. It is possible that, for the prescribed drop tests for normal conditions of transport, some fuel elements may defect and then oxidation will proceed. As before, the release fraction of radionuclides from the radioactive source to the package cavity could increase but again the containment system will remain leaktight and package safety will not be compromised.

The calculations show that the temperature of the packaging components may range from -40°C to 148°C, Section 7.3, Package Thermal Design, demonstrates that the selected packaging components can accommodate this temperature range.

The drop tests that were conducted on the prototype, see Appendix A, Section 4.0, and the selection of the packaging components demonstrate that the package has been designed for an ambient temperature range of -40°C to 38°C.

The results in Table 7.1 show that, for any particular packaging component, the temperature gradient across that component will be less than 2°C and therefore any thermal stresses within the components will be negligible.

The results show that, after loading the packaging with the maximum decay heat, at least 50 hours will be required before the package reaches thermal equilibrium.

Finally, the maximum operating pressures can be assessed for the case where the package has been loaded undervater. Two situations will be addressed,

a) for the usual situation where the package cavity has been drained and vacuum dried and no residual moisture remains, and

b) for the unusual situation where the package cavity has been drained and vacuum dried but some residual moisture remains.

From Table 7.1, assume that the bulk air temperature in the draver cavity is about the same as the shipping can temperature or 150°C. The free air volume in the package cavity is estimated to be 0.01 m^3 which is simply the draver cavity volume minus the fuel bundle volume and disregarding the can volume. If the package initial temperature were 20°C at the time of loading and if the pressure were 101.3 kPa, then at equilibrium the partial pressure of the air would be 146.2 kPa. If, some of the fuel elements defected as a result of the drop tests for normal conditions of transport, there would be a very small increase in the total cavity pressure due to the partial pressure of the released Kr-85 gas. However, the increase in the total cavity pressure will be small due to the relatively large free air volume within the package cavity. For situation a) the estimated pressure is about 150 kPa (1½ atmospheres) and this is considered to be the maximum normal operating pressure for the package. The package has been adequately designed for this situation.

For situation b), assume the air is saturated with moisture. At 150°C, the partial pressure due to the moisture would be about 462 kPa (from Steam Tables) and the total cavity pressure would be about 612 kPa (6 atmospheres). Even though this is not considered to be a normal operating pressure, the package has been adequately designed for this situation.

7.5 Accidental Conditions of Transport

7.5.1 General

One aspect of accident conditions of transport is the regulatory thermal test of 800°C for 30 minutes. The results of this thermal test on a prototype package are described below. As a consequence of the various tests that make up the hypothetical accident conditions of transport, the package must maintain a certain degree of radiation shielding and containment integrity. These criteria are evaluated in detail in Sections 8 and 9 of this report. The main purpose of this Section is to establish the package time-temperature profile both during and after the regulatory thermal test.

7.5.2 Fire Test

A pool type fire test was carried out at Ontario Hydro's Wesleyville Fire Test Facility on 1993 March 3. The results are described in Report No. B93-11-P, Reference 27. The prototype package was supported above a 4.5 m diameter fuel pan which contained a layer of kerosene floating on water.

Thermocouples around and on the package measured flame and package temperatures during the test. Uniform fire cover and average flame temperatures above 800°C were observed during the 30 minute fire test duration.

Flame temperatures were measured by twelve 1.6 mm diameter K-type thermocouples that surrounded the package, about 76 mm from its surface.

7.5.3 Prototype Package

Prior to the fire test the prototype package had been subjected to the regulatory mechanical tests. Consequently, the package was in a damaged state. During the mechanical tests, the support frame was not included. Similarly, this component was not included in the fire test. The containment flange cap screw were not re-torqued nor were the torques measured after the last series of mechanical tests (9m side drop test and 9m oblique drop test) prior to the fire test.

For the fire test the package cavity axis was in a horizontal orientation. The package contained a simulated radioactive payload in its cavity but without any simulated decay heat load. Ten thermocouples were attached to the prototype. Five 1.6 mm diameter K-type thermocuples measured external package temperatures and five similar thermocouples measured internal package temperatures. Package temperatures were recorded both during the fire test and 24 hours thereafter. Figure 7.1 shows the thermocouple locations.

Temperature indicators were attached to the inner faces of the front and rear flanges and the outer elements of the fuel bundle assembly.

Figures 7.2 through 7.6 show the prototype prior to, during and after the fire test.

7.5.4 Fire Test Results

The following data has been extracted from Reference 27 and highlights the results of the fire test. At the beginning of the test the ambient and package temperatures were 4°C.

Figure 7.7 shows the instantaneous flame temperature for the <u>average</u> of the 12 thermocouple measurements (from Graph No. 3, Plot T1 of Reference 27). The results indicate considerable fluctuation in the environment temperature but also indicates that the environment exceeds 800°C.

Figure 7.8 (a) and 7.8 (b) show the instantaneous package external surface temperatures. The results show considerable variation from one location on the package to another during the fire but these variations subside after the fire. The return of the package external surface temperatures to normal conditions occurs gradually.

Figures 7.9 and 7.10 show the instantaneous package internal surface temperatures. During the test some thermocouples measured cyclic temperature variations. After the fire was extinguished this phenomenon ceased and all the thermocouples measured temperatures that are characteristics of the anticipated results.

All of the wood inside the impact limiters had been consumed.

The temperature indicators provided the following results (Reference 11, Appendix A), Front Flange: 240 to 250°C, Rear Flange: 225 to 255°C, Fuel Bundle: 121°C.

7.5.5 Discussion of Results

The initial main flask body and lead shield insert temperatures were 4°C, or, according to Table 7.1, between about 42 and 49°C less than the temperatures for these components for normal conditions of transport where, the ambient temperature is 38°C and solar insolation is neglected, but the decay heat is included. This deficiency is offset by the facts that,

a) the fire environment and package were preheated for about 1½ minutes before the average flame temperatures reached 800°C, and

b) the average flame temperature exceeded 800°C for the duration of the test. Reference 27 shows that the average flame temperature, i.e. T1, measured between 900 and 990°C during the test. As calculated in Appendix B, it is estimated that this excessive thermal environment will transfer about 40% more heat to the package than an 800°C thermal environment, primarily by radiation heat transfer mechanisms.

For the purposes of this assessment it has been assumed that these opposing variations offset each other equally. In order to check the validity of this assumption, a finite difference analysis was used to compare the following two cases.

	Case 1	Case 2
Ambient Temperature	38°C	4°C
Solar Insolation	No	No
Decay Heat	160 W	0 W
Package Temperatures	47°C	4°C
Environment	800°C	950°C
Test Time	30 minutes	30 minutes

The calculational results which are given in Appendix B show that the actual fire test is more severe than the regulatory thermal test and consequently the assumption is valid.

From Figure 7.8 (a) the maximum package surface temperatures range from 420 to 800°C at the time the fire is extinguished and decreased to a range of 220 to 310°C ten minutes later. From Figure 7.8 (b) the package surface temperatures range from about 100 to 150°C four and one half hours after the fire and essentially remain at this level for the next 20 hours. The main flask body is virtually unaffected by any of these temperature conditions; the radiation shielding and structural integrity of the main flask body will remain intact.

From Figure 7.10 the maximum internal body temperature reached 266°C (measured in the front valve cavity 9 hours after the test was started). This result indicates that the lead shield insert will remain intact as a result of the fire test since the melting temperature of lead is 325°C. Also from Figure 7.10 the maximum internal body temperatures in the elastomeric 'O'-ring seal areas range from about 210 to 220°C. In general, these temperatures occur about 10 hours after the start of the test and remain at this level for about seven hours. Then, the temperatures decrease slowly. The upper temperature limits for a time exposure of 10 hours as showed in Figure 7.11, Reference 24, are:

Ethylene Propylene:	193°C
Fluorocarbon:	243°C.

These data indicate that the sealing performance of the fluorocarbon 'O'-rings should be adequate and that the sealing performance of the ethylene propylene 'O'-rings is marginal.

Because the valve cavity temperature reached 266°C, it exceeded the temperature limit of 93°C (Reference 25) for the valve stem insert material (PCTFE, polychlorotrifluoroethylene). This material has a melting temperature of 220°C to 245°C. As a result of the fire tests, a valve with a stellite stem insert (315°C valve rating) has now been specified for the package.

The results show that the package internal temperatures will be around 200°C. Obviously, the irradiated fuel sheath temperatures will exceed 200°C. Because fuel sheath failures will likely occur as the result of the regulatory mechanical tests, oxidation of the UO_2 fuel will occur. Consequently, this concern needs to be addressed in Section 8, Containment Evaluation.

The package internal pressure will be assessed for the case where the package has been loaded underwater. Two situations will be addressed,

a) for the usual situation where the package cavity has been drained and vacuum dried and no residual moisture remains, and,

b) for the unusual situation where the package cavity has been drained and vacuum dried but some residual moisture remains.

For both of these situations an estimate will have to be made for the cavity bulk air temperature because this data was not recorded during the fire test other than the temperature indicators on the dummy fuel bundles. This will be done as follows. In Section 7.4.3 the cavity bulk air temperature was assumed to be the same as the shipping can temperature and, according to Table 7.1, the shipping can temperature was about 85°C greater than the inside steel shield temperature. This data and assumption will be retained in this estimate. In Figure 7.10, the time period between 10 and 20 hours represents quasi-equilibrium temperatures for the internal body temperatures, i.e. the inside steel shield. The temperatures ranged from about 170°C to 220°C (excluding TC#8 which measured air temperatures) and the mean temperature was about 180°C during this time period. Therefore, the cavity bulk air temperature is estimated to be 265°C. The free air volume in the package is about 0.01 m^3 and if the package temperature and pressure were 20°C and 101.3 kPa respectively at the time of loading, then under accident conditions of transport the partial pressure of the air would be 186 kPa. There would be a very small additional pressure from any Kr-85 gas that escapes from any defected fuel elements. For situation a) the estimated pressure is about 200 kPa or about 2 atmospheres. The package has been adequately designed for this situation.

For situation b), assume the air is saturated with moisture. At 265°C the partial pressure due to the moisture would be about 5170 kPa (from Steam Tables) and the total cavity pressure would be about 5370 kPa or about 53 atmospheres.

Because the results showed that all the wood in the impact limiters would be consumed as a result of the fire test, a minor modification was made to their design. Three 10 mm thick pieces of non combustible insulation (Marinite P) have been specified in the design. This insulation is located between the wood and the end faces of the main flask body and its purpose is to restrict the transfer of heat from the burning wood to the end faces.

TC #1 Flask Top
TC #2 Flask Side
TC #3 Flask Bottom
TC #4 Flask Side
TC #5 Cover Plate Interspace
TC #6 Rear Cover Plate Seal
TC #7 Rear Flange Seal
TC #8 Valve Cavity
TC #9 Front Flange Seal
TC #10 Flask Corner

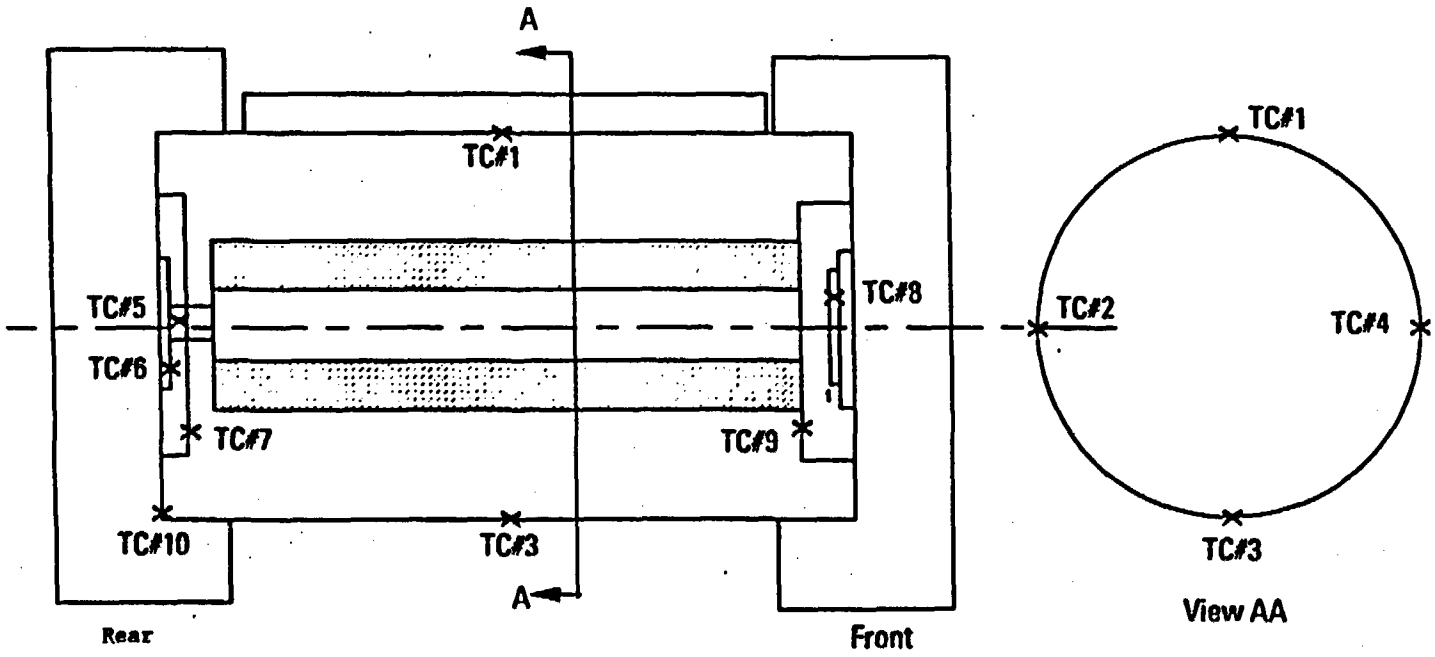

FIGURE 7.1 THERMOCOUPLE LOCATIONS

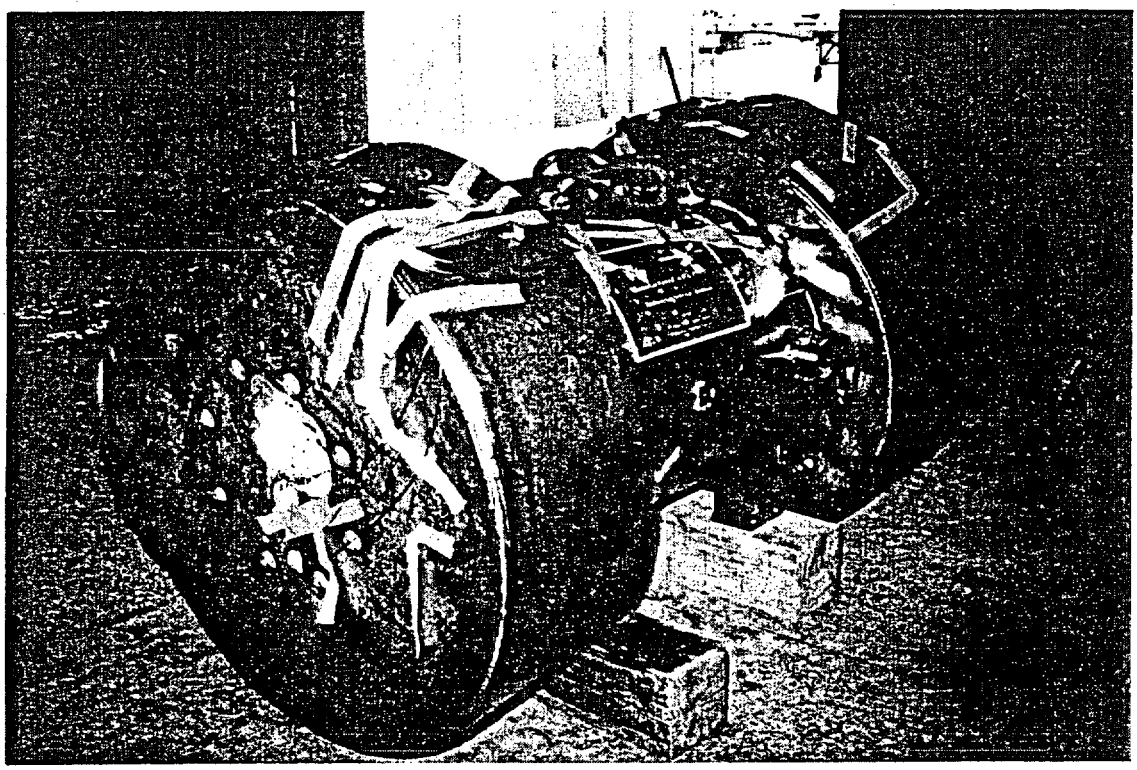

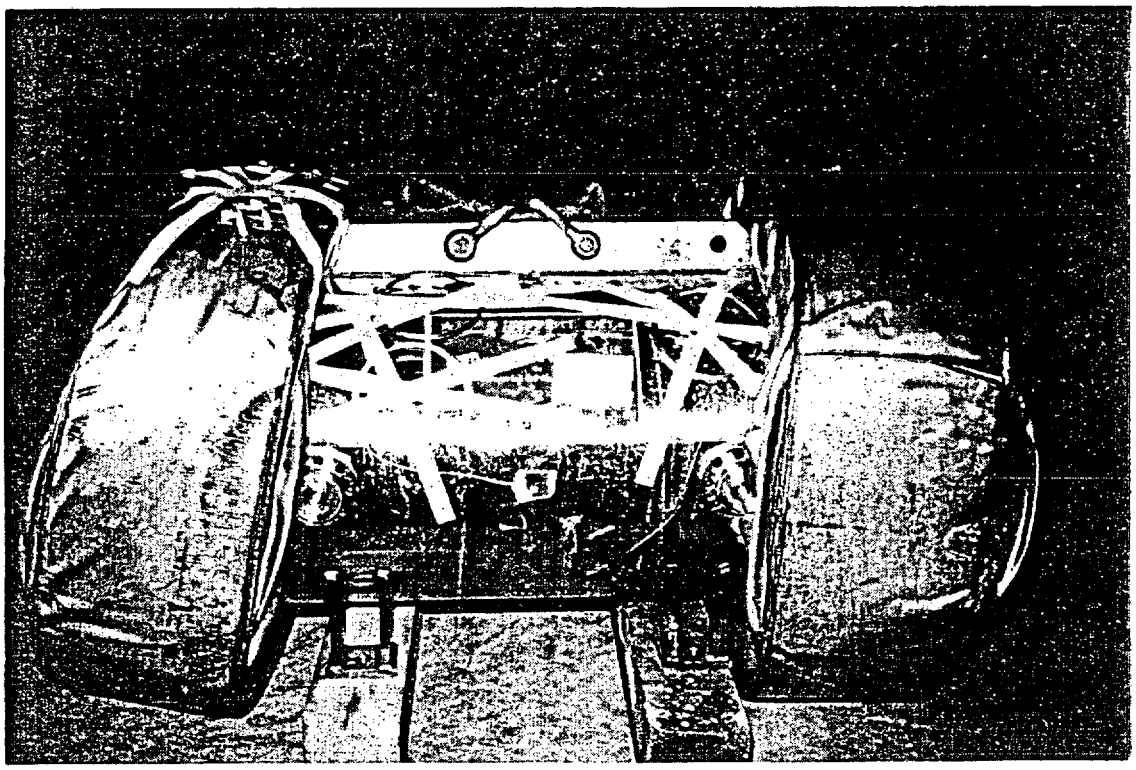

FIGURE 7.2 PHOTOGRAPHS OF PACKAGE PRIOR TO FIRE TEST

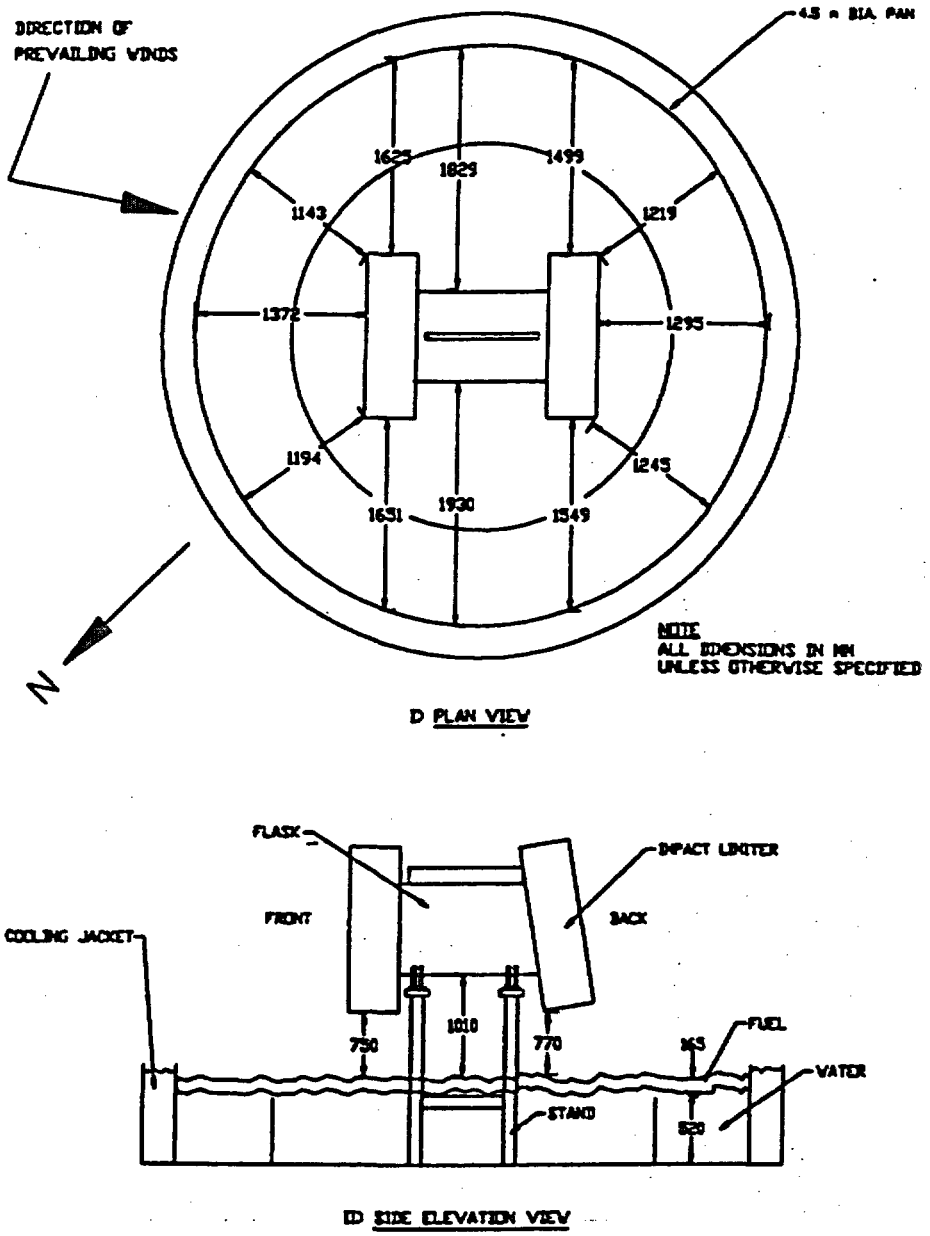

FIGURE 7.3 PACKAGE ARRANGEMENT IN FIRE PAN

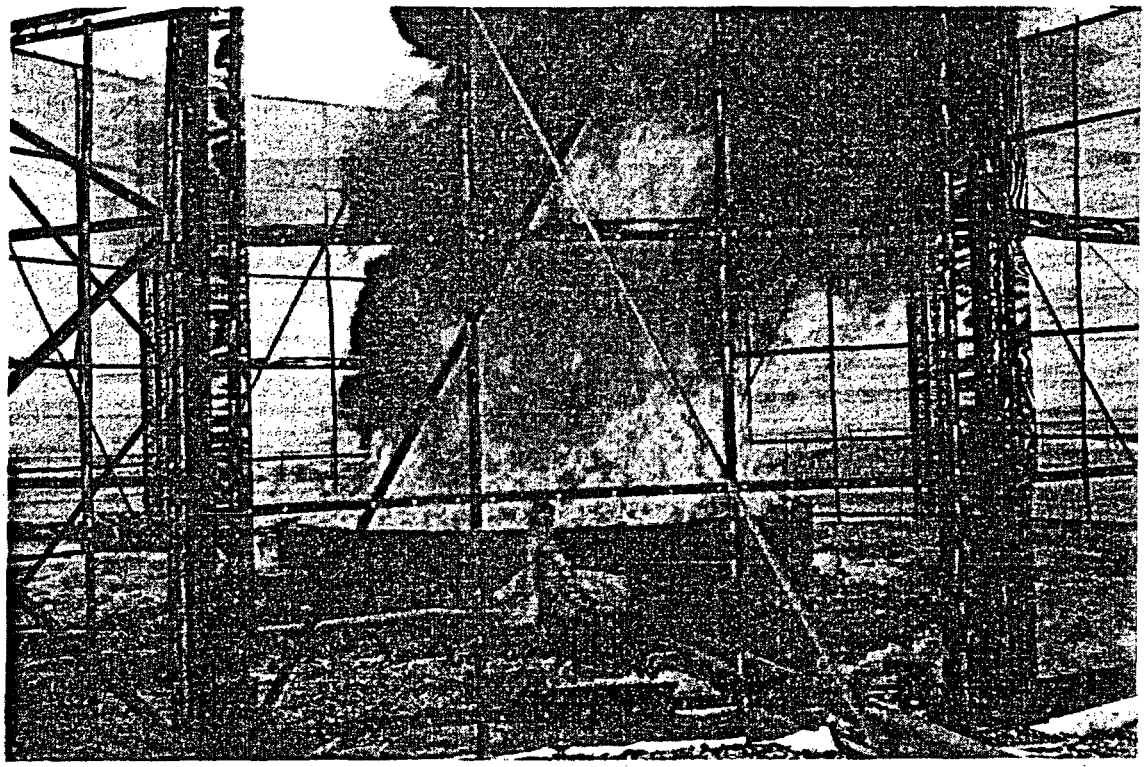

FIGURE 7.4 PHOTOGRAPH OF FULLY DEVELOPED POOL-FIRE

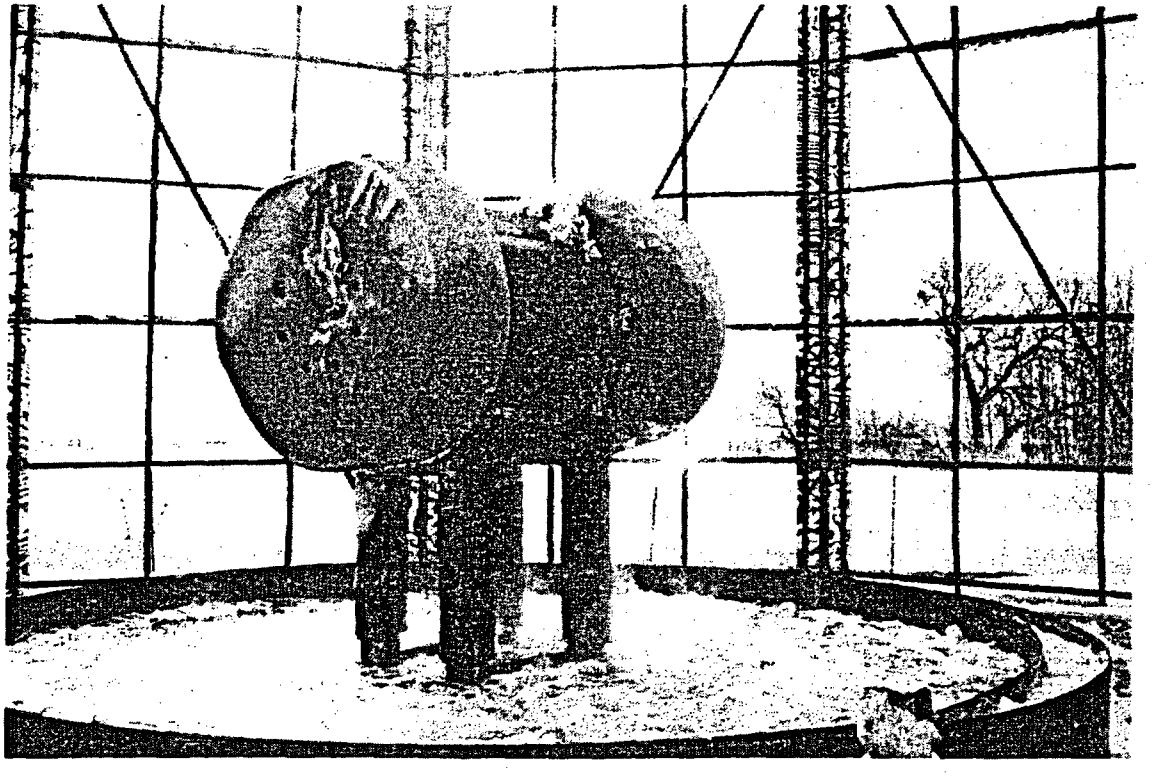

FIGURE 7.5 PHOTOGRAPH OF PACKAGE IMMEDIATELY AFTER TERMINATION OF POOL-FIRE

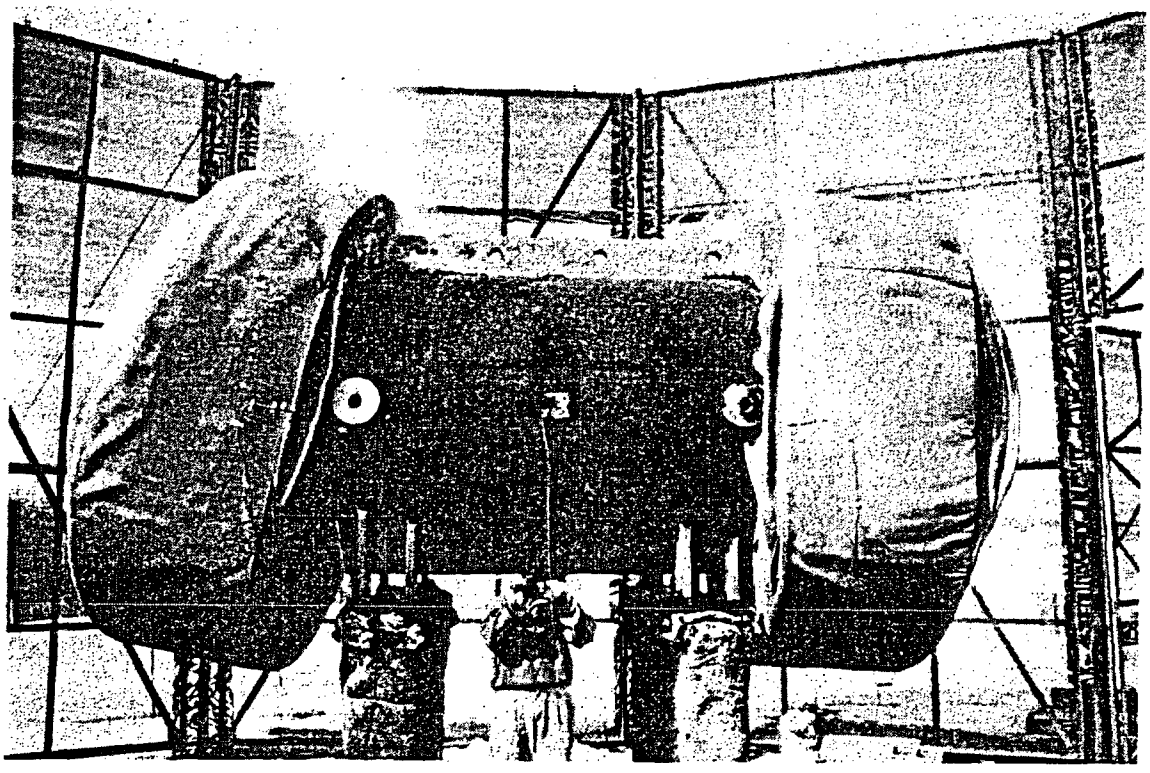

FIGURE 7.6 PHOTOGRAPH OF PACKAGE 15 MINUTES AFTER TERMINATION OF POOL-FIRE

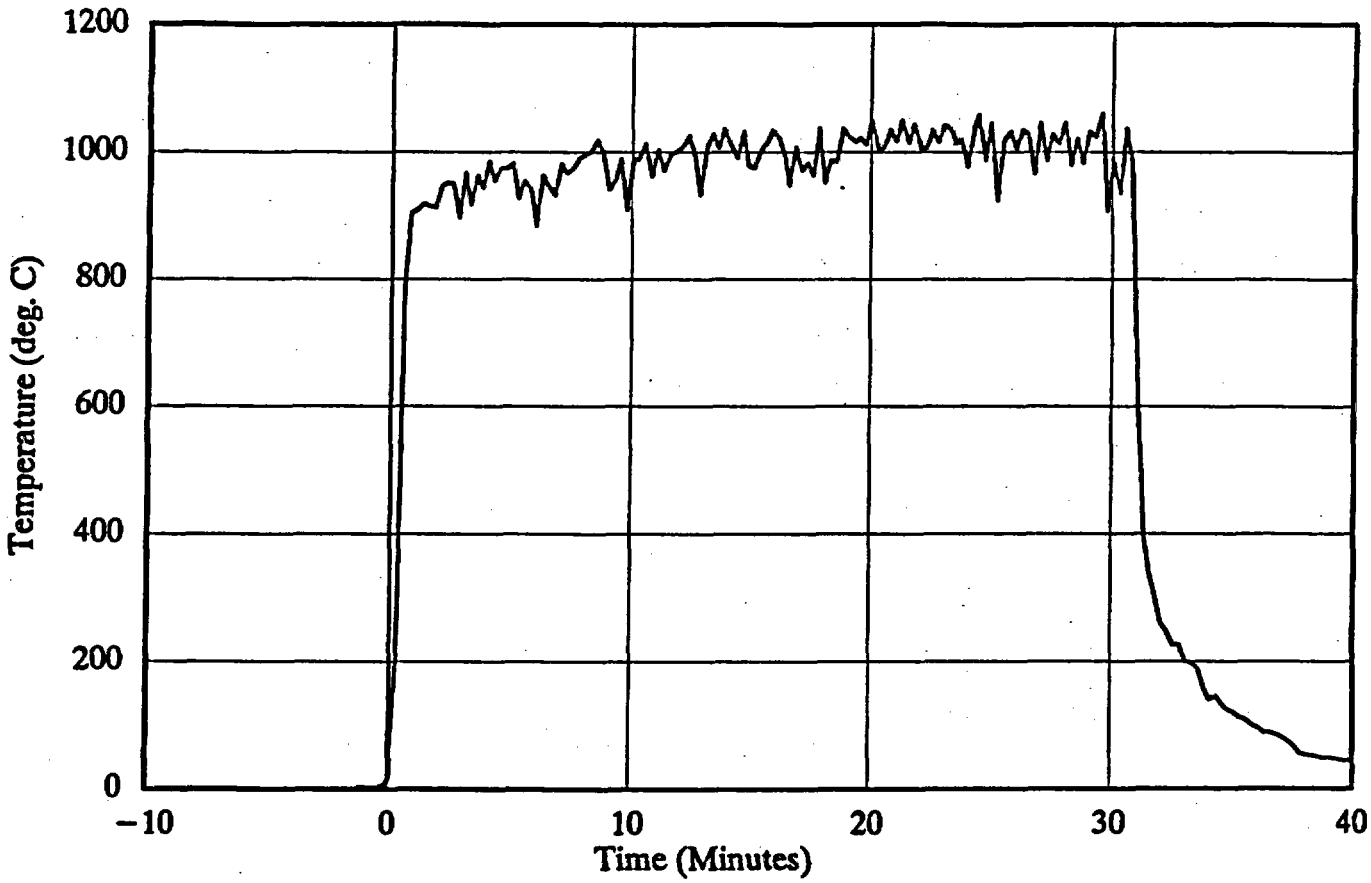

FIGURE 7.7 INSTANTANEOUS AVERAGE FLAME TEMPERATURE

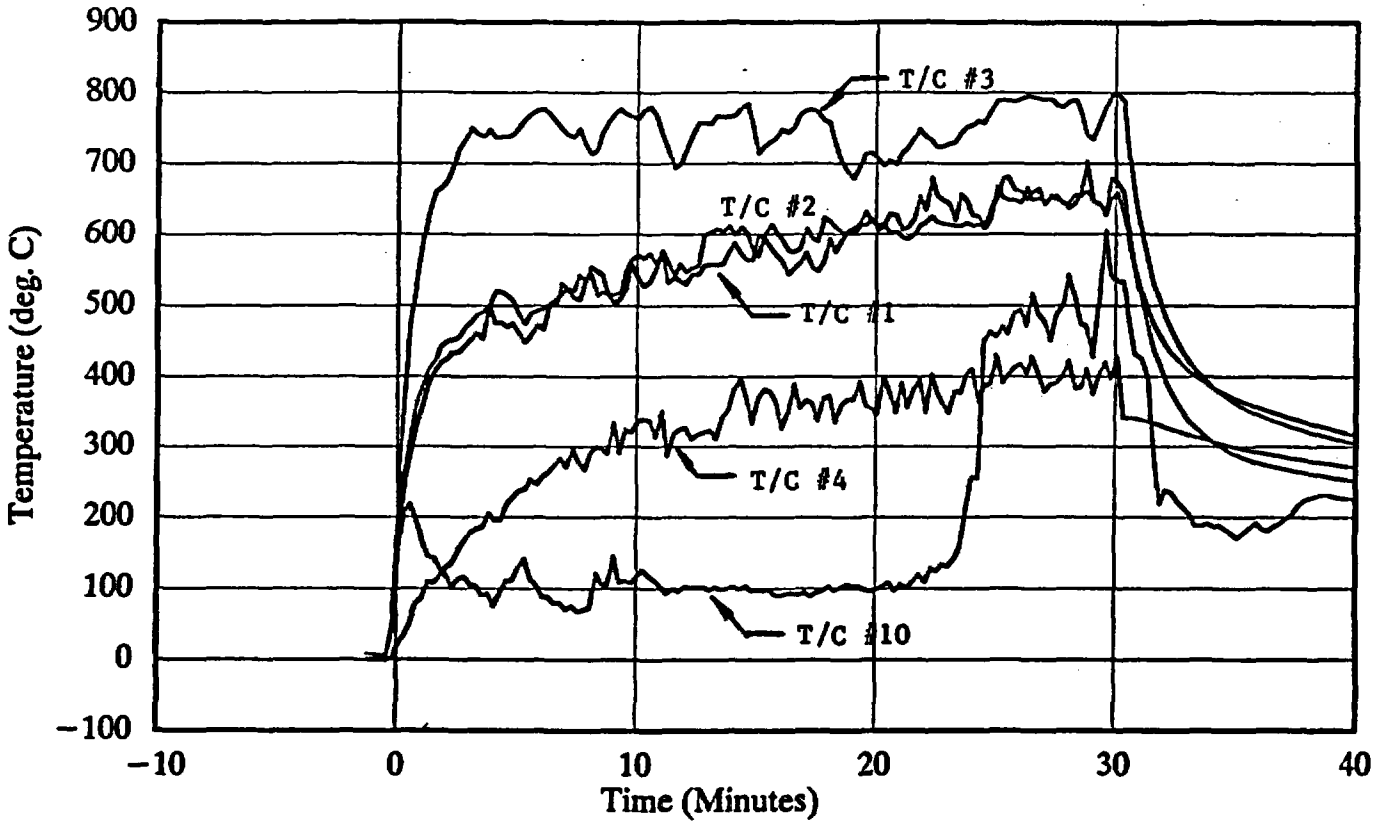

FIGURE 7.8(a) PACKAGE SURFACE TEMPERATURES FROM 0 TO 40 MINUTES

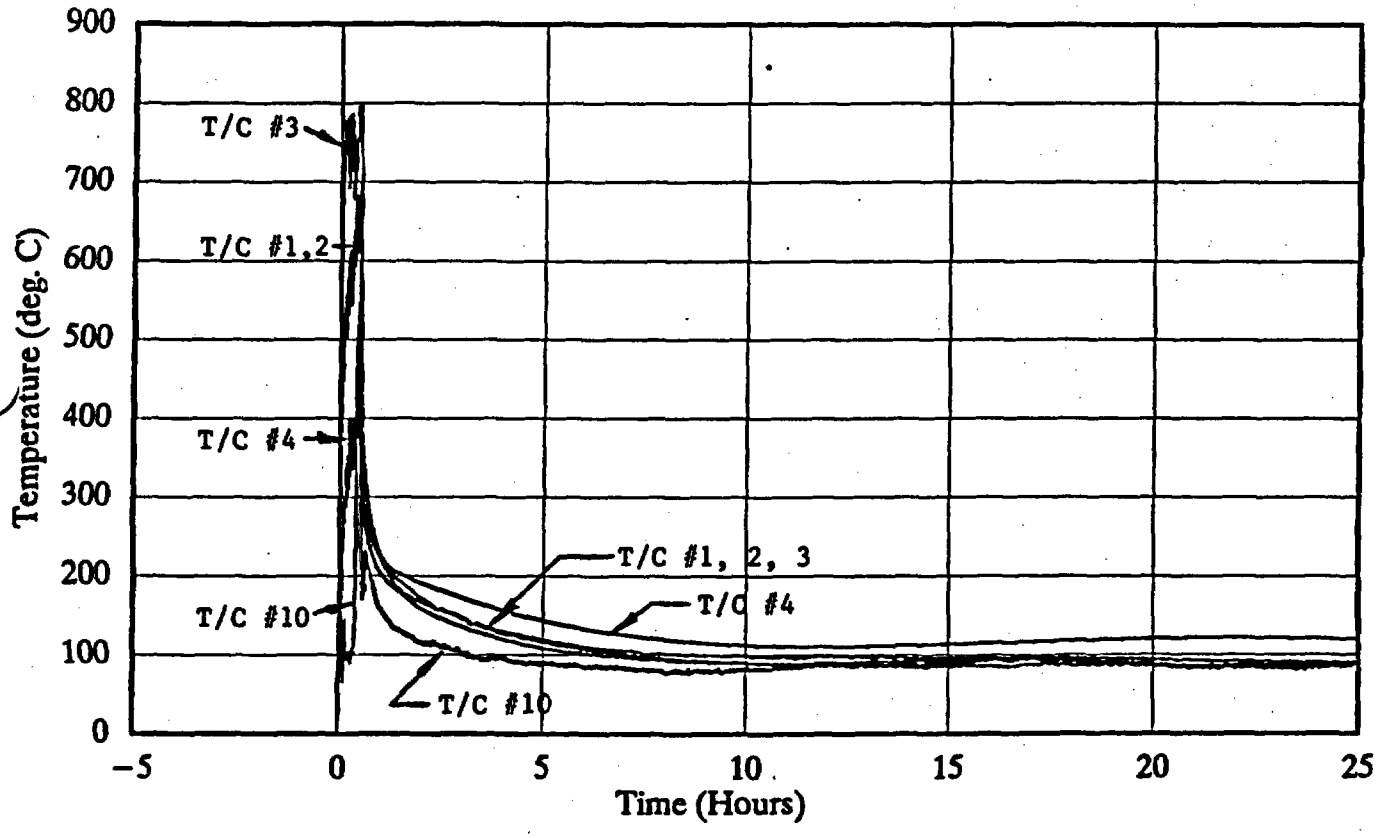

FIGURE 7.8(b) PACKAGE SURFACE TEMPERATURES FROM 0 TO 25 HOURS

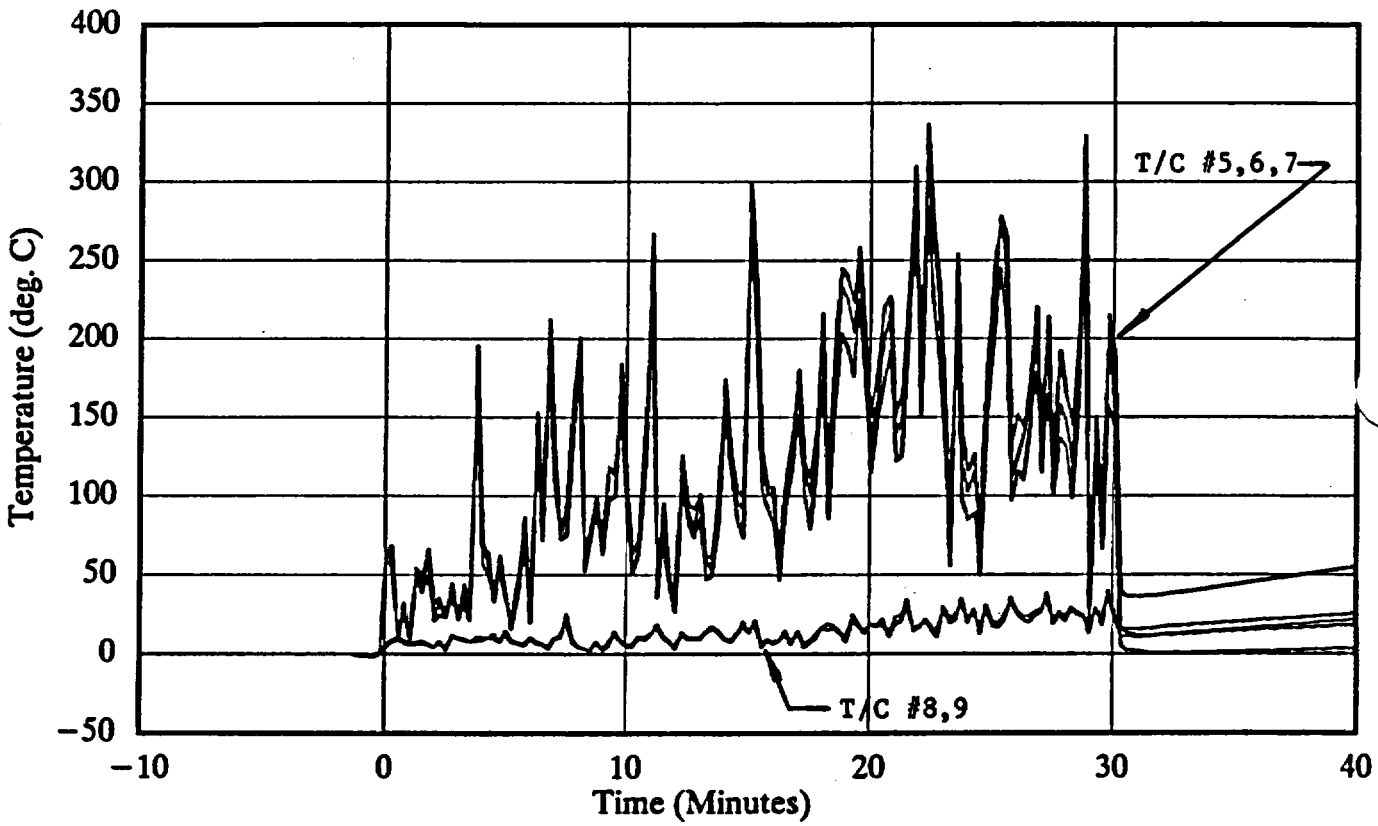

FIGURE 7.9 INSTANTANEOUS INTERNAL PACKAGE TEMPERATURES: 0 TO 30 MINUTES

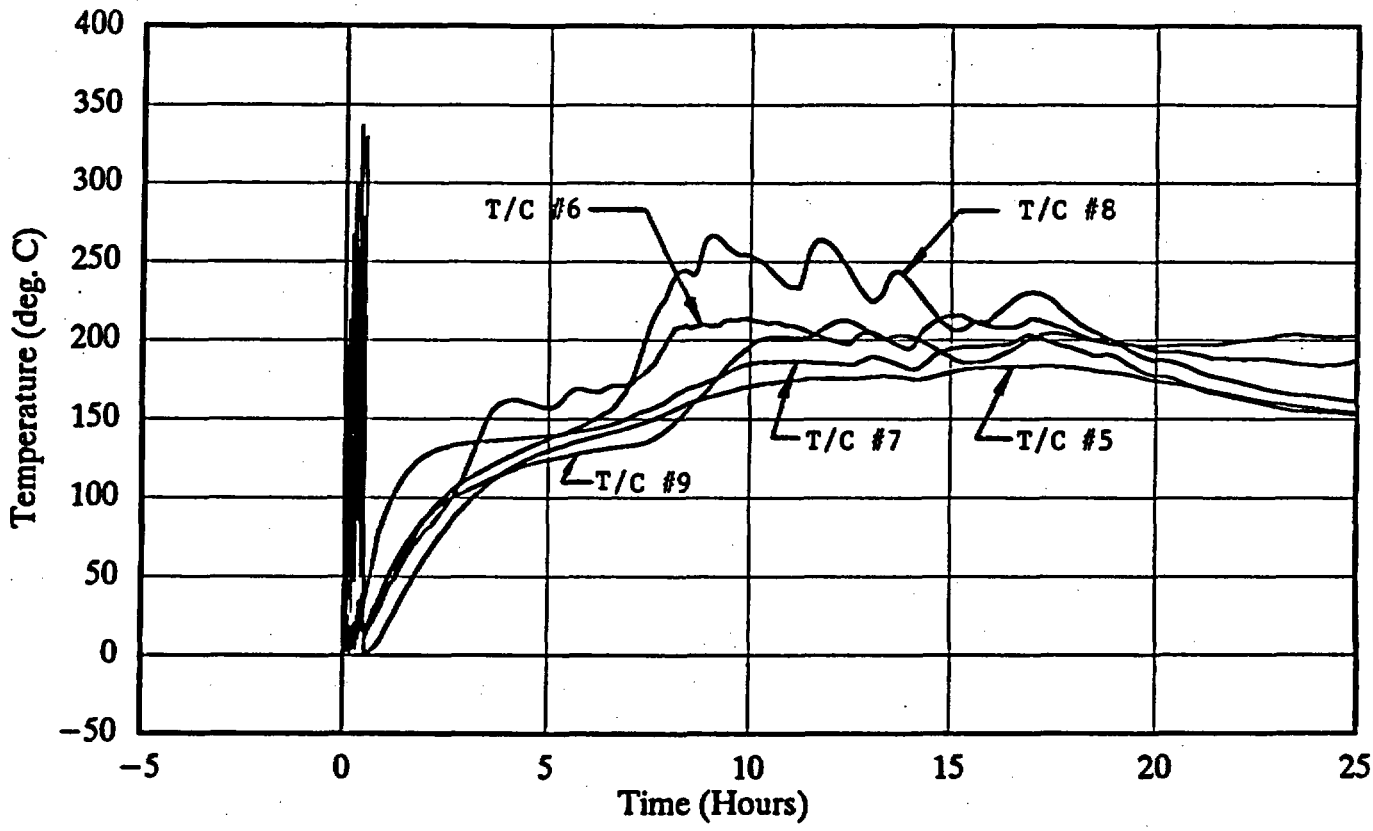

FIGURE 7.10 INSTANTANEOUS INTERNAL PACKAGE TEMPERATURES: 0 TO 25 HOURS

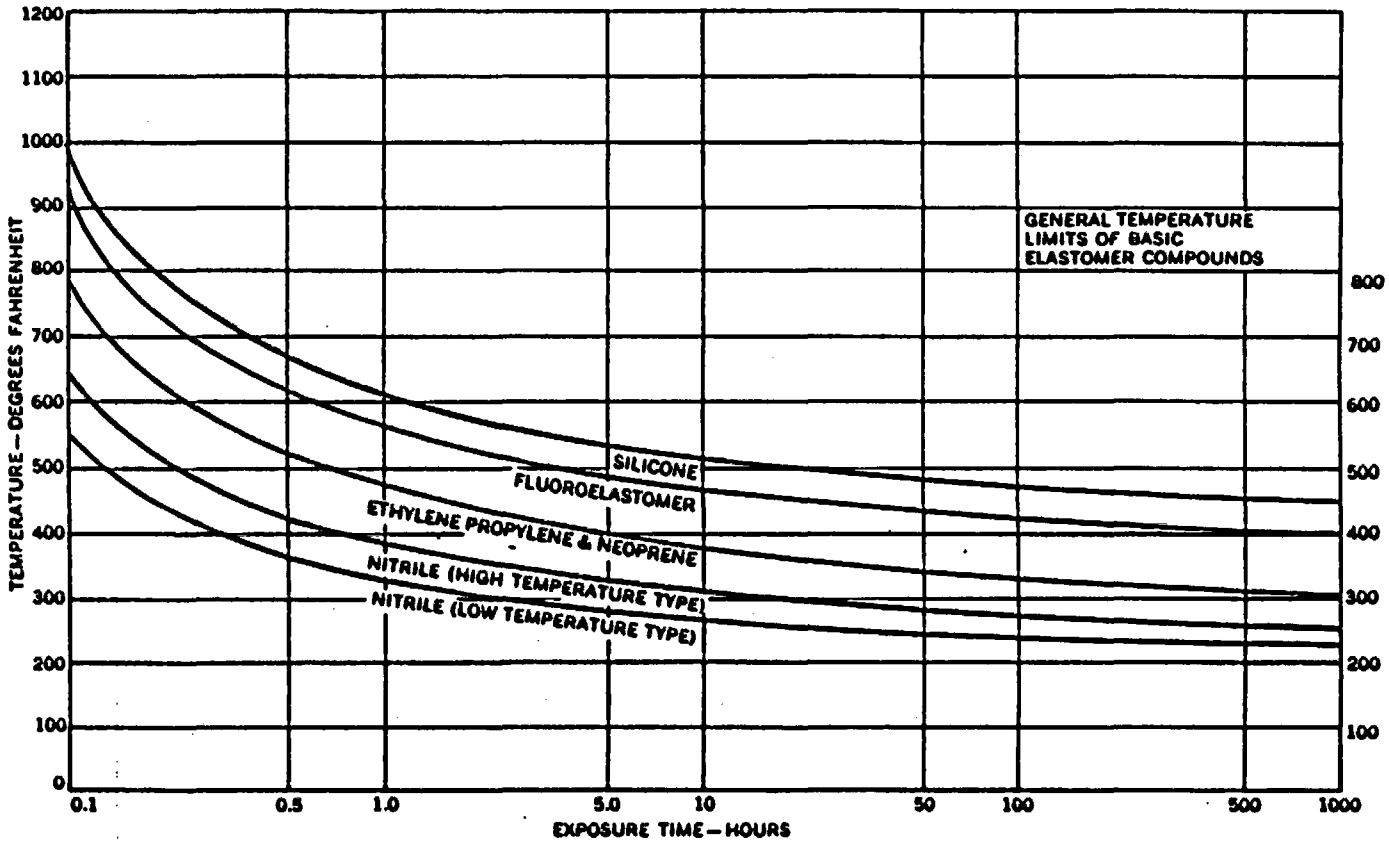

Figure 7.11 GENERAL TEMPERATURE LIMITS OF BASIC ELASOMER COMPOUNDS (From Figure A3-6 of Ref[illegible] 24)

8.0 CONTAINMENT EVALUATION

8.1 General

The package containment system consists of:

- the main flask body
- the front closure flange
- the front valve/tubing assembly
- the rear closure flange, and
- the rear cover plate.

The closure flanges and rear cover plate are sealed with two O-rings: the inner O-ring is ethylene propylene and the outer O-ring is fluorocarbon. Each closure flange and rear cover plate contains a port for leakage testing the space between the O-rings after assembly and prior to shipment. The valve assembly also has a front cover plate which contains a single fluorocarbon O-ring and a port to facilitate leakage testing.

The design criteria for containment of the radioactive contents are,

a) under normal conditions of transport, the package shall restrict the loss of radioactive contents to not more than 10^{-6} A_2 per hour, and,

b) under accident conditions of transport, the package shall restrict the accumulated loss of radioactive contents in a period of one week to not more than 10 A_2 for Kr-85 and not more than A_2 for all other radionuclides.

Because radioactive material could not be used during the prototype test program, the containment analyses are based on measured gaseous leakage rates and consequently Reference 19 is used extensively.

Reference 19 defines "leaktight" as a leakage rate of 1×10^{-8} Pa.m³/s (1×10^{-7} atm cm³/s) or less based on dry air at 25°C and for a pressure differential of 101.3 kPa against a vacuum of 1 kPa or less. According to Reference 19, this definition applies to radioactive material in any physical form, e.g. gas, liquid or solid, and, if it has been demonstrated that the containment system is "leaktight", the system is considered to comply with the regulatory containment requirements. This approach greatly simplifies demonstration of compliance for this package because the package has been designed for multipurpose use and it is difficult to provide an accurate description of all the radionuclides that will be transported. However, an assessment has been made in Appendix C, to show that the use of the "leaktight" concept is appropriate.

8.2 Potential Release Scenarios and Considerations

Shipments of irradiated power reactor channel tube sections or irradiated test specimens will consist of components in solid form and so, the radioactive material that will be potentially available for release will be

in particulate form. Usually only a few radionuclides will be present and in most cases the predominant radionuclide will be Zr-95. As a representative case, Appendix C evaluates a containment analysis that is based on a pressure tube section that is made of Zr-2.5 wt% Nb metal and has the maximum permissible activity of 3000 A_2 or 2700 TBq. In this analysis, it was determined that the containment requirements were much more restrictive for normal conditions of transport than for accident conditions of transport. Further, it was calculated that the required equivalent air leakage rate would range between 1.16×10^{-6} and 4.81×10^{-2} $Pa.m^3/s$ for normal conditions of transport. These values are considered to represent extreme cases and a realistic value is considered to be midway between the extremes or about 1×10^{-4} $Pa.m^3/s$. The conclusion is that the use of the concept leaktight, i.e. 1×10^{-8} $Pa.m^3/s$ is valid.

A containment analysis for irradiated CANDU fuel bundles and elements is more complex. The representative case that is given in Appendix C is based on the analytical approach that is used in the USA. This approach considers four sources of release,

a) the residual contamination from the storage pool,

b) the fuel element zirconium alloy sheaths,

c) "crud" which includes such things as corrosion and activation products from the reactor coolant system which adhere to the fuel element surfaces, and,

d) the irradiated uranium which is a source of fission products and actinides.

Source a) is of secondary significance and can be disregarded. The analysis highlights many considerations and results which are included in Section C.4. The main conclusions are:

a) the analysis is based on the use of release fractions for which data is limited and variable;

b) the containment requirements for the radioactive gases is no more restrictive than that for the radionuclides in particulate form;

c) the containment requirements for normal conditions of transport are more restrictive than those for accident conditions of transport;

d) for normal conditions of transport the required equivalent air leakage rate ranges between 1×10^{-4} and 1×10^{-5} $Pa.m^3/s$ and under the most pessimistic assumptions the minimum value is about 1×10^{-6} $Pa.m^3/s$;

e) the use of the concept leaktight, i.e. 1×10^{-8} $Pa.m^3/s$ is valid; and

f) it is important to ensure that the package cavity is vacuum dried whenever it has been loaded in a storage pool.

8.3 Helium Leakage Test Results on Prototype Package

The helium leakage test results on the prototype package are given in Reference A11. The following is a summary of those procedures and the test results.

1) Figure 8.1 shows the test set-up that was used in all cases. This method allows the simultaneous testing of,

   a) the bellows seal valve assembly,

   b) the inner O-ring on the front closure plate,

   c) the inner O-ring on the rear closure plate, and

   d) the inner O-ring on the rear cover plate.

2) the helium mass spectrometer leak detector had a test sensitivity of 1×10^{-9} Pa.m^3/s capable of measuring helium leaks to less than 1×10^{-8} Pa.m^3/s.

3) The test gas was a mixture of air and helium. The partial pressure of air was approximately 20×10^3 Pa and that of the helium was approximately 80×10^3 Pa. The duration of each leak test was not less than five minutes.

4) After the prototype was assembled in preparation for the impact tests, no helium leakage was detected that was equal to or greater than 5×10^{-9} Pa.m^3/s.

5) After a 0.9 m vertical drop onto the rear impact limiter, a 1 m vertical puncture drop onto the rear impact limiter, a 9 m vertical end drop onto the front impact limiter and a 1 m vertical puncture drop onto the front impact limiter, no helium leakage was detected that was equal to or greater than 5×10^{-9} Pa.m^3/s.

6) The package was disassembled for inspection and after re-assembly, no helium leakage was detected that was equal to or greater than 4×10^{-9} Pa.m^3/s.

7) After a 9 m side drop test, a 9 m oblique drop test (cavity axis at about 61° from horizontal) and the thermal test, no helium leakage was detected that was equal to or greater than 3.5×10^{-9} Pa.m^3/s.

8) After disassembly, the O-rings were inspected. Visually, the O-rings were in good condition with the exception of the valve cover plate O-ring. In one location, the valve cover plate O-ring had degraded. [NOTE: This O-ring is <u>not</u> required for containment. The purpose of this O-ring is to facilitate leakage testing of the valve/tubing assembly.] Hardness measurements after testing were as follows:

	Fluorocarbon	Ethylene Propylene
Front Flange	72/73.5	78/82
Rear Flange	71/72.5	80/83
Valve Cover Plate	69/71.5	Not Applicable
Rear Cover Plate	72/73.5	78/82
Manufacturer's Specification	75	80

9) The PCTFE (polychlorotrifluoroethylene), "KEL-F" stem insert on the valve had melted as a result of the fire test; however, containment was still maintained by the fluorocarbon O-ring in the Cajon VCO union/blind nut arrangement.
[NOTE: As a result of the thermal test, the specification for the valve stem insert was changed from "KEL-F" to Stellite with a temperature rating of 315°C].

The impact and thermal tests on a prototype demonstrated that the package will maintain an equivalent air leakage rate of 1×10^{-8} Pa.m³/s or better; therefore, the package is considered to be leaktight and satisfies regulatory containment requirements.

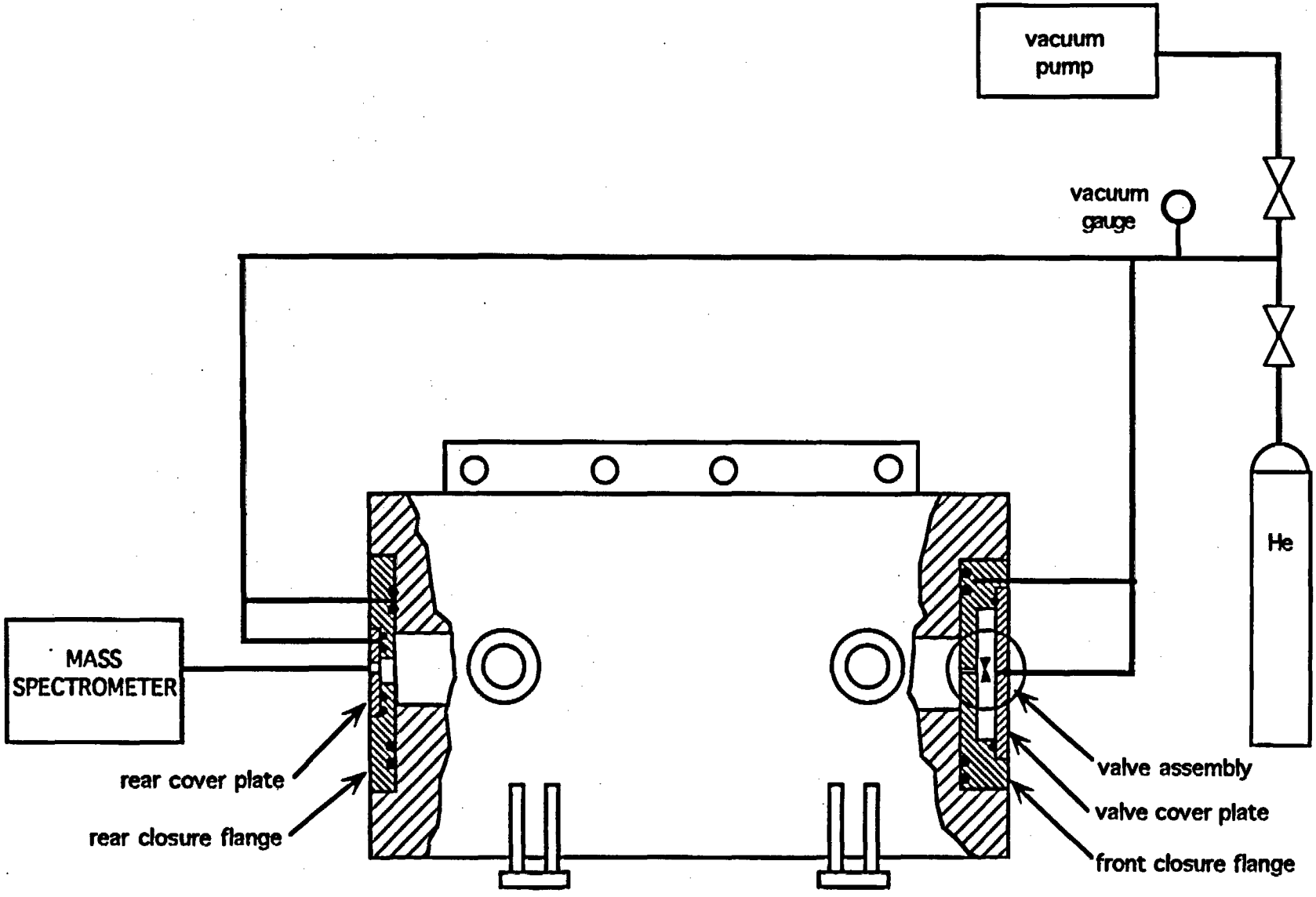

FIGURE 8.1 HELIUM LEAK TEST SET-UP

9.0 SHIELDING EVALUATION

9.1 Summary

The shielding requirements for the package will be controlled by the radiation levels from the irradiated fuel rather than the irradiated power reactor channel tube sections or the test specimens.

Table 4.1 summarizes the calculated results and the regulatory requirements. For irradiated CANDU fuel, only gamma radiation has been considered because radiation levels from neutron sources are not significant below burnups of 1730 GJ/kg U, Reference 29. For a maximum burn-up of 1150 GJ/kg U, the effect of neutron radiation would increase the the total radiation level by 15 to 23% in the radial direction.

The gamma radiation levels for routine, normal and accident conditions of transport are the same because the prototype test results showed that the package shielding properties will not be affected by the prescribed impact and thermal tests.

The results show that the package design complies with the regulatory requirements.

9.2 Shielding Description

Gamma shielding in the radial direction is provided by the main stainless steel body with a radial thickness of approximately 219 mm (8.625 in.) and a cylindrical lead insert. Because the drawer is square, the lead thickness varies from a minimum of 30 mm (1.167 in.) to a maximum 65 mm (2.563 in.).

The drawer with 279 mm (11 in.) stainless steel plugs at each end together with the sealing and support flanges provide the necessary gamma shielding in the axial direction. The impact limiters do not provide any significant shielding and are neglected from the analysis.

Neutron shielding is not required for this packaging.

9.3 Source Specification

The packaging is designed to transport irradiated CANDU fuel or irradiated reactor components or irradiated test specimens.

For the purposes of this shielding analysis an irradiated natural uranium dioxide CANDU fuel bundle has been considered. The reference design is a Pickering fuel bundle with the following characteristics:

Burn-up	-	1150 GJ/kg of initial uranium
Cooling time	-	180 days
Uranium mass	-	19.86 kg

It should be noted that the average bundle burnup for CANDU fuel is 650 GJ/kg U.

TABLE 9.1 PACKAGE RADIATION LIMITS FOR AN IRRADIATED CANDU FUEL BUNDLE WITH A BURNUP OF 1150 GJ/kg U AND 180 DAYS COOLING

CONDITION OF TRANSPORT	CONTACT WITH PACKAGE		1M FROM PACKAGE SURFACE		AT VEHICLE OUTER SURFACES	2M FROM OUTER LATERAL SURFACES
	Radial mSv/h	Axial mSv/h	Radial mSv/h	Axial mSv/h	mSv/h	mSv/h
Routine						
• Calculation	0.321	0.091	0.043	0.008	0.048*	0.008*
• Non Exclusive Use Requirements	2.0	2.0	0.1	0.1	---	---
• Exclusive Use Requirements	10.0	10.0	---	---	2.0	0.1
Normal						
• Calculation	0.321	0.091	0.043	0.008		
• Non Exclusive Use Requirements	2.4	2.4	---	---		
• Exclusive Use Requirements	12.0	12.0	---	---		
Accident						
• Calculation	0.321	0.091	0.043	0.008		
• Non Exclusive Use Requirements	---	---	10.0	10.0		
• Exclusive Use Requirements	---	---	10.0	10.0		

* Radial dose rates for a vehicle that is 2.6 metres wide

Tables 2 and 3 of Reference 23 give activity and mass of individual radioisotopes for a burn-up of 1150 GJ/kg U and a decay period of 0.5 years. The data was generated by computer program CANIGEN which is a modified version of General Electric's ORIGEN. The natural uranium in the UO_2 fuel pellets was defined as having the following isotope composition:

U-234	0.0054 wt.%
U-235	0.7110 wt.%
U-238	99.2836 wt.%

Based on this data the total activity will be approximately 1380 TBq (37,300 Curies).

9.3.1 Gamma Source

The photon release rates after 0.5 years cooling from the irradiated fuel with the given isotopic composition were calculated by CANIGEN for the following sources.

(a) Fission Products

Fission products are defined as those isotopes which are either formed directly in fission, or are produced by subsequent radioactive decay or neutron capture by an isotope formed directly in fission. The photon spectrum from fission products is given in Table 9.2

Table 9.2
Fission Product Photon Spectrum

Mean Energy (MeV)	Photons/sec per kg of Initial Uranium
0.30	3.611 E + 12
0.63	2.285 E + 13
1.10	7.041 E + 11
1.55	1.625 E + 11
1.99	1.221 E + 11
2.38	1.565 E + 10
2.75	1.200 E + 09
3.20	3.791 E + 07
	TOTAL 2.747 E + 13

(b) Actinides

The actinide group is strictly comprised of all those isotopes above and including actinum in the periodic table. It includes all the heavy elements initially in the fuel (uranium) and those that are formed by a combination of neutron capture and radioactive decay in these heavy elements.

In CANIGEN, the daughter products of these isotopes are also grouped under this classification. The photon spectrum for the actinides are given in Table 9.3.

TABLE 9.3
Actinides Photon Spectrum

Mean Energy (MeV)	Photons/sec per kg initial uranium
0.03	7.072 E + 07
0.04	3.977 E + 09
0.06	8.426 E + 08
0.10	2.262 E + 07
0.15	5.404 E + 07
0.20	4.008 E + 07
0.30	2.481 E + 07
0.63	1.125 E + 08
1.10	2.108 E + 07
1.55	6.211 E + 01
1.99	1.562 E + 01
2.38	6.445 E + 00
2.75	5.230 E + 02
	TOTAL 5.166 E + 09

The total photon source for both fission products and actinides is given in Table 9.4.

Neutron activiation of the Zircaloy-4 fuel sheath and structural components have been neglected because the activity of these components is insignificant compared to the total activity of the fission products.

Table 9.4
Total Photon Spectrum

Mean Energy (MeV)	Photons/sec per kg initial uranium
0.03	7.072 E + 07
0.04	3.977 E + 09
0.06	8.426 E + 08
0.10	2.262 E + 07
0.15	5.404 E + 07
0.20	4.008 E + 07
0.30	3.616 E + 12
0.63	2.285 E + 13
1.10	7.041 E + 11
1.55	1.625 E + 11
1.99	1.221 E + 11
2.38	1.565 E + 10
2.75	1.200 E + 09
3.20	3.792 E + 07
	TOTAL 2.748 E + 13

9.3.2 Neutron Source

Neutrons are produced from spontaneous fission of the transplutonium isotopes and by (α,n) reactions in which high energy α-particles emitted by the actinides react with light elements (mainly oxygen) to produce neutrons.

Though most of the transuranium elements undergo α decay and have a small probability of spontaneous fission, the buildup of these transuranium neutron sources is not significant below exposures of approximately 1730 GJ/kg U (20,000 MWD/MTU), Reference 29. Above 1730 GJ/kg U, the isotopes curium-242 and curium-244 represents a significant neutron source.

From Reference 23, the neutron emission from irradiated fuel with 6 months decay at different burnup rates is as follows:

	Neutron Emission (n/s)	
	650 GJ/kg U	1150 GJ/kg U
spontaneous fission	1.675×10^5	1.024×10^6
(α,n) reactions	7.090×10^4	2.989×10^5
TOTAL	2.384×10^5	1.323×10^6

The highest neutron source (spontaneous fission) is curium-242 which represents 60 to 70% of the total neutron emission rate depending on the burnup.

9.4 Shield Model Description

9.4.1 Normal Conditions of Transport

(a) Radial Model

The model used for gamma shielding analysis is shown in Figure 9.1(a). In this configuration, the source was modelled as a cylinder with a homogeneous mixture of UO_2, and zirconium. The source was located in the centre of the package cavity. The shields were modelled as cylindrical shells. All stainless steel components such as the drawer and shield insert cladding were lumped with the main flask body as listed in Table 9.5.

Table 9.5
Steel Shielding Thicknesses

Component	Thickness (mm)
Flask	219.6
Insert outer shell	7.94
Insert inner shell	9.53
Drawer (cover)	3.18
TOTAL	240.25

The perforated stainless steel fuel can was neglected from the analyses.

The shield insert was also modelled as a cylindrical shell. An equivalent inner diameter was calculated to maintain the same cross-sectional area. The equivalent radial thickness used for the lead was 54.4 mm.

A comparison between the shielding model and package design is shown in Figure 9.2.

(b) Axial Model

The axial model used for gamma shielding is shown in Figure 9.1(b). As with the radial configuration, the source was also modelled as a cylinder with a homogeneous mixture of UO_2, and zirconium. The shielded drawer and closure/support flanges were modelled as steel slabs. The total shield thickness used was 330 mm of stainless steel. The valve cover plate and the rear cover plate were neglected from the analysis as were the impact limiters.

9.4.2 Accident Conditions of Transport

Under accident conditions, no loss of shielding occurred as a result of the prototype tests. There will be no change in radial or axial shielding configurations. The configuration of fuel elements may change under impact conditions, which may change the self-shielding of the elements, however, there will be negligible effect on the radiation levels. Therefore the radiation level, at 1 metre under accident conditions will be approximately the same as that for normal conditions of transport which is less than 10 mSv/h requirement.

9.5 Material Densities

The material densities used for gamma shielding analyses are given in Table 9.6 and Table 9.7. The fuel bundle is asssumed to be an homogenized mixture over a volume of 4.076×10^{-3} m^3.

Table 9.6
Fuel Bundle Density

	Density (kg/m^3)
Fuel Bundle	
UO_2 (91.7%)	5527
Zr (8.39%)	500
Air (> 1%)	4.91
	TOTAL 6031.9

Table 9.7
Shielding Density

		Density (kg/m^3)
Stainless Steel (304)		
	Fe (74%)	5824
	Ni (8%)	712
	Cr (18%)	1294
	TOTAL	7830
Lead	Pb	11300
Air Gap	Air	1.22

9.6 Gamma Shielding Evaluation

The gamma radiation levels were calculated at the package surface and 1 metre from the surface for axial and radial direction using MICROSHIELD Version 3.12 Reference 30.

MICROSHIELD is a point kernal code based on ISOSHLD II. Dose build-up factors using the geometric progression method are used to account for secondary radiation as a result of Compton scattering. The most predominant shield material, stainless steel, is used to calculate dose build-up factors.

Flux-to-dose rate conversion factors are given in Table 9.8.

The calculated results, which are given in Table 9.1, show that the package provides adequate gamma shielding in radial and axial directions for all conditions of transport.

Table 9.8
Flux-to-Dose Conversion Factors

Energy (MeV)	Dose Conversion Factor mSv/h per photon/cm² sec
0.100	1.500 E - 6
0.150	2.592 E - 6
0.250	4.900 E - 6
0.350	7.210 E - 6
0.475	9.690 E - 6
0.650	1.352 E - 5
0.825	1.650 E - 5
1.000	1.930 E - 5
1.225	2.254 E - 5
1.475	2.596 E - 5
1.700	2.907 E - 5
1.900	3.154 E - 5
2.100	3.360 E - 5
2.300	3.542 E - 5
2.500	3.800 E - 5
2.700	3.996 E - 5
3.000	4.290 E - 5
3.600	4.752 E - 5
4.500	5.445 E - 5
5.500	6.187 E - 5
6.600	7.062 E - 5
8.000	8.080 E - 5
9.000	8.704 E - 5
10.000	9.243 E - 5

9.7 Neutron Shielding Evaluation

The following simplified analysis calculates the neutron dose rates in the radial direction. In the analysis, the following assumptions were made:

i) because there is no hydrogenous shielding, neutrons are not attenuated;

ii) there is no self-absorption of the source; and

iii) neutron multiplication is neglected.

For a cylindrical source, the radial dose rate at the perpendicular bisection can be given by the following equation (Reference 31):

$$D = c \frac{So}{2\pi Ld} \tan^{-1} \frac{L}{2d}$$

where,

So = neutron emission rate, n/s

d = radial distance from the source axis, cm

L = length of source, cm

c = conversion factor, $\frac{mrem/h}{n/s.cm^2}$

Substituting the following values at the surface of the package and at 1 metre from the surface,

So = 1.323×10^6 n/s (from Reference 23, for a burnup of 1150 GJ/kg U)

d = 38.1 cm (on contact)
= 138.1 cm (1 m from surface)

L = 49.53 cm

c = 0.155 $\frac{mrem/h}{n/s.cm^2}$ (from Reference 32 App. E., integrated over a fission neutron energy spectrum and a Quality Factor = 10)

would produce the following neutron dose rate:

D contact = 10.0 mrem/h (0.1 mSv/hr)

D 1m = 0.85 mrem/h (0.0085 mSv/hr)

Compared with the calculation gamma radiation levels given in Table 9.1, the increase in total radiation levels including neutron radiation will be approximate 31% on contact and 20% at 1 metre from the radial surface of the package.

For normal burnup of CANDU fuel of approximately 650 GJ/kg U (180 MWD/kg U), the neutron source will decrease to 2.384×10^5 n/s. As a result, the neutron dose rate will decrease accordingly by a factor of five.

9.8 Alternative Shielding Configurations

9.8.1 Axial Shielding Plugs

In cases where the drawer is not installed, axial shielding plugs can be used at each end of the shield insert to provide the required axial gamma shielding. The 178 mm (7 inches) long plugs are fabricated from poured lead and clad in stainless steel. As described in Section 9.4.1(b), if the 279 mm (11 inches) stainless steel ends of the drawer were replaced with 162 mm (6.375 inches) of lead (neglecting the stainless steel cladding), the package radiation level in the axial direction would be as follows:

on contact - 0.165 mSv/h
at 1 metre - 0.009 mSv/h

These levels are below the radiation limits specified in Table 9.1.

9.8.2 Shield Insert No. 2

Shield Insert No. 2 can be used in place of the drawer and corresponding shield insert without compromising the gamma shielding integrity of the package. The cylindrical insert is fabricated from poured lead and clad in stainless steel. The insert has a 178 mm (7 inches) inner diameter and a 321 mm (12.625 inches) outer diameter with 57 mm (2.25 inches) of lead.

The drain end of the insert has 140 mm (5.5 inches) of lead and 35 mm (1.375 inches) of steel to provide axial shielding. The removeable top plug of the insert has 146 mm (5.750 inches) of lead and 25 mm (1 inch) of steel for axial shielding at the front closure end.

The radial and axial gamma shielding models are shown in Figures 9.3 and 9.4 respectively.

The radiation levels for a 6 month cooled CANDU fuel bundle with a burnup of 1150 GJ/kg U is shown in Table 9.9.

TABLE 9.9 Radiation Levels with Shield Insert No. 2

Location	Radial mSv/h	Axial mSv/h
Contact with Package	0.348	0.150
1m from Package Surface	0.046	0.009

The results are similar to that shown in Table 9.1 and below the allowable limits.

9.8.3 Shield Insert No. 3

Shield insert no.3 is designed to transport CANDU pressure tube specimens from the Wolsung-1 reactor. Three - 30" lengths of 4.46" diameter pressure tube fit into a basket 10-3/8" outside diameter. This basket fits into the 10½" inside diameter of the insert.

The insert radial shielding consists of 1" (25 mm) of steel. The axial shielding consist of 6" (154 mm) of lead. The lower end of the insert has a drain tube embedded in the lead.

Gamma spectroscopy measurements performed on samples of Wolsung pressure tubes (1995 Feb.) indicate the following activity.

Isotope	Activity (Ci/g)	Activity in 25 kg (Ci)
Co-60	.51 E-3	12.8
Zr-95	8.8 E-3	220
Nb-94	.38 E-3	9.5
Nb-95	20.2 E-3	505

From Microshield 4.0 the radial radiation dose level with a "smeared" source in insert no. 3 in the IMT flask is 50 mR/H (0.5 mSv/h) on contact and 9 mR/h (.09 mSv/h) at 1 m from the package.

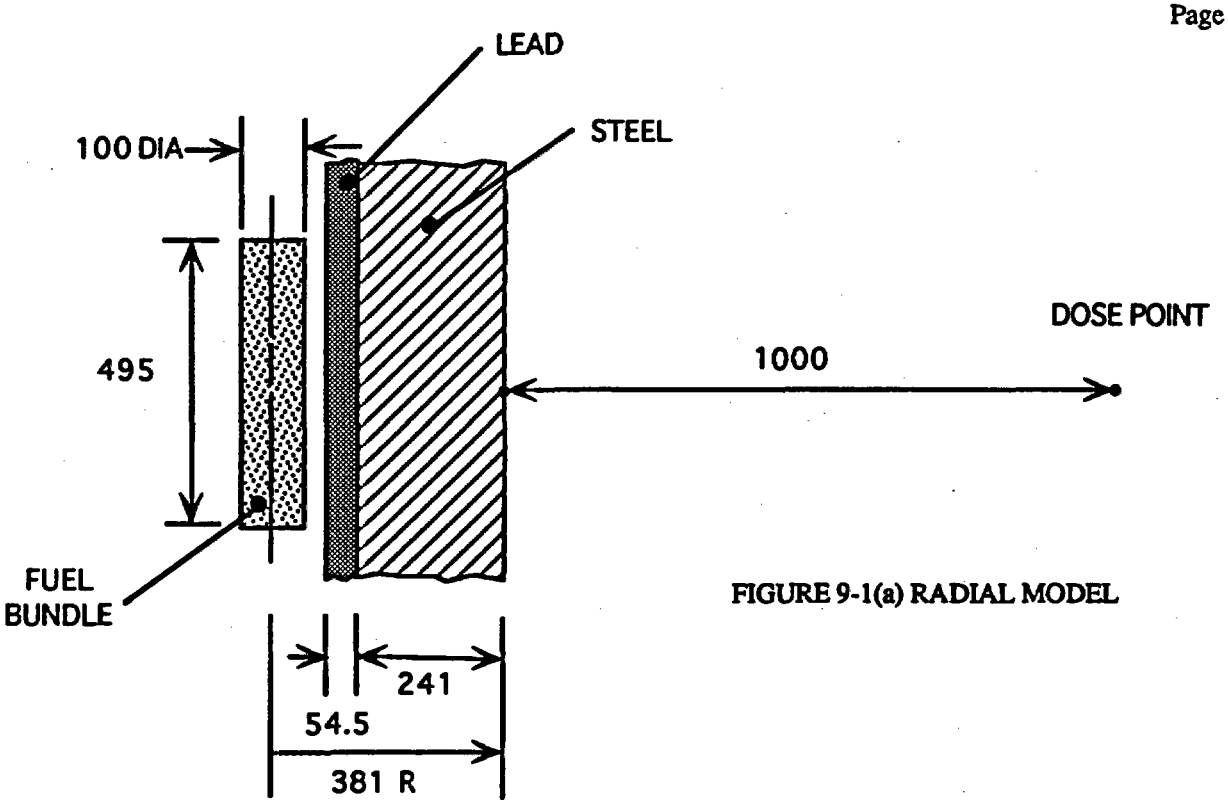

FIGURE 9-1(a) RADIAL MODEL

NOTE: All dimensions in mm

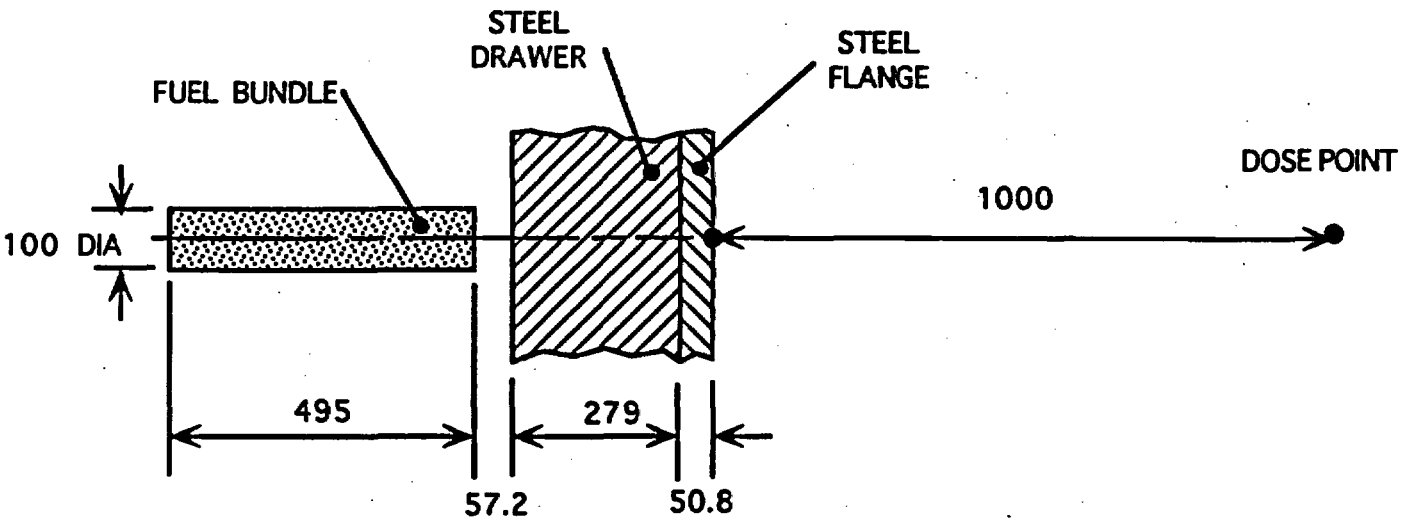

FIGURE 9-1(b) AXIAL MODEL

FIGURE 9-1 GAMMA SHIELDING MODELS

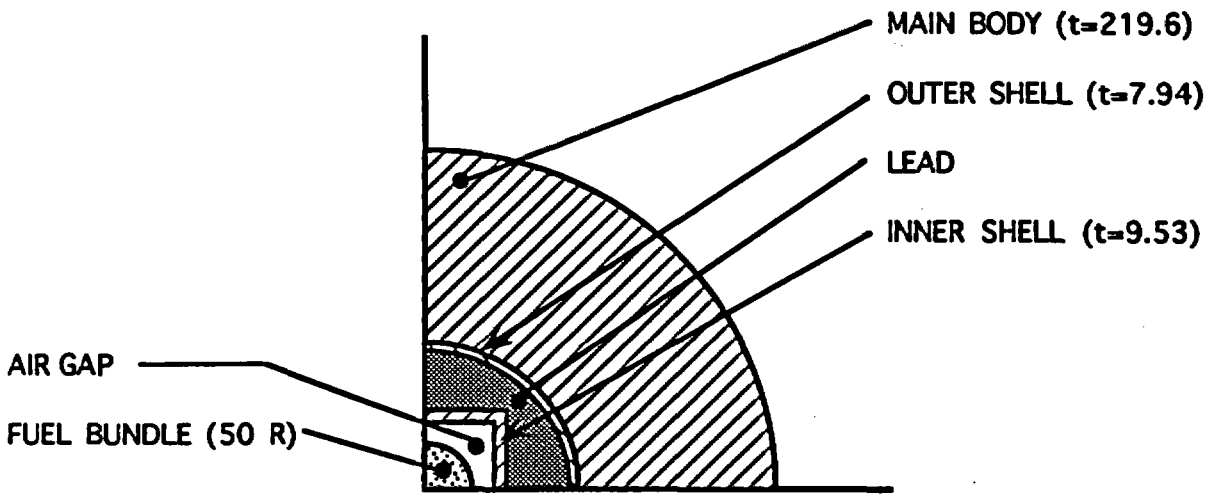

FIGURE 9-2(a) RADIAL CROSS-SECTION OF PACKAGE

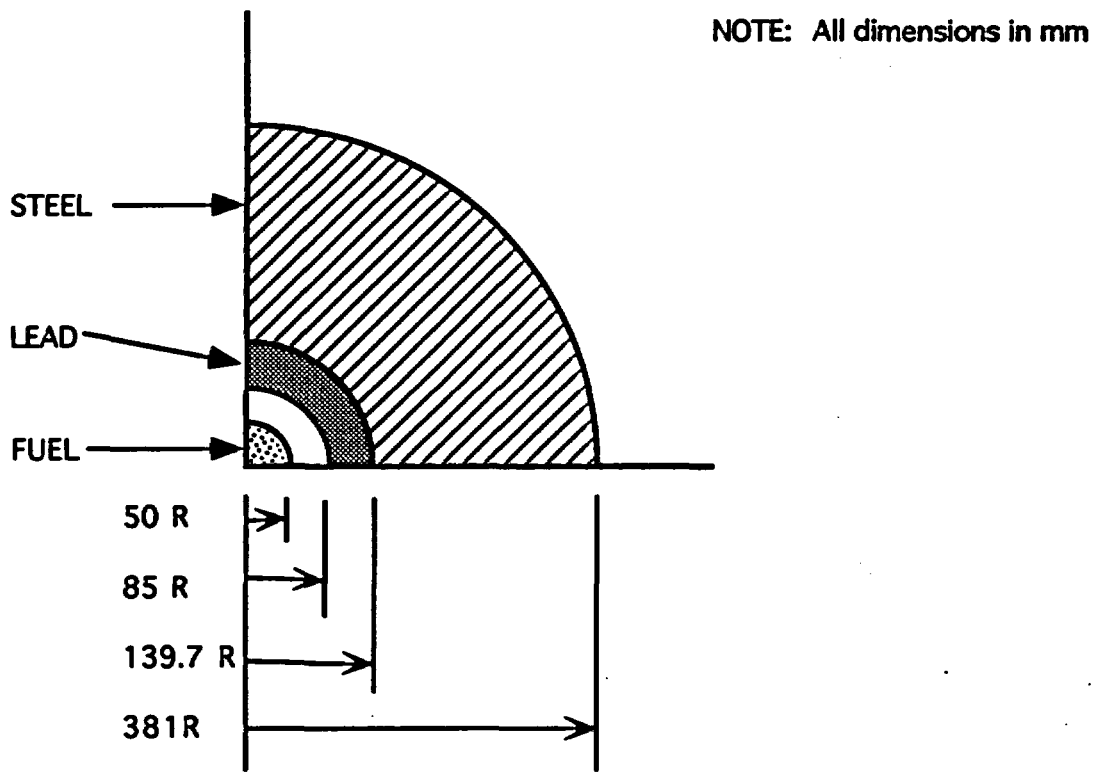

FIGURE 9-2(b) RADIAL GAMMA SHIELD MODEL

FIGURE 9-2 COMPARISON BETWEEN PACKAGE DESIGN AND RADIAL SHIELD MODEL

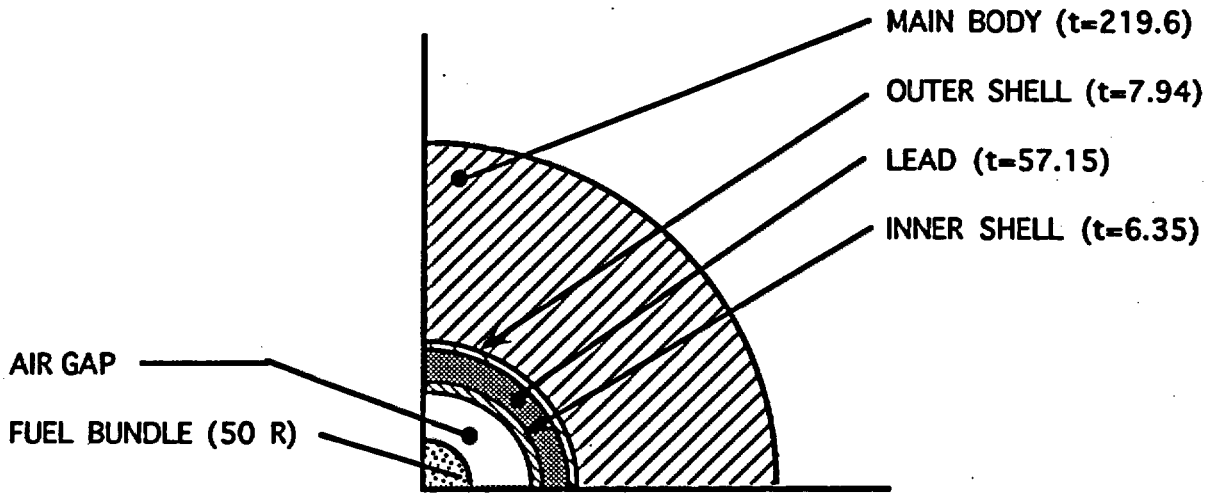

FIGURE 9-3(a) RADIAL CROSS-SECTION OF PACKAGE WITH SHIELD INSERT NO. 2

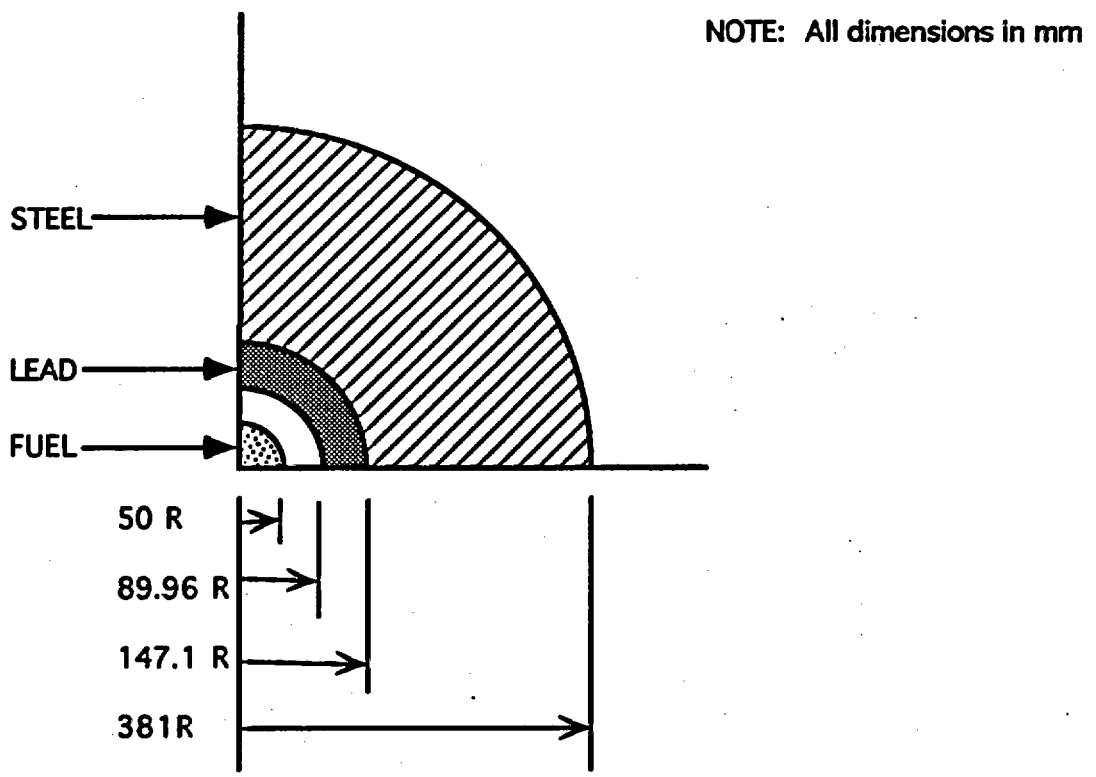

FIGURE 9-3(b) RADIAL GAMMA SHIELD MODEL

FIGURE 9-3 COMPARISON BETWEEN PACKAGE DESIGN WITH SHIELD INSERT NO. 2 AND RADIAL SHIELD MODEL

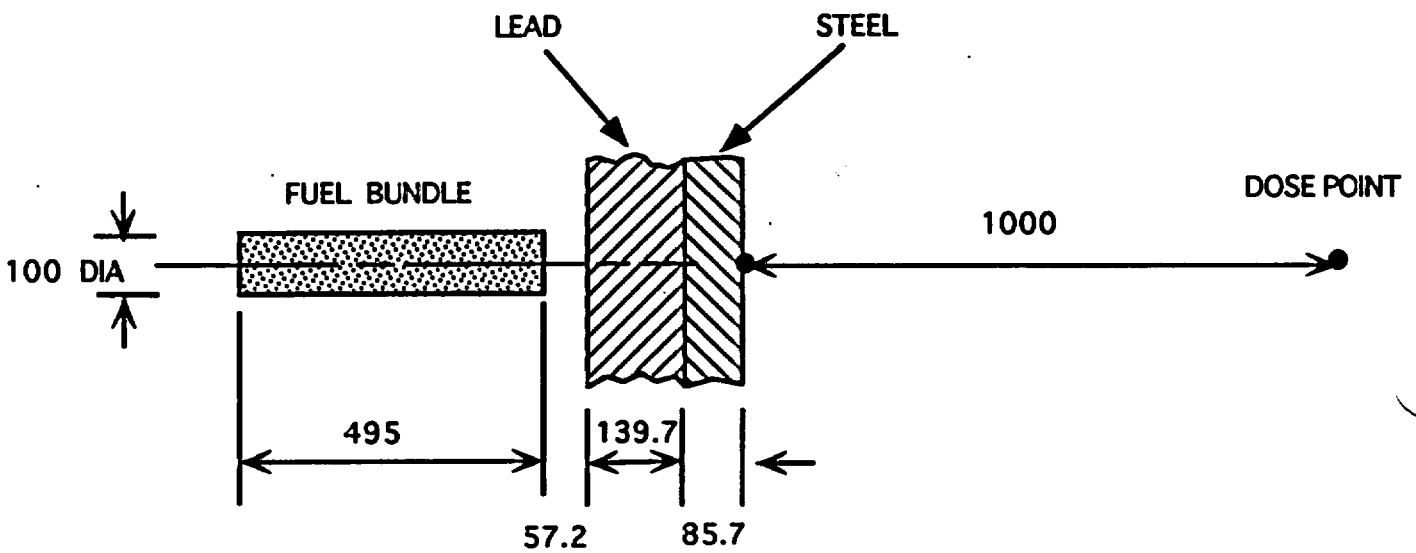

NOTE: All dimensions in mm

FIGURE 9-4 AXIAL GAMMA SHIELDING MODEL WITH SHIELD INSERT NO. 2

10.0 ASSESSMENT OF COMPLIANCE

The Atomic Energy Control Board has developed Canadian regulations, Reference 1, which permit the use of the IAEA recommendations that are contained in Safety Series No. 6, Reference 2. In this section, Sections IV, V and VII of Safety Series No. 6 will be reviewed paragraph by paragraph. Sections I, II and III are of a general nature; the package design and shipments will comply with these sections but a detailed review will not be included here. A detailed review of Section VII is not included because this section pertains to the Competent Authority and administrative requirements.

NOTE: The number in the margin corresponds to the paragraph in Safety Series No. 6.

Package Inspection Requirements

401 The design pressure of the containment system exceeds 35 kPa. Section A.3 of Appendix A shows that the containment system is designed for pressures as high as 5.37 MPa. As part of the fabrication program the containment system will be leakage tested before first shipment to ensure that the design criteria are satisfied (see Reference 8). Similarly, the gamma radiation shielding components will be checked with a calibrated source to confirm their effectiveness. The radioactive decay heat is not significant enough to warrant a check of the heat transfer characteristics of the package.

402 Reference 12, the operating procedures, describes how the requirements of this paragraph will be fulfilled.

Transport of Other Goods

403 through 406 No comment, accepted as written.

Other Dangerous Properties of Contents

407 The radioactive contents do not possess other dangerous properties such as explosiveness, flammability, pyrophoricity, chemical toxicity and corrosiveness.

Requirements and Controls for Contamination and for Leaking Packages

408 Reference 12, the operating procedures require that the non-fixed contamination on the external surfaces of the package shall not exceed the levels specified in Table III.

409 Overpacks or freight containers may be used occasionally. If they are to be used the limits in Table III will not be exceeded.

410 through 413 Reference 12, the operating procedure require compliance with these paragraphs.

414 Not applicable because the radioactive contents will be Type B quantities.

Requirements and Controls for Transport of Excepted Packages

415 through 420 Not applicable because, for the authorized radioactive contents, the package will not be designated as "Excepted".

421 No comments, accepted as written.

Requirements and Controls for Transport of LSA Material and SCO in Industrial Packages or Unpacked

422 through 427 Not applicable because the radioactive contents will be Type B quantities.

Determination of Transport Index TI

428 through 431 No comments, accepted as written

Limits on Transport Index and Radiation Level for Package and Overpacks

432 through 434 No comment, accepted as written.

Categories

435 No comment, accepted as written.

Marketing, Labelling and Placarding

436 through 439 A nameplate with the appropriate data will be applied to each packaging. Paragraph 437 is not applicable because the radioactive contents are Type B quantities.

440 through 442 The package will be labelled with two appropriately completed labels.

443 through 445 No comment, accepted as written.

Consignor's Responsibilities

446 No comment, accepted as written

447 Reference 12, the operating procedures requires that the transport documents be properly prepared.

448 through 451 The consignor's declaration will be included with the transport documents.

452 No Comment, accepted as written.

453 454 Reference 12, the operating procedures required that the appropriate information will be provided to the carrier.

455 through 459 No comment, accepted as written.

Transport

460 through 475 No comment, accepted as written.

476 477 Not applicable because the package will not be transported by post.

Storage in Transit

478 through 482 No comment, accepted as written.

Customers Operations

483 No comment, accepted as written.

Undeliverable Consignments

484 No comment, accepted as written.

Requirements for Radioactive Materials

501 through 504 Not applicable because the radioactive contents will not be designated as LSA-III or special form.

General Requirements for All Packagings and Packages

505 The package is designed with a lifting bar and trunnions so that it can be easily and safely handled and transported. The package is designed with a support frame so it can be properly secured on the conveyance during transport.

506 The lifting attachments, lifting bar and trunnions will not fail when used in the intended manner. A factor safety of 3, which should cover snatch liftings has been used in the design of the lifting attachments (see Sections 6.3.7, 6.3.8 and 6.3.9). Failure of the lifting attachments will not result in the ability of the package to meet the other requirements of the regulations.

507 Not applicable because there are no other features on the outer surface of the package that could be used to lift the package.

508 Because the external surfaces of the packaging are machined stainless steel, the package can easily be decontaminated.

509 Because the outer surface of the package is cylindrical and transported horizontally, the package will not collect or retain water.

510 Not applicable because there are no features added to the package at the time of transport.

511 Based on previous experience with the Interproject flask, the package should be capable of withstanding the effects of any acceleration, vibration or vibration resonance which may arise under routine transport conditions without deterioration in the effectiveness of the closing devices.

512 Notwithstanding the irradiation of the elastomeric seals, the structural materials of the packaging are physically and chemically compatible with each other and with the radioactive contents.

513 Under transport conditions, the valve is inaccessible which will prevent any unauthorized operation. The cavity housing the valve is sealed with a fastened cover plate. In addition, the impact limiter is installed at the end of the package over top of the valve cover plate.

514 Not applicable, the radioactive material contents do not have any other dangerous properties.

Additional Requirements for Packages Transported by Air

515 The calculated surface temperature of the packaging at an ambient temperature of 38°C (100°F) with no solar insolation is 47°C which is below the design limit of 50°C (see Section 7.4.3).

516 The elastomeric seals specified for the packaging have a temperature range of -54°C to 204°C (see Section 7.3). Therefore the integrity of the containment would not be impaired if the packaging was exposed to ambient temperatures ranging from -40°C to 55°C.

517 Not applicable because the radioactive materials is not liquid.

Requirements for Industrial Packages

518 through 523 Not applicable because the radioactive contents will be Type B quantities

Requirements for Type A Packages

524 The package is designed to meet the requirements specified in paragraphs 505-517 (see above).

525 The smallest overall external dimension of the package is not less than 10 cm.

526 A seal will be incorporated at each end of the package which will provide evidence that the package has not been opened.

527 The forces in the tiedown attachments under normal and accident conditions will not impair the ability of the package to meet the requirements of the Regulations (see Sections 6.3.7 and 6.3.9).

528 There will be no degradation of the packaging materials within the temperature range of -40°C to 70°C. The elastomeric seals have a temperature range of -54°C to 204°C (see Section 7.3).

529 The design, fabrication and manufacturing is/will be in accordance with ASME Boiler and Pressure Vessel Code (see Appendix A and Reference 8).

530 The containment system is securely closed by cap screws which cannot be opened unintentionally or by pressure which may arise within the package (see Appendix A.3.2.2 and A.3.3.2).

531 Not applicable because there is no special form radioactive material.

532 Not applicable because the containment system is not a separate unit of the package.

533 Not applicable because there is no radiolytic decomposition of liquids nor generation of gas by chemical reaction and radiolysis.

534 The containment system can retain its radioactive contents under a reduction of ambient pressure to 25 kPa.

535 The valve is a bellows seal type valve; therefore, the only leakage past the seat needs to be considered. Any leakage past the seat will be retained by the "Cajon" tube plug. The valve and associated tubing is enclosed and sealed with a cover plate together with a elastomeric O-ring.

536 Not applicable because there is no radiation shield which encloses a component of the package specified as a part of the containment system.

537 Under tests for normal conditions of transport there will be no change in shielding integrity and no loss or dispersal of the radioactive contents (see Section 6.3.2.2.).

538 Not applicable because the radioactive material is not liquid.

539 Not applicable because the radioactive material is not liquid.

540 Not applicable because the radioactive material is not gaseous.

Requirements for Type B Packages

541 The package is designed to meet requirements specified in paragraphs 505-517 and paragraphs 525-538 notwithstanding paragraph 548(a) (see above).

542 Impact and thermal tests have shown that the integrity of the shielding will not be affected under accident conditions (see Section 9.4.2). Therefore the radiation will not exceed 10 mSv/h (1 rem/h) at 1 m from the surface of the package with the maximum radioactive contents which the package is designed to carry.

543 Heat generated within the package will not adversely affect the containment or shielding integrity of the packaging if the package where left unattended for one week (see Section 7.4.3).

544 With an ambient temperature of 38°C and the heat generated within the package by the radioactive contents, the calculated surface temperature is 46°C, which is below the acceptable limit of 50°C (see Section 7.4.3).

545 No comment, accepted as written.
546

547 Prototype package testing showed that the impact limiters will remain effective if the package is subjected to the mechanical tests specified for normal and accident conditions of transport (see Section A.4.6.1). The impact limiters are fabricated from wood encased in 1/8" thick stainless steel sheet. This will prevent the wood from being damaged during routine handling and transportation.

548 Prototype package testing showed that the regulatory containment requirements will be satisfied (see Section 8.3).

549 The package meets the requirements for Type B packages as specified in paragraphs 541-548 (see above).

550 Not applicable because the irradiated nuclear fuel has a maximum activity of 2000 TBq (54000 Curies) (see Section 3.2).

551 There are no filters or mechanical cooling systems.

552 There is no pressure relief systems.

553 Prototype package testing showed that the level of stress in the containment system would not attain values which would adversely affect the package in such a way that it would fail to meet the applicable requirements (see Sections 6.3.2, 6.3.3 and 6.3.5).

554 The maximum normal operating pressure is 150 kPa which is less than 700 kPa gauge (see Section 7.4.3).

555 With an ambient temperature of 38°C and the heat generated within the package by the radioactive contents the calculated surface temperature is 46°C which is below the acceptable limit of 85°C (see Section 7.4.3).

556 If the package were subjected to an ambient temperature range from -40°C to 38°C, the containment system and the shielding system will not be impaired. The elastomeric seals have a temperature range of -54°C to 204°C (see Section 7.3). The containment system is fabricated from austenitic stainless steel which does not have a nil ductility transition temperature. Therefore brittle fracture of the containment system will not occur at -40°C (see Section 6.3.2.3).

557 Not applicable because the package complies with Type B(U)
558 requirements.

Requirements for Packages Containing Fissile Material

559 through 568 Not applicable because the natural uranium fuel does not qualify as Fissile Material as defined in the regulations.

Demonstration of Compliance

601 Demonstration of compliance was completed by calculations and full scale prototype testing (Appendix A).

602 The principle regulatory requirements for this package are containment of the radioactive contents and provision for adequate gamma radiation shielding. Acceptance was demonstrated by helium leakage test procedures and radiation shielding calculations respectively.

Test for LSA-III Material

603 Not applicable because the radioactive contents are not designated as LSA-III.

Tests for Special Form Materials

604 through 613 Not applicable because the radioactive contents are not designated as special form.

Tests for Packages

614 through 628 The prototype package was tested in accordance with these paragraphs. The test procedures and results are given in Section A4 of Appendix A.

629 Calculations (see Section A6 of Appendix A) show that package can withstand the external pressure if it were immersed under a head of water of 15 metres.

630 Not applicable because the activity of the irradiated fuel is 2.0 TBq (54000 Curies) (See Section 3.2).

631 through 633. Not applicable because the radioactive contents do not qualify as "Fissile Material" as defined in the regulations.

11.0 REFERENCES

1. Atomic Energy Control Board, SOR/91-304, Transport Packaging of Radioactive Material Regulations, Amendment, 9 May 1991.

2. International Atomic Energy Agency Safety Series No. 6 "Regulations for the Safe Transport of Radioactive Material 1985 Edition" (As Amended 1990), Vienna 1990.

3. AECL Research, "Irradiated Material Transportation Packaging Quality Assurance Plan", Engineering and Design Division Document No. 24.

4. Canadian Standards Association, CAN3-Z299.2-85, "Quality Assurance Program - Category 2".

5. AECL Research, "Design Quality Assurance Manual", Engineering and Design Division Document A-13900-DP-1.

6. AECL Research, "Engineering and Design Working Procedures", Engineering and Design Division Document A-13900-DP-2.

7. Canadian Standards Association, CAN3-N286.2-86, "Design Quality Assurance for Nuclear Power Plants".

8. AECL Research, "Irradiated Material Transportation Packaging Technical Specification", Engineering and Design Division Document A-13318-SP-1.

9. Canadian Standards Association, CAN3-Z299.3-85, "Quality Assurance Program - Category 3".

10. NATO-AQAP-1 (Allied Quality Assurance Publications), "Requirements for an Industrial Quality Control System".

11. AECL Research, "Irradiated Material Transportation Package Test Specification for Prototype Testing", Engineering and Design Division Document A-13318-SP-2.

12. AECL Research, "Irradiated Material Transportation Package Operating Procedures", Engineering and Design Division Document A-13318-PR-4.

13. Canadian Standards Association, CAN3-N286.0-82, "Quality Assurance Program Requirements for Nuclear Power Plants."

14. Canadian Standards Association, CAN-N286.5, "Quality Assurance Program Requirements for Nuclear Power Plants."

15. J.L. Crosthwaite, "CANDU Irradiated-Fuel Handbook", Atomic Energy of Canada Limited, WNRE-371, 1979 January.

16. I.R. Emerton to R. Lesco, AECL memorandum, "Irradiated Material Transportation Package", RMR-91-031, 1991 January 29, Engineering and Design Division Job File 13318.

17. International Atomic Energy Agency, "The Physical Protection of Nuclear Material", Information Circular, INFCIRC/225/Rev. 2, December 1989.

18. American Society of Mechanical Engineers Boiler and Pressure Vessel Code Section III, "Rules for Construction of Nuclear Power Plant Components", Division I Appendices, Appendix I "Design Stress Intensity Values, Allowable Stress, Material Properties, and Design Fatigue Curves, 1992 Edition.

19. American National Standard "For Radioactive Materials - Leakage Tests on Packages for Shipment", ANSI N14.15-1987.

20. American Society of Mechanical Engineers Boiler and Pressure Vessel Code Section III, "Rules for Construction of Nuclear Power Plant Components", Division I Appendices, Appendix F "Rules of Evaluation of Service Loadings with Level D Service Limits", 1992 Edition.

21. U.S. Nuclear Regulatory Commission, Regulatory Guide 7.6, "Design Criteria for the Structural Analysis of Shipping Cask Containment Vessels".

22. International Atomic Energy Agency, Safety Series No. 37, "Advisory Material for the IAEA Regulations for the Safe Transport of Radioactive Material (1985 Edition) Third Edition (As Amended 1990).

23. L.J. Clegg and J.R. Coady, "Radioactive Decay Properties of CANDU Fuel Volume 1: The Natural Uranium Fuel Cycle", Atomic Energy of Canada Limited, AECL-4436/1, January 1977.

24. Parker Seal Group, "Parker O-Ring Handbook", March 1982.

25. NUPRO Company, "B" Series Bellows Sealed Valves", Catalogue N-390-1, March 1991.

26. Y. Liner et. al, "Temperature Analysis of Irradiated Material Transportation Package", CRL Thermalhydraulics Development Branch Report ARD-TD-318 COG-92-03, January 1992.

27. R. Zane, "Pool Fire Testing of the IMT Package for Atomic Energy of Canada Limited", Ontario Hydro Report B93-11-P, April 23, 1993.

28. AECL Research, "Irradiated Material Transportation Package Procedure for Prototype Drop Testing", Engineering and Design Division Document A-13318-PR-2.

29. H.S. Bailey et. al., "Neutron Shielding Problems in the Shipping of High Burnup Thermal Reactor Fuel", Nuclear Technology, Volume 17, March 1973.

30. Microshield Manual, Version 3.12, Grove Engineering Inc.

31. A.T. Jeffs, "Gamma and Neutron Dose Rates During Fabrication and Storage of BLW(PB) Fuel", CRNL Report 1159 (BLW(PB)-FPR-N8), July 1974.

32. US National Council on Radiation Protection and Measurements, "Protection Against Neutron Radiation", NRCP No. 38 (1971).

APPENDIX A - STRUCTURAL ANALYSES

A.1 General

This Appendix contains supplemental information for other parts of the safety analysis report and specifically for Section 6, Structural Evaluation. The Appendix consists of five parts,

a) the impact analysis of the package as a result of 9 metre drop tests,

b) detailed analyses of the package components that could affect containment,

c) a description of the procedures and results for the prototype package test program,

d) detailed analyses of the package handling and tiedown components, and

e) detailed analyses of the package components when subjected to an external pressure of 150 kPa.

A.2 Impact Analysis

A.2.1 Impact Limiter Load-Deflection Characteristics

The type of wood and wood grain are oriented to provide the greatest amount of energy absorption on impact. Balsa wood is located at the ends of the limiter such that the grain is oriented parallel to the package axis. Redwood is placed at the limiter sides with the grain direction radial to the package. At the corners of the limiter, the grain of the redwood is oriented at a 45° angle. For end, side and oblique (45°) drops, the impact orientation will be parallel to the wood grain.

Under large strains, wood will crush at a constant stress/force until strain hardening occurs at approximately 50 to 90% strain. According to Reference 1, redwood and balsa wood have the following typical crush strengths parallel to the grain.

- Balsa wood 500 to 2000 psi
- Redwood 4500 to 6500 psi.

Actual tests were conducted on balsa wood and redwood specimens (Reference 2). The constrained compression test results (typical) parallel and perpendicular to the grain were as follows:

	Parallel (psi)	Perpendicular (psi)
Redwood	6500	1200
Balsa wood	1500	120

For the purposes of the analyses, nominal values were used, 1600 psi for balsa wood and 5000 psi for redwood.

(i) Flat End Impact

For impact onto the flat end of the package, the impact foot print is the projected area of the main flask body. Therefore, the crush area and crush force are constant as follows:

$$A_c = \pi r_f^2$$

$$F_c = A_c \cdot \sigma_c$$

where,

r_f - radius of the flask body

= 15 inches

σ_c - crush strength of balsa wood

= 1600 psi

(ii) Horizontal Side Impact

For impact onto the horizontal side of the package, the crush area is,

$$A_c = 2L\ [d\ (2r_L - d)]^{1/2}$$

where,

L - projected length of the main flask body (side length of the two impact limiters)

= 12 inches (6 inches per limiter)

r - outer radius of the limiter, and

= 24 inches

d - limiter deformation

therefore, the crush force is

$$F_c = A_c\ \sigma_c$$

where,

σ_c - crush strength of redwood

= 5000 psi

(iii) Oblique Angle Impact

For an oblique drop through the centre of gravity, the impact angle with respect to the package vertical axis is 60.9°. At the corners of the impact limiter, the grain of the redwood is oriented at a 45° angle. To account for impacts not parallel to the grain, Hankison formula, Reference 3, can be used to determine crush strengths as a function of grain angle:

$$\frac{N}{P} = \frac{Q/P}{\sin^n \emptyset + Q/P \cos^n \emptyset}$$

where,

$\emptyset$ - grain angle

Q - crush strength perpendicular to the grain

P - crush strength parallel to the grain

N - crush strength as a function of the grain angle

n - empirical constant

To calculate the ratio of N/P for redwood, the following values were used:

$\emptyset = 15°$

n = 2.0 from Reference 4

Q/P = 0.20 from Reference 4

For the given values above, the N/P ratio equals 0.79. Therefore, the crush strength of redwood at 15° from the grain direction would be 3950 psi (5000 x 0.790).

As with the side impact, the crush area and crush force are a function of deformation. The crush footprint (A_c) can be approximated by a truncated ellipse as follows:

$$A_c = \{1/2\ [rl - c\ (r - d)]\}\ /\cos \theta$$

where,

l - arc length, circular segment

$$= 2r \sin^{-1} \left[\frac{c}{2r} \right]$$

c - chord length, circular segment

$$= 2\ [d\ (2r - d)]^{1/2}$$

θ - impact angle

d - limiter deformation

The crush area is also limited by the projected area of the flask. The crush force is therefore given by,

$$F_c = A_c \sigma_c$$

where,

σ_c - crush strength of redwood at a grain angle of 15°

= 3950 psi

A.2.2 Accelerations

Because the package is quite robust and has a small slenderness ratio (length/diameter = 1.8), the package can be treated as a rigid body. The maximum rigid body deceleration and impact limiter deformations can be determined using Figures A1, A2 and A3 as follows:

Energy to be Absorbed, $E = Wh$

$$= (13000)\ (360)$$

$$= 4.68 \times 10^6 \text{ in-lbs}$$

From Figure A1, A2 and A3, the maximum deceleration can be determined as follows:

$$a = \frac{F_{max}}{W}$$

For each of the impact orientations, the maximum decelerations and impact limiters deformation are given in the table below.

As a comparison, a simple one-dimensional computer code (FMPASC and QUASC) was used (See Reference 5). For dynamic analysis, SCANS models the package as an elastic beam and the impact limiters as forces that change with impact analyses uses a one-dimensional beam model. Each node in the beam has two translational degrees of freedom and one rational degree of freedom. The impact code was an explicit time-history integration scheme in which equilibrium is formulated in terms of the global external forces and internal force resultants. This formulation allows the code to track large rigid-body motion. Thus the oblique impact problem can be calculated from the initial impact through essentially rigid-body rotation to secondary impact. The results of the SCANS analysis are also tabled below.

Impact Orientation	Decelerations g's		Deformation inch	
	SCANS	Rigid Body	SCANS	Rigid Body
Flat End	90.2	88	4.2	4.0
Horizontal Side	128.8	119	4.2	3.8
Oblique Angle (60.9°)	122.1	115	7.1	6.8

From the test results given in Reference 6, a comparison with the analytical results is as follows:

Impact Orientation	Decelerations g's		Deformation inch	
	Calculated	Test	Calculated	Test
Flat End	90.2	180[1]	4.2	3
Horizontal Side	128.8	95[2]	4.2	4
Oblique Angle	122.1	94	7.1	7.5

[1] derived from measured peak decelerations

[2] derived based on average decelerations.

For the purposes of the package containment component analyses, an impact load of 200 g's has been assumed regardless of the impact orientation.

A.3 Package Containment Component Analyses

A.3.1 Design Criteria

The components that will be analyzed include the containment flanges and their cap screws and the cap screws that secure the drawer and the lead shield insert. Where evaluation of the flanges and cap screws under accident conditions of transport is assessed (either due to impacts or internal gas on vapour pressures), the design criteria in Appendix F, Article F-1000, "Rules for Evaluation of Service Loadings with Level D Service Limits", Section III of the ASME Code, Reference 5, have been used. Where evaluation of the flanges and cap screws under internal gas or vapour pressures for normal conditions of transport is assessed the design criteria in NB-3000, "Rules for the Construction of Nuclear Power Plant Components", Section III of the ASME Code, Reference 6, have been used.

A.3.2 Closure Flanges

A.3.2.1 Under Impact Conditions

This analysis uses the mass of the front closure flange (115 kg) but assumes that the flange is a flat plate 50.8 mm (2 inches) thick. By making this simplifying assumption, the analysis becomes applicable to the rear closure flange (60 kg) as well.

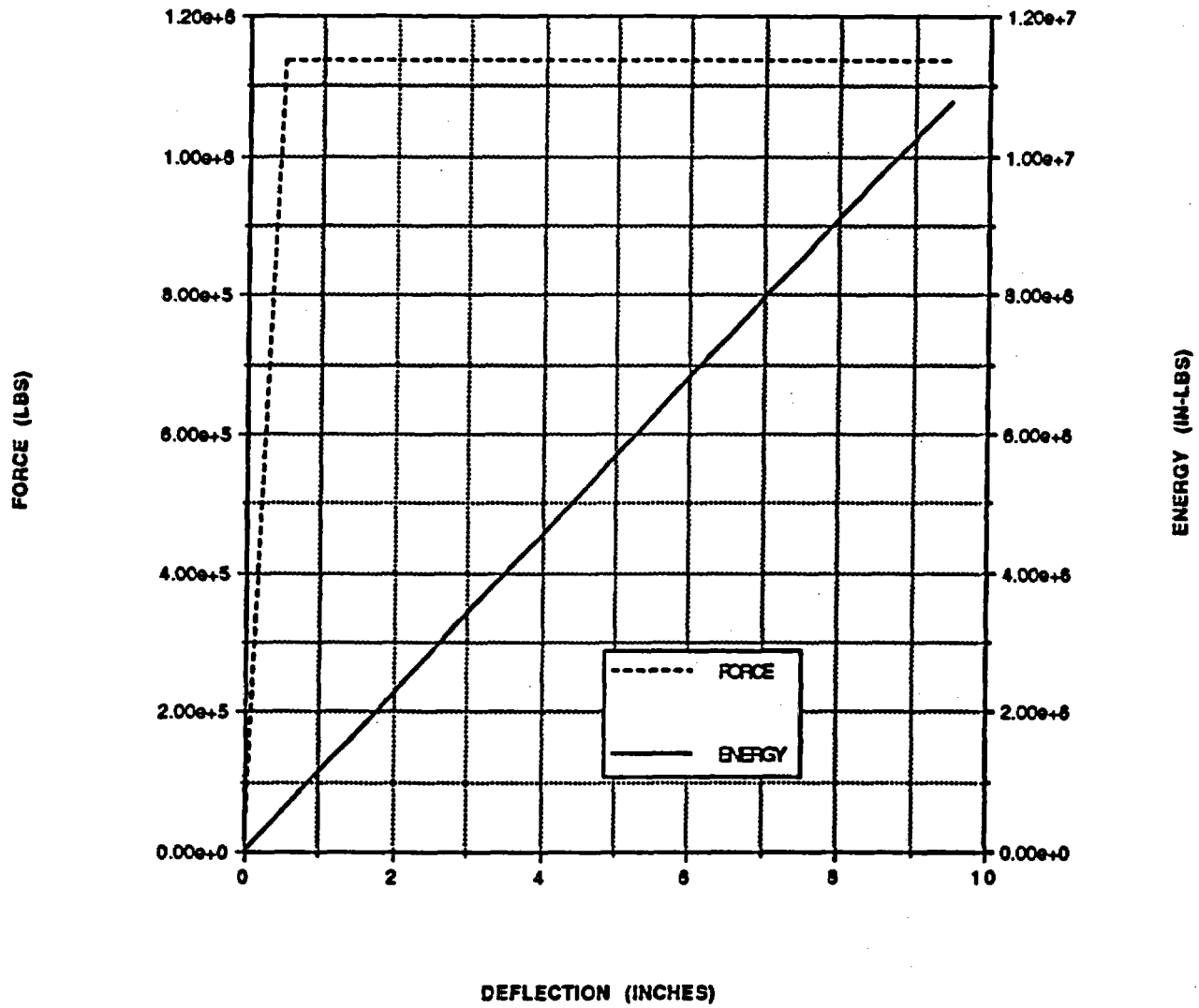

FIGURE A.1 LOAD DEFLECTION CHARACTERISTICS FOR END IMPACT

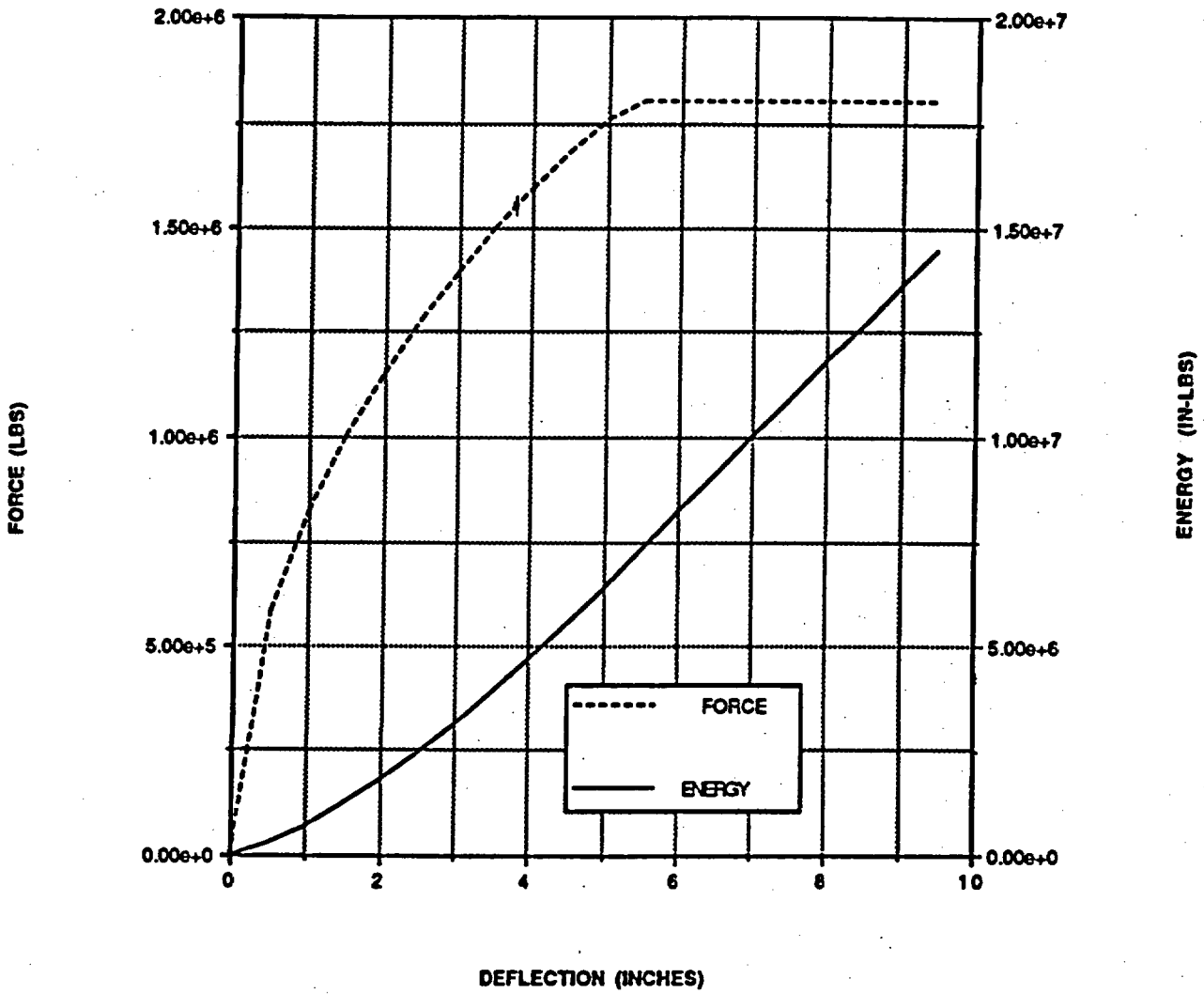

FIGURE A.2 LOAD DEFLECTION CHARACTERISTICS FOR SIDE IMPACT (FOR TWO IMPACT LIMITERS)

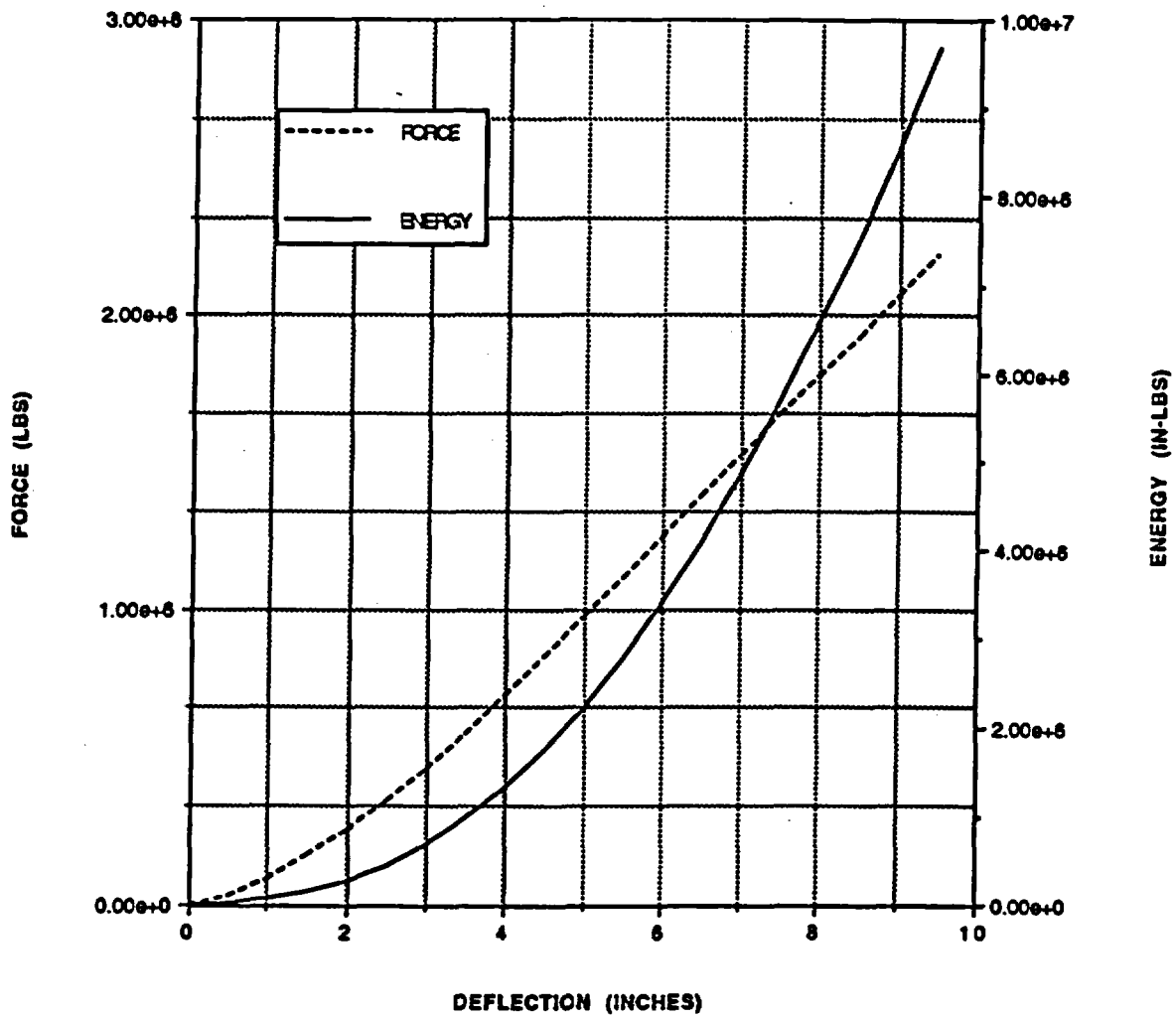

FIGURE A.3 LOAD DEFLECTION CHARACTERISTICS FOR OBLIQUE IMPACT

Inertia forces on the valve cover and rear cover plates are not significant.

For end impacts, inertia loading will induce bending stresses in the containment flanges. The maximum bending stresses will occur at the centre of the flange on one surface. Assuming the flange (impact end) is pinned at the bolt circle diameter, the stresses from Reference 9 are as follows:

Radial bending stress, $S_r = q\left[\frac{3}{8t^2}(3+\nu)R^2\right]$

Tangential bending stress, $S_t = S_r$

Longitudinal stress, $S_l = 0$

Shear stress, $\tau = 0$ (at the surface)

Assuming the inertia load is distributed evenly across the flanges then,

$$q = \frac{Wg}{\pi R^2}$$

and substituting,

$\nu = 0.3$ (Poisson's ratio)

Therefore, $S_r = S_t = \frac{Wg}{\pi R^2}\left[\frac{3}{8t^2}(3+0.3)R^2\right]$

$$= 0.394\,\frac{Wg}{t^2}$$

For a mass of 115 kg, the force

$W = 115\ (9.807)$
$= 1128$ N
$t = 50.8$ mm, or 5.08×10^{-2} m, and,
$g = 200$ for an end impact

Therefore, $S_r = S_t = \frac{0.394\ (1128)\ (200)}{(5.08 \times 10^{-2})^2}$

$= 34.4$ MPa

A.3.2.2 Under Internal Gas or Vapour Pressure

A.3.2.2.1 Front and Rear Closure Flanges

From Section 7.4.3, the Maximum Normal Operating Pressure was determined to be 1.5×10^5 Pa for the gas or vapour within the package containment system. However, in the unusual case where residual moisture may remain in the cavity, the pressure could rise to 6.1×10^5 Pa. This pressure will be used in the analysis. The temperature of the closure is about 62°C (from Table 7.1). Both flanges will be considered as flat plates, 50.8 mm thick. As in Section A.3.2.1:

Radial bending stress, $S_r = q\ [\frac{3}{8t^2}\ (3 + \nu)R^2]$

Tangential bending stress, $S_t = S_r$

Longitudinal stress, $S_l = 0$

Shear stress, $\tau = 0$ (at the surface)

q = the internal pressure on the flange
= 6.1×10^5 Pa.

Note: This value represents an *absolute* pressure and, when it is used, takes account of any reduction in ambient pressure.

t = 50.8 mm

$\nu = 0.3$

R = the outside radius of the inner "O"-ring
= 183 mm

Therefore,

$$S_r = S_t = 6.1 \times 10^5\ [\frac{3}{8(50.8)^2}\ (3 + 0.3)(183)^2]$$

$$= 9.8 \text{ MPa}$$

As a result of the thermal test, the internal gas or vapour pressure could be as high as 53.7×10^5 Pa, according to Section 7.5.5. The temperature of the closure flanges is about 200°C from Figure 7.10.

In this case,

$$S_r = S_t = 53.7 \times 10^5\ [\frac{3}{8(50.8)^2}\ (3 + 0.3)(183)^2]$$

$$= 86.3 \text{ MPa}$$

A.3.2.2.2 Rear Cover Plate

The analyses are the same as those in Section A.3.2.2.1 except that the plate thickness t = 22.2 mm and the outside radius of the inner O-ring = R = 59.6 mm.

Therefore, for normal conditions of transport,

$$S_r = S_t = 6.1 \times 10^5\ [\frac{3}{8(22.2)^2}\ (3 + 0.3)(59.6)^2]$$

$$= 5.4 \text{ MPa}$$

After the thermal test,

$$S_r = S_t = 53.7 \times 10^5 \left[\frac{3}{8(22.2)^2}(3 + 0.3)(59.6)^2\right]$$

$$= 47.5 \text{ MPa}$$

A.3.2.3 Combined Loadings

A.3.2.3.1 Front and Rear Closure Flanges

For normal conditions of transport, the maximum loadings will consist of a load due to an end impact plus a load due to internal gas or vapour pressure. From Sections A.3.2.1 and A.3.2.2.1, the stresses may be added, thus,

$$S_r = S_t = 34.4 + 9.8$$
$$= 44.2 \text{ MPa}$$

(This is a conservative calculation because the 15.5 MPa value actually pertains to a 9 m end impact.)

For accident conditions of transport, the maximum loading on the closure flanges will be the same as above, thus,

$$S_r = S_t = 44.2 \text{ MPa}$$

As a result of the thermal test, the maximum loading will be due to the load from the internal gas or vapour pressure only.

Thus, from Section A.3.2.2.1

$$S_r = S_t = 86.3 \text{ MPa.}$$

A.3.2.3.2 Rear Cover Plate

For both normal and accident conditions of transport, the maximum loading will be due to the load from the internal gas or vapour pressure only because the load due to the plate inertia is insignificant.

For normal conditions of transport,

$$S_r = S_t = 5.4 \text{ MPa, and}$$

as a result of the thermal test,

$$S_r = S_t = 47.5 \text{ MPa.}$$

A.3.2.4 Stress Intensities

For SA-182 F304, or SA-240 Type 304 from ASME Section II, Part D:

S_u = 503 MPa at 62°C (prorated)

S_u = 444 MPa at 200°C

S_y = 190 MPa at 62°C (prorated)

S_y = 143 MPa at 200°C

S_m = 138 MPa at 62°C (allowable stress intensity)

S_m = 129 MPa at 200°C (allowable stress intensity)

For normal conditions of transport and, according to Article NB3221.3 of the ASME Code, Reference (8), the calculated stress intensity shall not exceed 1.5 S_m. Therefore, the allowable stress intensity

$$S_m \text{ (allowable)} = (1.5)(138) = 207 \text{ MPa.}$$

The calculated stress intensity is 44.2 MPa for the front and rear closure flanges and 5.4 MPa for the rear cover plate. Therefore, the design criteria are satisfied.

For accident conditions of transport and, according to article F1331.1 of the ASME Code, Reference 7, the stress intensities (twice the maximum shear stress) resulting from the general primary membrane stresses shall not exceed the lesser of 2.4 S_m or 0.7 S_u.

At 62°C,

$2.4\ S_m$ = 331 MPa and
$0.7\ S_u$ = 352 MPa

At 200°C,

$2.4\ S_m$ = 310 MPa and
$0.7\ S_u$ = 311 MPa

Also, the stress intensity resulting from the sum of the primary membrane stresses and the primary bending stresses shall not exceed 150% of the allowable stress intensity for general primary membrane stresses (as calculated above).

At 62°C,

$$S_m \text{ (allowable)} = 1.5\ (331) = 497 \text{ MPa}$$

At 200°C,

$$S_m \text{ (allowable)} = 1.5\ (310)$$
$$= 465 \text{ MPa}$$

The calculated stress intensities are due to primary bending stresses for the front and rear closure flanges were:

$$S_m \text{ (calculated)} = S_r - S_1 = 44.2 \text{ MPa at } 62°C, \text{ and}$$
$$S_m \text{ (calculated)} = S_r - S_1 = 86.3 \text{ MPa at } 200°C.$$

Therefore, the design criteria are satisfied.

The calculated stress intensity for the rear cover plate was,

$$S_m \text{ (calculated)} = S_r - S_1 = 47.5 \text{ MPa at } 200°C.$$

Therefore, the design criteria are satisfied.

A.3.3 Flange Cap Screws

From the analyses in Section A.3.2, it is apparent that the maximum stresses of the cap screws will occur for accident conditions of transport. Therefore, an analysis for normal conditions of transport is not included.

A.3.3.1 Under Impact Conditions

For the front and rear closures, the force acting on the cap screws would be the inertia load on the closure flanges due to impact. Because the front closure flange (115 kg) is twice as heavy as the rear closure flange, the inertial forces generated by the front closure will be the highest. Therefore, only these loads will be considered as follows:

Impact Orientation	Cap Screw Tension Loads kN	Cap Screw Shear Loads kN
Side	0	225.6
Oblique at 60°	195.4	112.8

There are a total of eight cap screws. The minor root diameter of the cap screw is 21.57 mm and the stress area per cap screw is 3.65×10^{-4} m^2. Assuming that the impact loads are distributed evenly over the entire cap screw area, the stresses for each cap screw are:

Impact Orientation	Tensile Stress MPa	Shear Stress MPa
Side	0	77.3
Oblique at 60°	66.9	38.6

A.3.3.2 Under Internal Gas or Vapour Pressure

A.3.3.2.1 Front and Rear Closure Flange Cap Screws

At the time of any impact accident, the internal pressure could be as high as 6.1×10^5 Pa. The force on the closure would be,

$$F = \pi R^2 P$$

where R = the outside radius of the inner O-ring
= 183 mm

Therefore, $F = 64{,}180$ N

The minor root diameter of the cap screw is 21.57 mm and the stress area is 3.65×10^{-4} m². The tensile stress for each bolt is,

$$S = \frac{64{,}180}{(8)(3.65 \times 10^{-4})}$$

$$= 22.0 \text{ MPa}$$

After the thermal test, the internal pressure could be as high as 53.7×10^5 Pa.

Then, $F = 564{,}977$ N, and

$S = 193.5$ MPa

A.3.3.2.2 Rear Cover Plate Cap Screws

The analyses are the same as those is Section A.3.3.2.1 except that the outside radius of the inner O-ring is R=59.6 mm, the minor root diameter of the capscrew is 3.8 mm and the stress area is 4.5×10^{-5} m².

At the time of impact,

$$F = \pi\ (0.0596)^2\ (6.1 \times 10^5)$$

$$= 6800 \text{ N, and}$$

$$S = \frac{6800}{(8)(4.5 \times 10^{-5})}$$

$$= 18.9 \text{ MPa}$$

After the thermal test, the internal pressure could be as high as 53.7×10^5 Pa.

Then,

$F = 59925$ N, and
$S = 166.5$ MPa

A.3.3.3 Combined Loadings

A.3.3.3.1 Front and Rear Closure Cap Screws

According to paragraph F-1335 of the ASME Code, Reference 7, the design criteria are:

Allowable Tensile Stress F_{tb}: smaller of 0.7 S_u and S_y

Allowable Shear Stress, F_{tv}: smaller of 0.42 S_u and 0.6 S_y

Combined Tensile and Shear Stress: $\left(\frac{f_t}{F_{tb}}\right)^2 + \left(\frac{f_v}{F_{tv}}\right)^2 < 1$

where,

S_u - ultimate tensile strength, MPa
S_y - yield strength, MPa
f_t - computed tensile stress, MPa
f_v - computed shear stress, MPa

The fasteners for the closure flanges are 1" - 8 UNC-2A cap screws fabricated from ASME SA-193 Class 1C 8BS with the following properties:

S_u = 646 MPa at 62°C (prorated)
S_u = 565 MPa at 200°C
S_y = 307 MPa at 62°C (prorated)
S_y = 204 MPa at 200°C

Therefore, at 62°C

F_{tb} = 307 MPa, and
F_{tv} = 184 MPa

At 200°C,

F_{tb} = 204 MPa, and
F_{tv} = 122 MPa

For the combined effects of impact and internal pressure, simply add a tensile stress of 22 MPa (due to internal pressure) to the cap screw stresses tabled in Section A.3.3.1. For vertical end impact, the cap screw is not subjected to tensile loads, therefore, only horizontal side and oblique angle impacts need to be considered.

Impact Orientation	Tensile Stress MPa	Shear Stress MPa	Combined Stress Ratio
Side	22	77.3	0.22
Oblique at 60°	88.9	38.6	0.16
Design Criteria	307	184	1

From the above, the calculated stress values satisfy the design criteria.

After the thermal test, no impact loads need be considered and so the combined bolt stress remains as 193.5 MPa. This value satisfies the design criteria of 204 MPa at 200°C.

In the event that the drawer locking cap screw is not installed, the impact of the drawer and its contents would increase the inertia loads and stresses on the front cap screws.

Consider an oblique impact only, the additional impact load would be:

$$F = 2\ (115 + 24.5)(9.807)(200)\ \cos 30$$
$$= 474\ \text{kN}$$

Where the co-efficient 2 represents the assumed dynamic amplification factor and the factor 9.807 converts kilograms to a force in Newtons.

The additional cap screw stress is:

$$S = \frac{474}{(8)(3.65 \times 10^{-4}}$$

$$= 162\ \text{MPa}$$

Then, the total cap screw stress would be

$$S = 88.9 + 162$$
$$= 250.9\ \text{MPa}$$

which still satisfies the design criteria.

A.3.3.3.2 <u>Rear Cover Plate Cap Screws</u>

For the rear cover plate, the inertia load due to the plate mass is negligible and so the cap screw stresses will be the same as those given in Section A.3.3.2.2.

At the time of impact,

$$S = 18.9 \text{ MPa at } 62°C$$

After the thermal test,

$$S = 166.5 \text{ MPa at } 200°C$$

The design criteria for these two situations are 307 and 204 MPa respectively.

A.3.4 Lead Shield Insert

A.3.4.1 Cap Screws

The shield insert cap screws secure the insert to the main flask body and will prevent additional impacts on the front closure. From Table 7.1, the temperature of the insert would be approximately 67°C. The eight 1" - 8UNC 2A cap screws are fabricated from ASME Section II, Part D, SA 564 Type 630 H1100 material which has the following properties:

S_u = 965 MPa at 38°C
S_u = 965 MPa 67°C

S_y = 795 MPa at 38°C
S_y = 763 MPa at 67°C (prorated)

Stress Area = $3.65 \times 10^{-4} m^2$

The allowable tensile and shear stresses at 67°C are:

$$F_{tb} = 0.7\ S_u$$

$$= 676 \text{ MPa and}$$

$$F_{tv} = 0.42\ S_u$$

$$= 405 \text{ MPa}$$

The force acting on the cap screws is the inertia load of the shield insert (670kg). Thus,

$$F = 6561g \text{ N}$$

Assuming that this force is distributed equally amongst the cap screws, the cap screw stress is:

$$S = \frac{F}{A}$$

$$= \frac{6561\ g}{(8)(3.65 \times 10^{-4})}$$

$$= 2.25\ g \text{ MPa}$$

Because the insert is laterally constrained by the flask body, shear stress cannot develop in the cap screws as a result of inertia loads acting on the insert from horizontal side impacts. Under end and oblique impacts, the cap screws will be subjected to tensile loads.

Therefore the stresses due to end and oblique angle impacts are tabled below.

Impact Orientation	Stresses		
	Tensile MPa	Shear MPa	Combined Stress Ratio
End	450	0	0.443
Oblique at 60°C	390	225*	0.641
Design Criteria	676	405	1

* Insert is laterally constrained by the flask body; therefore shear stresses are minimized.

A.3.4.2 Flange-to-Shell Welds

In addition to the cap screws, the integrity of the welds must be maintained under impact conditions to prevent additional impact loads on the front closure. The rear flange of the insert, bolted to the main flask body, is welded to the outer shell (6.345×10^{-3}m full penetration weld). For an end impact, the inertia loads acting on the welds is,

$$F = (6561)\ (200\ g's) = 1312\ kN.$$

Longitudinal Stress

$$S_L = \frac{\text{Impact Load}}{\text{weld area}}$$

$$= \frac{1312}{(0.305)\pi\ (6.345 \times 10^{-3})}$$

$$= 172.3\ MPa$$

Stress Intensity $S = 172.3$ MPa

Assuming the weld has the same minimum properties as the base material ASME SA 240 304L or SA 312 TP304L:

At 67°C S_y = 160 MPa

S_u = 470 MPa

S_m = 115 MPa

For accident conditions of transport and according to Article F1331.1 of the ASME Code, the stress intensity (twice the maximum shear) shall not exceed the lesser of 2.4 S_m or 0.7 S_u. Therefore,

$$S_{allowable} = 276 \text{ MPa} > 172.3 \text{ MPa}$$

A.4 Prototype Package Testing

A.4.1 Introduction

Various series of destructive tests were completed on a prototype package with a simulated fuel bundle assembly in order to demonstrate compliance with regulatory transportation requirements and to collect data for research purposes.

In all, three 9 metre drop tests, two 1 metre puncture tests, one 0.9 metre drop test and one 30 minute 800°C thermal test were completed on the same prototype package. All of the drop tests were completed at the Chalk River Laboratories Drop Test Facility. The fire test was completed at Ontario Hydro's Fire Test Facility at Wesleyville. The prototype package was equipped with accelerometers, strain gauges and thermocouples in order to collect information on declerations, cap screw strains and package temperature profiles.

High speed, normal speed and still camera photography were used throughout the tests.

The objectives of the test program were,

a) to assess the performance of the impact limiters for different impact orientations,

b) to determine any reduction in the gamma radiation shielding properties of the package, particularly with respect to the lead shield insert,

c) to demonstrate that the containment system remains leaktight (1×10^{-8} Pa.m^3/s) after impact tests alone and after the cumulative effects of impact tests and a thermal test,

d) to obtain the level of stress in the flange closure cap screws as a result of 9 metre drop tests,

e) to assess the effect of 9 metre drop tests on irradiated fuel bundle assemblies,

f) to obtain packaging component temperature data as a result of the thermal test, and

g) to assess the condition of the packaging components as a result of the hypothetical accident test conditions.

A.4.2 Prototype Test Specimen

The test prototype details are shown on the following drawings:

CRL Drawing Number	Title
E-5580-A-34	Assembly Shipping Flask
E-5580-A-35	Assembly Shipping Drawer
E-5580-SA-14	Package Sub-Assembly
E-5580-SA-15	Sub-Assembly and Details Shielding Insert
E-5580-91	Details Shipping Drawer
E-5580-92	Details Flask Body
E-5580-93	Details Impact Limiter
E-5580-94	Details Shipping Frame
D-5580-95	Details Main Closure
D-5580-96	Details Valve Cover Plate
D-5580-97	Details Rear Closure
D-5580-98	Details Lifting Trunnions and Shear Discs
C-5580-99	Details Rear Cover Plate.

Tapped holes were provided in the flask body for mounting individual accelerometers or triaxial accelerometer blocks. Up to 6 accelerometers could be installed and each could record up to 2500g's.

Access ports through the ends of the impact limiters were provided for conducting helium leak tests of all the flange seals.

Eight strain gauge bolts, 25 mm (inch) diameter, were installed, four for the front flange and four for the rear flange.

Four access ports through the side of each impact limiter were provided for strain gauge bolt lead wires.

For the fire test, ten 1.6 mm stainless steel, chromel-alumel thermocouples were attached to the package, five to the external surface and five to the internal components.

Temperature indicators were attached to the inside faces of the front and rear flanges and the outer elements of the simulated fuel bundle assembly.

Neither the package support frame nor the weather cover were included in the tests.

A simulated fuel bundle represented the radioactive contents. Except for the use of lead instead of UO_2 pellets, the simulated bundle was identical to a 28 element CANDU fuel bundle assembly.

A.4.3 Test Procedures

References 10, 11 and 12 give complete details about the prototype test specification and procedures. The following summarizes the test procedures in order of completion.

1) Assemble package and conduct helium leak test.

2) Complete a 0.9 m vertical, rear end drop test, a 1 m vertical, rear end puncture test, a 9 m vertical, front end drop test and a 1 m vertical front end puncture test.

3) Repeat helium leak test.

4) Disassemble package, inspect, measure and photograph results.

5) Reassemble package and repeat helium leak test.

6) Complete a 9 m horizontal side drop test, a 9 m oblique rear end drop test and a 30 minute open pool fire test.

7) Conduct helium leak test.

8) Disassemble package, inspect, measure and photograph results.

A discussion of the critical impact test orientations is as follows:

(a) Puncture Tests

Under accident conditions, puncture loads can be expected because impact surfaces are not necessarily flat. As a result thin walled packages are sensitive to puncture loads with respect to both loss of containment integrity and loss of thermal insulation. Because the flask body has 225 mm thick stainless steel walls, puncturing of the flask body and loss of containment is very unlikely. Two areas on the package which are vulnerable to puncture is the rear cover plate and valve assembly. As a result, two puncture tests were conducted at the following locations:

(i) front end limiter at the axis centre (location of the valve cover plate); and

(ii) rear end impact limiter at the axis centre (location of the rear cover plate).

(b) 9 m Drop Tests

The 9 m drop test unto an unyielding surface is designed to simulate the impact/crash loads that can be expected in the event of an accident. Drop tests were conducted to verify containment integrity of package (structural integrity) and the structural integrity of the wood impact limiters. Three 9 m drop tests were conducted with the package orientation described below:

1. End drop on the front (valve cover end) with the cylindrical axis of the package perpendicular to the impact surface.

   In this orientation, the lead shield insert cap screws and drawer cap screw will be subjected to tensile loads. Failure of these cap screws would result in an additional impact load from the shield insert on the front closure flange. The front closure flange and valve cover plate will be subjected to loads from the compression of the front impact limiter. Under these impact conditions, no tensile loads due to impact will be imposed on the front or rear flange cap screws.

2. Side drop with the cylindrical axis of the package parallel to the impact surface.

   Under these impact conditions, the main flask body will be subjected to bending stresses; however, the stresses will be relatively low because the flask has thick walls (225 mm). In addition, the closure flanges and cap screws will be subjected to shearing forces.

3. Oblique angle/centre of gravity drop on the rear impact limiter with the cylindrical axis rotated 60° from the horizontal.

   In this impact orientation, the package will be subjected to the following loading conditions:

   - bending loads on the rear closure flange
   - tensile loads on the rear closure cap screws
   - bending loads on the rear support flange for the shield insert.

A.4.4 Acceptance/Rejection Test Criteria

The radioactive related hazards associated with this package are excessive loss of gamma radiation shielding and loss of containment integrity. For the two series of tests above a leakage rate of more than 1×10^{-8} Pa.m^3/s from the containment system indicates rejection. This rate is based on the flow of dry air at 25°C for a pressure differential of 101.3 kPa against a vacuum of 1 kPa or less. Acceptance or rejection of the package due to excessive loss of gamma radiation shielding shall be assessed with reference to the regulatory requirements that are given in Table 9.1.

A.4.5 Prototype Test Results

The following summarizes the test results and observations that are given in detail in References 6 and 13.

1. Prior to the drop tests the containment system was leakage tested. The helium leakage rate was less than 5×10^{-9} Pa.m^3/s. (Section 8, Containment Evaluation, provides more information on the leakage test procedures).

2. No visible damage occurred to the package as a result of the 0.9 m vertical, rear end drop test.

3. As a result of the 1 m vertical, rear end puncture test the depth of penetration of the 150 mm steel bar was approximately 247 mm. The torque on the impact limiter cap screws measured from 0 to 20 N.m (after the two drop tests). The initial torque was 108 N.m.

4. As a result of the 9 m vertical, front end drop test the overall package height shortened by about 74 mm. The overall height of the front impact limiter shortened by about 11.5 mm. The circumferential corner of the impact limiter bulged slightly. The torque on the impact limiter cap screws measured from 0 to 20 N.m. The initial torque was 68 N.m.

5. As a result of the 1 m vertical, front end puncture test the depth of penetration of the 150 mm steel bar was approximately 181 mm.

6. After the series of drop tests described above the containment system was leakage tested. The helium leakage rate was less than 5×10^{-9} Pa.m^3/s.

7. The front impact limiter was removed and the following observations were recorded.

   a) The valve cover plate cap screws were badly bent and the cover plate had collapsed inwardly, approximately 16 mm. Torque measurements on the cap screws were not meaningful. The valve handle was broken.

   b) The torque on the front flange cap screws measured from 0 to 108 N.m. The initial torque was 135 N.m.

   c) Five of the rear cover plate cap screws were bent and the torque on five of them, not necessarily the same five, measured 0 N.m.

   d) The torque on the rear flange cap screws measured from 68 to 129 N.m. The initial torque was 135 N.m.

   e) The torque on the lead shield insert cap screws measured from 0 to 88 N.m. and that on the drawer cap screws measured 183 N.m. The initial torques were 305 N.m.

8. The prototype package was reassembled and the containment system was leakage tested. The helium leakage rate was less than 4×10^{-9} $Pa.m^3/s$.

9. As a result of the 9 m horizontal side drop test both impact limiters were flattened at the area of impact as shown in Figure A4. The height of the trunnions above the impact target measured 50 mm at the rear and 70 mm at the front. Prior to impact the height was approximately 168 mm. A part of the stainless steel encasement of the front impact limiter split and so some wood was exposed.

10. As a result of the 9 m oblique rear end drop test, the rear impact limiter deformed as shown in Figure A5.

11. After the series of drop and fire tests described above the containment system was leakage tested. The helium leakage rate was less than 3.5×10^{-9} $Pa.m^3/s$.

12. As the package was disassembled the following observations were recorded.

    a) The torque on seven of the front valve cover plate cap screw measured from 7 to 20 N.m, the eighth cap screws was damaged. The initial torque was 20 N.m.

    b) The torque on the front flange cap screws measured from 122 to 203 N.m. The initial torque was 135 N.m.

    c) The torque on all the rear cover plate cap screws measured 0 N.m. The initial torque was 7 N.m.

    d) The torque on the rear flange cap screws measured from 68 to 190 N.m. The initial torque was 135 N.m.

    e) The torque on the lead shield insert cap screws measured from 0 to 95 N.m and that on the drawer cap screw measured 81 N.m. The initial torques were 305 N.m.

    f) The valve cover plate O-ring seal was stuck to the cover plate at several places. At one place the O-ring had melted slightly.

    g) The compression set for the ethylene propylene O-rings was greater than that for the flurocarbon O-rings for both front and rear flanges. These O-rings were in good condition and pliable.

    h) For the simulated fuel bundle, all the elements had broken away from the end plates. The element sheaths all appeared in good condition.

A.4.6 Discussion

Leakage tests showed that the containment system remained leaktight (less than 1×10^{-8} Pa.m^3/s) for all the drop and fire tests.

There was no loss of gamma radiation shielding as a result of testing. There was no evidence of the lead insert melting during the fire test.

As discussed in Section 7.5, no excessive temperatures were recorded during the fire test.

A discussion of each package component is given in the following sections.

A.4.6.1 Impact Limiters

The impact limiters performed satisfactorily although the limiter deformation was less than the calculated values. For example for the vertical front end drop test the measured deformation was about 74 mm and the calculated was 106.7 mm. Other test data showed that the various cap screws were not overstressed as a result of deceleration forces. In the fire test, the balsa wood and redwood burned entirely. This is not a basis for rejection of the design. However, as a result of this observation, the design was modified (see drawing E-5580-847) to include three 12.5 mm (0.5 in.) discs of Marinite P insulation. This insulation will reduce heat transfer from the burning wood to the front and rear flanges.

A.4.6.2 Front Flange

The front flange, its cap screws and its O-ring seals performed satisfactorily. Although some loss of torque occurred, the cap screws were not overstressed and they maintained a leaktight closure.

A.4.6.3 Rear Flange

The rear flange, its cap screws and its O-ring seals performed satisfactorily. Although some loss of torque occurred, the cap screws, were not overstressed and they maintained a leaktight closure.

A.4.6.4 Valve Cover Plate

Although the valve cover plate fulfilled its function, the performance of this component was deemed unsatisfactory for the puncture test because the plate had collapsed inwardly, the valve handle broke and some cap screws were damaged. Consequently, the valve cover plate was redesigned by thickening the plate, providing minimum cutouts for valve clearance, and a counter sinking the cap screw heads (see drawing D-5580-80).

The PCTFE (polychlorotrifluoroethylene), "KEL-F" stem insert on the valve had melted as a result of the fire test; however, containment was still maintained by the fluorocarbon O-ring in the Cajon VCO union/blind nut arrangement. As a result of the thermal test, the specification for the valve stem insert was changed from "KEL-F" to Stellite with a temperature rating of 315°C.

A.4.6.5 Rear Cover Plate

Although the rear cover plate maintained a leaktight closure, the performance of this component was deemed unsatisfactory because the cap screws have a tendency to lose their torque in impact accidents. Consequently the rear cover plate was redesigned by increasing the plate thickness, counter sinking the cap screw heads, and increasing the cap screw sizes (see drawing C-5580-82).

A.4.6.6 Lead Shield Insert

The lead shield insert and its cap screws performed satisfactory. Although some loss of torque occurred, the cap screws retained the insert without being overstressed. As a result of the fire test, the lead shielding did not melt.

A.4.6.7 Drawer Locking Cap Screw

The cap screw performed satisfactory. Although some loss of torque occurred, the cap screw retained the drawer without being overstressed.

A.4.6.8 Simulated Fuel Bundle

The end plates of the fuel bundle were badly damaged. As a result, the fuel elements had broken away from the end plates. A visual examination of the elements showed no sheath damage.

A.5 Package Handling and Tiedown Component Analysis

A.5.1 Tiedown Analysis

The following tiedown analysis calculated the loads acting on the tiedown components depending on the mode of transportation and the method in which the package is secured to the conveyance. The design loads are taken from IAEA Safety Series No. 37 Appendix VIII entitled, "Acceleration Values and Calculation Methods for Package Tiedown Forces" (Reference 14).

A.5.1.1 Road and Sea Transportation

Design Loads:

Longitudinal	± 2 g
Laterial	± 2 g
Vertical	3 g down, 2 g up.

The vertical acceleration includes gravity and are actual absolute factors experienced by the package. The loads are assumed to be applied simultaneously.

Design Criteria:

The applied stress will not exceed the yield strength of the components.

Assumptions:

i) tiedowns are flexible and cannot support compression; and

ii) package is not chocked (blocked) to the conveyance.

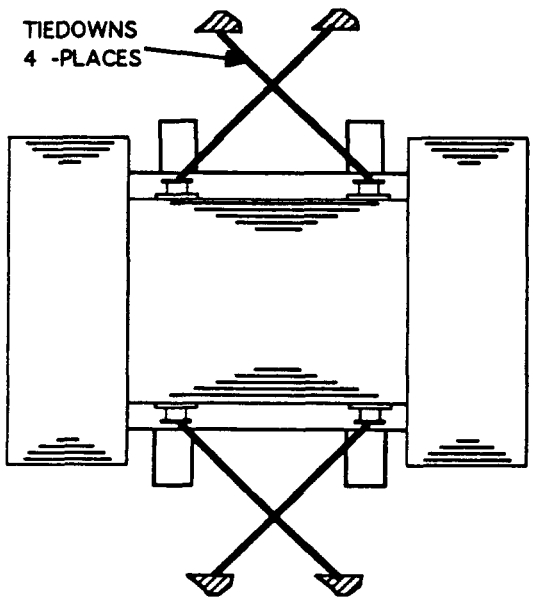

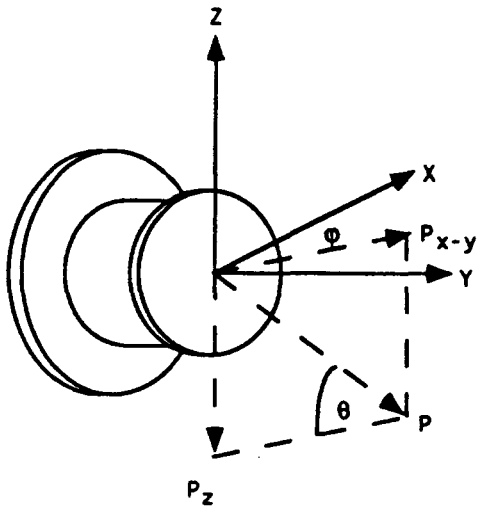

In general

$$P^2 = P^2_{xy} + P_z^2 \qquad P_{xy} = P \cos \phi$$

$$P_x = P \cos \phi \cos \theta$$

$$P_y = P \cos \phi \sin \theta$$

$$P_z = - P \sin \phi$$

Loads due to 2 g in the longitudinal direction (direction of travel) and assuming only two tiedown members can support the load.

$$\Sigma F_x = Ma_x \text{ in the x-direction}$$

and $P_{1x} = P_{3x}$ due to symmetry

$$2 P_{1x} \cos \phi \cos \theta = Wg_x$$

$$P_{1x} = \frac{Wg_x}{2 \cos \phi \cos \theta}$$

Loads dues to 2 g in the lateral direction (y-direction) and again assuming only two tiedown members can support the load.

$$\Sigma F_y = Ma_y \text{ in the y-direction}$$

and $P_{1y} = P_{4y}$ due to symmetry

$$2 P_{1y} \cos \phi \sin \theta = Wg_y$$

$$P_{1y} = \frac{Wg_y}{2 \cos \phi \sin \theta}$$

Loads due to 2 g in the vertical direction (z-direction) and assuming all four tiedowns can support the vertical load upwardly

$$\Sigma F_z = Ma_z \text{ in the z-direction}$$

and $P_{1z} = P_{2z} = P_{3z} = P_{4z}$

$$4 P_{1z} \sin \phi = wg_z$$

$$P_{1z} = \frac{Wg_z}{4 \sin \phi}$$

Summing up the total load (maximum) acting on tiedown member No. 1 as follows:

$$P_1 = P_{1x} + P_{1y} + P_{1z}$$

$$= \frac{Wg_x}{2 \cos \phi \cos \theta} + \frac{Wg_y}{2 \cos \phi \sin \theta} + \frac{Wg_z}{4 \sin \phi}$$

Let,

$g_x = 2$
$g_y = 2$
$g_z = 2$
$\phi = 45°$
$\theta = 45°$
$W = 57968$ N (13,000 lbs)
$\mu = 0.3$

$$P_1 = W [2 + 2 + 0.707]$$

$$P_1 = 57968 (4.707)$$

$$P_1 = 273 \text{ kN } (61,190 \text{ lbs})$$

Resolving the tiedown forces in x, y, z coordinates

$$F_x = 137 \text{ kN}$$

$$F_y = 137 \text{ kN}$$

$$F_z = 193 \text{ kN}$$

A.5.1.1.1 <u>Component Analysis</u>

(a) <u>Shear Disc</u>

Diameter = 0.06 m (2.362 in.)

$$\text{Shear Area} = \frac{\pi}{4} (0.06)^2 = 0.0028 \text{ m}^2$$

$$\text{Shear Force} = [F_x^2 + F_z^2]^{1/2}$$

$$= [(137)^2 + (193)^2]^{1/2} = 236.7 \text{ N}$$

$$\text{Average Shear Stress} = \tau = \frac{V}{A} = \frac{236.7 \times 10^3}{0.0028} = 84.5 \text{ MPa}$$

For SA479 Type XM-19 $S_y = 380$ MPa

Therefore $\tau_{allowable} = 0.5\ S_y = 190 \text{ MPa} > 84.5 \text{ MPa}$

(b) Trunnions

Stress Area, $A = \frac{\pi}{4}(0.089^2 - 0.032^2) = 0.0054\ m^2$

Tensile Stress due to F_y

$$S_T = \frac{F_y}{A} = \frac{137 \times 10^3}{0.0054} = 25.4\ MPa$$

Bending stress due to F_z and F_x:

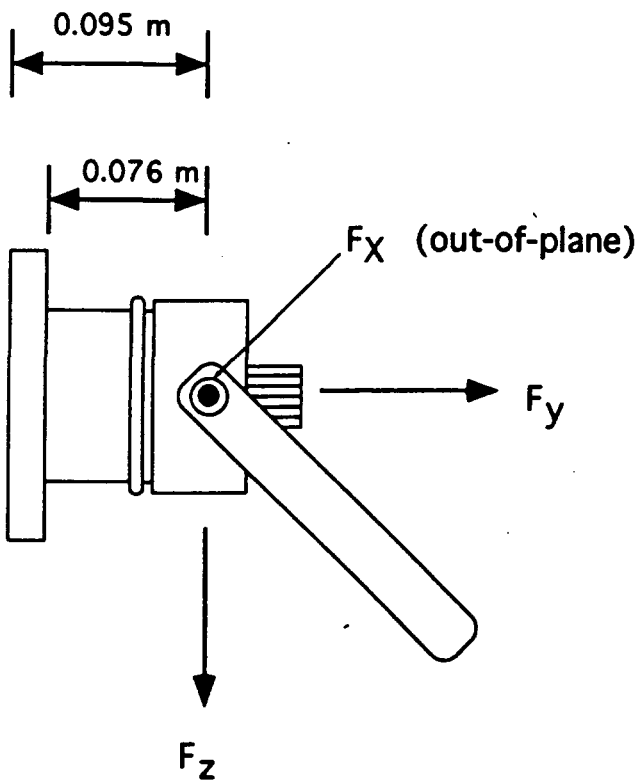

$$S_B = F_{xz} \cdot e \cdot \frac{c}{I}$$

where, $F_{xz} = [F_x^2 + F_z^2]^{1/2}$

$= [(137)^2 + (193)^2]^{1/2}$

$= 236.7$ kN

$F_{xz}.e = (236.7)(0.076) = 18$ kN.m

$c = 0.0889/2 = 0.0445$

$I = \frac{\pi}{64}[(0.0889)^4 - (0.0318)^4] = 3.02 \times 10^{-6}$ m^4

$$S_B = \frac{1.8 \times 10^3 (0.0445)}{3.02 \times 10^{-6}} = 265.1 \text{ MPa}$$

Total Tensile Stress

$S_{Total} = S_T + S_B$

$= 25.4 + 265.1$

$= 290.5$ MPa

Average Shear Stress due to F_x and F_z

$V = [F_x^2 + F_z^2]^{1/2} = 236.7$ kN

$$\tau = \frac{V}{A} = \frac{236.7 \times 10^3}{0.0054} = 43.8 \text{ MPa}$$

$$\text{Max. Shear Stress} = \left[\frac{(S_{Total})^2}{2} + \tau^2 \right]^{1/2}$$

$$= \left[\left(\frac{240.5}{2} \right)^2 + 43.8^2 \right]^{1/2}$$

$= 151.7$ MPa

For ASME SA479 Type XM-19

Therefore $\tau_{all} = (0.5)(S_y) = 190$ MPa > 151.7 MPa

(c) Cap Screws

Assume shear load is supported by shear disc; therefore only tension in cap screws needs to be considered:

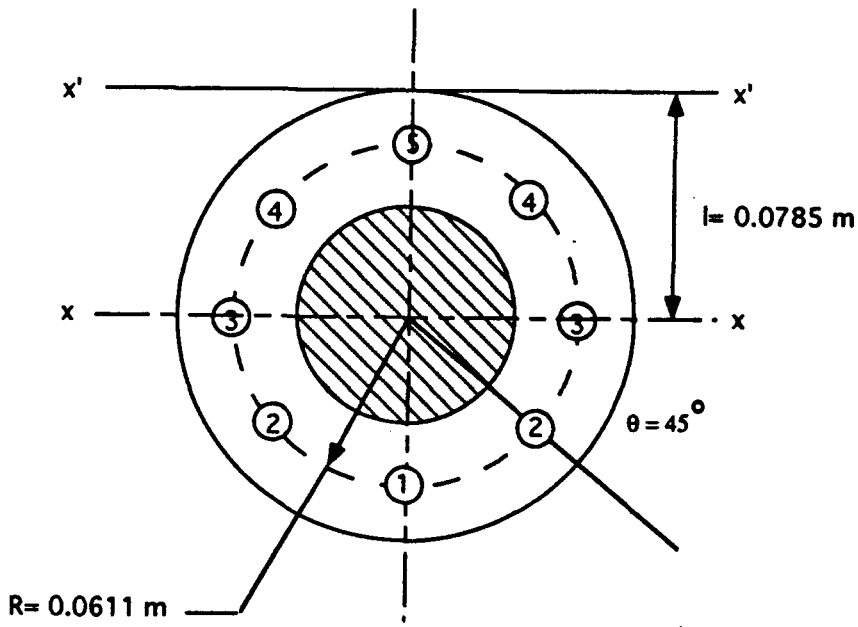

From Welding Research Council Bulletin 236 (Reference 15),

$$F_B = M \left[\frac{L/R + \cos (J-1)\,\theta}{NR\,[(L/R)^2 + 1/2]} \right]$$

The maximum tensile load will occur on cap screw located at position '1' due to a bending moment about $x^1 - x^1$.

where $M = (236.7)\,(0.0953) = 29.43$ kN.m

$R = 0.0611$ m

$L = 0.0785$ m

$\theta = 45°$

$N = 8$

$J = 1$

$$F_B = \frac{29.43 \times 10^3 \left[0.0785/0.0611 + \cos (1-1)\, 45° \right]}{8\,(0.0611) \left[\left[\frac{0.0785}{0.0611} \right]^2 + \frac{1}{2} \right]}$$

$$= \frac{29.43 \times 10^3\ (2.286)}{8(0.0611)(2.15)}$$

$$= 29.43 \times 10^3\ (2.175)$$

$$F_B = 49.1 \text{ kN}$$

Tensile Load due to F_y on cap screw located at position '1' is,

$$F_T = \frac{F_y}{8} = \frac{137}{8} = 17.1 \text{ kN}$$

Total Tension Load, $F_{Total} = F_B + F_T$

$$= 49.1 + 17.1$$

$$= 66.2$$

For 1/2" UNC Thread

Tensile Stress Area = 0.1419 in^2 (9.14×10^{-5} m^2) from CSA B1.1

$$\text{Tensile Stress} = \frac{66.2 \times 10^3}{9.14 \times 10^{-5}} = 724.3 \text{ MPa}$$

For ASME SA 564 Type 630 H1100

$$S_y = 795 \text{ MPa}$$

Therefore, $S_{allowable} = 795 > 724.3$ MPa

(d) <u>Safety Hoist Rings</u>

Each safety hoist ring has a rated capacity of 66.7 kN (15,000 lbs) with a factor of safety of 5 on the ultimate strength of 333.6 kN. This is less than the tiedown force of 273 kN.

A.5.1.2 <u>Rail and Air Transportation</u>

<u>Design Loads:</u>

Longitudinal	± 10 g
Lateral	± 2 g
Vertical	± 4 g

The vertical acceleration includes gravity and are actual absolute factors experienced by the package. The loads are assumed to be applied simultaneously.

Design Criteria:

The applied stress will not exceed the yield strength of the components.

Assumptions:

(i) tiedowns are flexible and cannot support compression,

(ii) package is chocked (blocked) to the conveyance; and

(iii) friction is neglected.

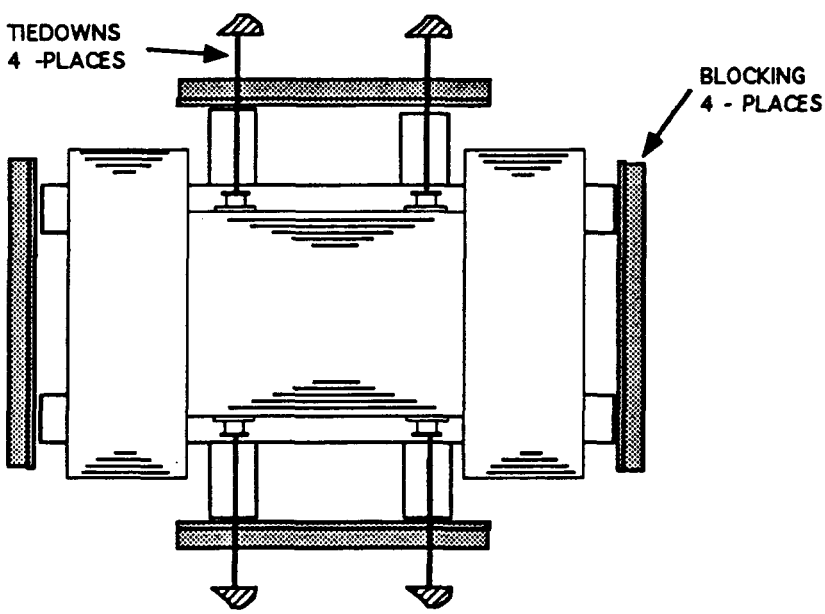

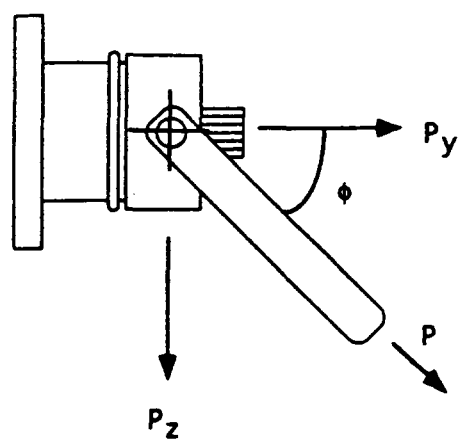

In general,

$$P = P_y^2 + P_z^2$$

$$P_y = P \cos \phi$$

$$P_z = P \sin \phi$$

$$P_x = 0$$

Tiedown loads due to 10 g in the longitudinal direction (direction of travel)

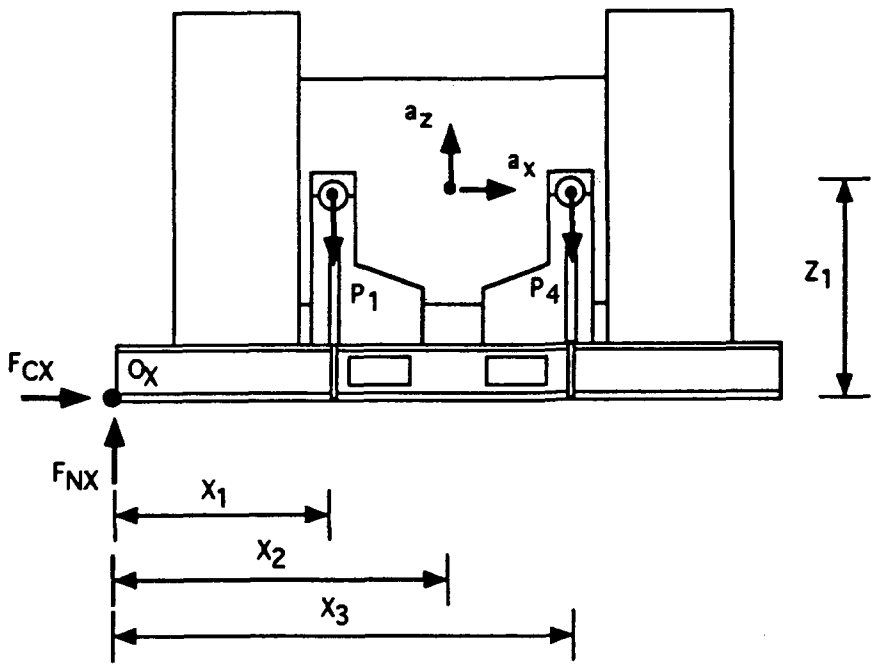

$$\Sigma M_{ox} = 0$$

and $P_{1x} = P_{3x}$

$P_{2x} = P_{4x}$ due to symmetry

$$Wg_x \, z_1 = 2 \, P_{1x} \sin \phi \, x_1 + 2 \, P_{4x} \sin \phi \, x_3$$

Assuming all tiedown members have the same stiffness then the tension in P_1 is directly proportional to the tension in P_4 due to rotation about 'O_x' as follows,

$$P_1 = \frac{\sqrt{x_1^2 + z_1^2}}{\sqrt{x_3^2 + z_1^2}} \, P_4$$

Therefore,

$$Wg_x \; z_1 = 2 \left[\frac{x_1^2 + z_1^2}{x_3^2 + z_1^2} \right]^{1/2} P_{4x} \sin \phi \; x_1$$

$$+ 2 \, P_{4x} \sin \phi \; x_3$$

$$= 2 \, P_{4x} \sin \phi \left\{ x_1 \left[\frac{x_1^2 + z_1^2}{x_3^2 + z_1^2} \right]^{1/2} + x_3 \right\}$$

$$P_{4x} = \frac{Wg_x \, z_1}{2 \sin \phi \left\{ x_1 \left[\frac{x_1^2 + z_1^2}{x_3^2 + z_1^2} \right]^{1/2} + x_3 \right\}}$$

Tiedown loads due to 5 g in the lateral direction (y-direction)

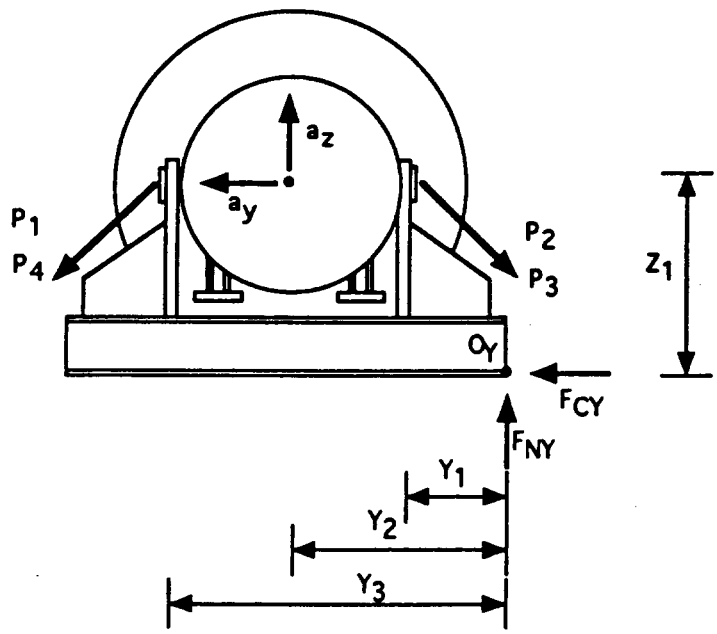

$$\Sigma M_{ox} = 0$$

and $P_{1y} = P_{4y}$ due to symmetry

$P_{2y} = P_{3y} = 0$ cannot support compression

$$M_{gy} z_1 = 2 P_{4y} \cos \phi z_1 + 2 P_{4y} \sin \phi y_3$$

$$P_{4y} = \frac{M_{gy} z_1}{2 (\cos \phi z_1 + \sin \phi y_3)}$$

Loads due to 4 g in the vertical direction (z-direction) and assuming all four tiedowns can support the vertical load upwards

$\Sigma F_z = Ma_z$ in the z-direction

and $P_{1z} = P_{2z} + P_{3z} = P_{4z}$

$$4P_{4z} \sin \phi = Wg_z$$

$$P_{4z} = \frac{W_{gz}}{4 \sin \phi}$$

Summing up the total load (maximum) acting on tiedown member No. 1 as follows:

$$P_{4x} = P_{4x} + P_{4y} + P_{4z}$$

$$= \frac{W_{gx} z_1}{2 \sin \phi \left\{ x_1 \left[\frac{x_1^2 + z_1^2}{x_3^2 + z_1^2} \right]^{1/2} + x_3 \right\}}$$

$$+ \frac{W_{gy} z_1}{2 (\cos \phi z_1 + \sin \phi y_3)}$$

$$+ \frac{W_{gz}}{4 \sin \phi}$$

Let $x_1 = 0.698$ m (27.5") $\quad g_x = 10$

$x_2 = 1.117$ m (44") $\quad g_y = 2$

$x_3 = 1.536$ m (60.5") $\quad g_z = 4$

$y_1 = 0.178$ m (7") $\quad \phi = 45°$

$y_2 = 0.609$ m (24") $\quad W = 57968$ N (13,000 lbs)

$y_3 = 1.193$ m (47")

$z_1 = 0.761$ m (30")

Substituting,

$$P_4 = \frac{(57968)\ (10)\ (0.761)}{2 \sin 45 \left[0.698 \left[\frac{0.698^2 + 0.761^2}{1.536^2 + 0.761^2} \right]^{1/2} + 1.536 \right]}$$

$$+ \frac{(57968)\ (2)\ (0.761)}{2\ (0.761 \cos 45 + 1.193 \sin 45)}$$

$$+ \frac{57968)\ (4)}{4 \sin 45}$$

$$P_4 = 57968\ (2.750 + 0.551 + 1.414)$$

$$= 57968\ (4.715)$$

$$= 273 \text{ kN}$$

Therefore, resolving the tiedown forces in the x, y, z coordinates

$$P_x = 0$$

$$P_y = 273 \cos 45$$

$$= 193 \text{ kN}$$

$$P_z = 273 \cos 45$$

$$= 193 \text{ kN}$$

Forces on the chocks neglecting friction,

In the x-direction,

$$\Sigma F_x = Ma_x$$

$$F_{cx} = Wg_x$$

$$= 57868\ (10)$$

$$= 580 \text{ kN}$$

In the y direction,

$$\Sigma F_y = Ma_y$$

$$2 P_{4y} \cos \phi + F_{cy} = Wg_y$$

$$F_{cy} = Wg_y - 2 P_{4y} \cos \phi$$

$$= (57968) (2) - (2) (57968) (0.55) \cos 45$$

$$= 70.8 \text{ kN}$$

Because of chocking, the chock forces will be transmitted to the trunnions of the package. Therefore in addition to the tiedown loads, the total loads acting on the trunnion (in position no. 4) will be as follows:

$$F_x = \frac{F_{cx}}{4} = \frac{580}{4} = 145 \text{ kN}$$

$$F_z = P_z = 193 \text{ kN}$$

$$F_y = P_y + \frac{F_{cy}}{4} = 193 + \frac{70.8}{4} = 210.7 \text{ kN}$$

$$F_z^1 = (P_{4x} + P_{4y}) \sin \phi$$

$$= 57968 (2.75 + 0.550) \sin 45$$

$$= 135.5 \text{ kN}$$

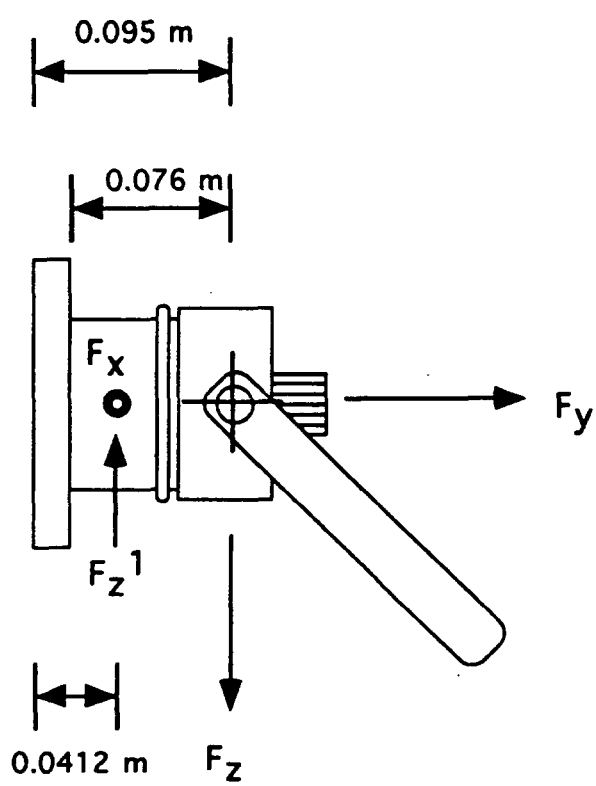

A.5.1.2.1 Component Analysis

(a) Shear Disc

Diameter, D = 0.06 m (2.302 in.)

Shear Area = $\frac{\pi}{4}(0.06)^2 = 0.0028 m^2$

Shear Force = $[\ F_x^2 + (F_z - F_z^1)^2\ ]^{1/2}$

$= [\ 145^2 + (193 - 135.3)^2\ ]^{1/2}$

= 156.1 kN

Average Shear Stress = $\tau = \frac{\upsilon}{A} = \frac{156.1 \times 10^3}{0.0028}$

= 55.8 MPa

For ASME SA 476 Type XM-19

Sy = 380 MPa

Therefore, $\tau_{allowable}$ = 0.5 Sy = 190 MPa > 55.8 MPa

(b) Trunnions

Stress Area, $A = \frac{\pi}{4}(D_o^2 - D_i^2)$

$= \frac{\pi}{4}(0.089^2 - 0.032^2)$

$= 0.0054 m^2$

Tensile Stress due to F_y

$S_T = \frac{F_y}{A} = \frac{210.7}{0.0054} = 39.0$ MPa

Bending Stress due to F_x and F_z

$S_B = M_{xz}\ \frac{c}{I}$

$M_{xz} = [\ M_x^2 + M_z^2\ ]^{1/2}$

$M_x = F_x \cdot e_x$

$= (145)\ (0.022)$

= 3.22 kN.m

$$M_z = F_z \cdot e_z - F_z^1 \, e_x$$

$$= (193)\ (0.076) - (135.3)\ (0.022)$$

$$= 11.7 \text{ kN.m}$$

$$M_{xz} = [\ 3.22^2 + 11.7^2\ ]^{1/2}$$

$$= 12.13 \text{ kN.m}$$

$$c = \frac{0.0889}{2} = 0.0445 \text{ m}$$

$$I = \frac{\pi}{64}\ [\ (0.0889)^4 - (0.0318)^4\ ]$$

$$= 3.02 \times 10^{-6} \text{ m}^4$$

$$S_B = \frac{(12.13)\ (10^3)\ (0.0445)}{3.02 \times 10^{-6}}$$

$$S_B = 178.7 \text{ MPa}$$

Total Tensile Stress

$$S_{TOTAL} = S_T + S_B$$

$$= 39.0 + 178.7$$

$$= 217.7 \text{ MPa}$$

Average Shear Stress due to F_x and F_z

$$V = [\ F_x^2 + (F_z - F_z^1)^2\ ]^{1/2} = 156.0 \text{ kN}$$

$$\tau = \frac{V}{A} = \frac{156.0 \times 10^3}{0.0054} = 28.9 \text{ MPa}$$

Maximum Shear Stress

$$\tau_{max} = \left[\left(\frac{S_{TOTAL}}{2} \right)^2 + \tau^2 \right]^{1/2}$$

$$= \left[\left(\frac{217.7}{2} \right)^2 + 28.9^2 \right]^{1/2}$$

$$= 112.6 \text{ MPa}$$

For ASME SA 479 Type XM-19

$$Sy = 380 \text{ MPa}$$

Therefore $\tau_{all} = 0.5\ Sy = 190 \text{ MPa} > 112.6 \text{ MPa}$

(c) Cap Screws

From Section A5.1.1.1(c), the maximum tensile load due to bending is as follows,

$$F_B = M_{xz} \quad 2.175$$

$$M_{xz} = [\ M_x^2 + M_z^2\ ]^{1/2}$$

$$M_x = F_x \cdot e_x^1$$

$$= (145)\ (0.0412)$$

$$= 5.98 \text{ kN.m}$$

$$M_z = F_z \cdot e_z^1 - F_z^1 \cdot e_x^1$$

$$= (193)\ (0.0953) - (135.3)\ (0.0412)$$

$$= 12.8 \text{ kN.m}$$

$$M_{xz} = [\ (5.98)^2 + (12.8)^2\ ]^{1/2} = 14.12$$

$$F_B = (14.12)\ (2.175)$$

$$= 30.7 \text{ kN}$$

Tensile load due to F_y on cap screws

$$F_T = \frac{F_y}{8} = \frac{210.7}{8} = 26.33 \text{ kN}$$

Total tensile load,

$$F_{TOTAL} = F_B + F_T$$

$$= 30.7 + 26.33$$

$$= 57.03 \text{ kN}$$

For 1/2" UNC Thread

Tensile Stress Area, $A = 9.14 \times 10^{-5}\ m^2$

$$\text{Tensile Stress} = \frac{57.03 \times 10^3}{9.14 \times 10^{-5}} = 624.0 \text{ MPa}$$

For ASME SA 564 Type 630 H1100

$$Sy = 795 \text{ MPa}$$

Therefore, $S_{allowable} = 795 > 624.0$ MPa

(d) Safety Hoist Rings

Each safety hoist ring has a rated capacity of 66.7 kN (15,000 lbs) with a factor of safety of 5 on the ultimate strength of 333.6 kN. This is less than the tiedown force of 273 kN.

(e) Air/Rail Shipping Frame (Drawing E-5580-113)

Under chocked conditions, the chocked forces, F_{cx} and F_{cy} will be transferred through the shipping frame. For the purposes of analysis assume each trunnion support location takes 25% of the chock loads as follows:

$$F_x = \frac{F_{cx}}{4} = \frac{580}{4} = 145 \text{ kN}$$

$$F_y = \frac{F_{cy}}{4} = \frac{70.8}{4} = 17.7 \text{ kN}$$

i) Stresses on Trunnion saddle

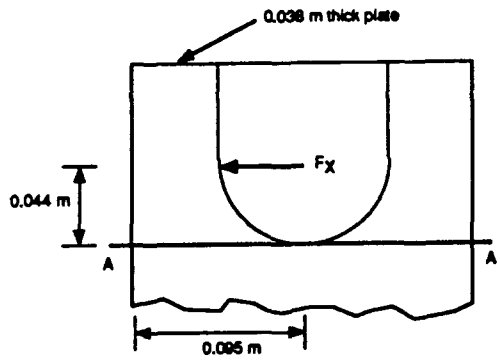

Stresses due to F_x at Section A-A

Bending Stress $S_B = \frac{Mc}{I}$

$$= \frac{(0.044)\ (145 \times 10^3)\ (0.095/2)}{\frac{1}{12}\ (0.038)\ (0.095)^3}$$

$$= 111.6 \text{ MPa}$$

Average Shear Stress $\tau = \frac{F}{A}$

$$= \frac{145 \times 10^3}{(0.038)(0.095)}$$

$$= 40.2 \text{ MPa}$$

$$\tau_{max} = \left[\left(\frac{111.6}{2} \right)^2 + 40.2^2 \right]^{1/2}$$

$$= 68.8 \text{ MPa}$$

For ASTM A36 Carbon Steel Sy = 250 MPa
Su = 400 - 500 MPa

Allowable Shear Stress,

$$\tau_{all} = 0.5\ Sy = 125 \text{ MPa} > 68.8 \text{ MPa}$$

Bending Stresses due F_y

Bearing Area of Trunnion

$$A_B = \frac{\pi}{8}\ (0.102^2 - 0.095^2)$$

$$= 5.28 \times 10^{-4}\ m^2$$

Bearing Stress

$$\tau_{BR} = \frac{F_y}{A_B} = \frac{17.7 \times 10^3}{5.28 \times 10^{-4}}$$

$$= 33.5 \text{ MPa}$$

For ASTM A36 Sy = 250 MPa > 33.5 MPa

For ASME SA 479 Type XM-19 Sy = 380 MPa > 33.5 MPa

(ii) Stresses on Gusset Support Fillet Welds

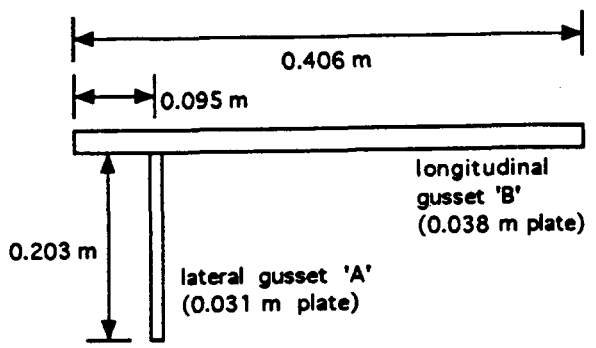

Stressed due to F_x and F_{zx}:

For the purposes of analysis, conservatively assume gusset plate B only takes the loads due to F_x and F_{zx}. Treating the weld as a line Reference 16:

Section Modulus Z_w about axis x-x

$$Z_w = bd + \frac{d^2}{3}$$

$$= (0.406)\ (0.038) + \frac{(0.406)^2}{3}$$

$$= 0.0704 \ \text{m}^2$$

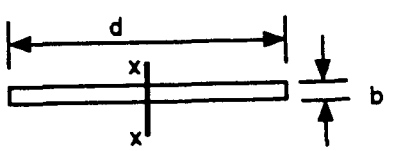

Bending Unit Load

$$f_B = \frac{M}{Z_w}$$

$$= \frac{F_x h_x - F_{zx} e_x}{Z_w}$$

$$= \frac{(145 \times 10^3)\ (0.558) - (112.7 \times 10^3)\ (0.406 - 0.095)}{0.0704}$$

$$= 6.514 \times 10^5 \text{ N/m}$$

Compressive Unit Load

$$f_c = \frac{F_{zx}}{L}$$

$$= \frac{112.7 \times 10^3}{2(0.406 + 0.038)}$$

$$= 1.269 \times 10^5 \text{ N/m}$$

Shear Unit Load

$$f_v = \frac{F_x}{L}$$

$$= \frac{14.5 \times 10^3}{2(0.406 + 0.038)}$$

$$= 1.633 \times 10^4 \text{ N/m}$$

Total Unit Load

$$f_{TOTAL} = [\ (6.514 - 1.269)^2 + (0.163)^2\ ]^{1/2} \times 10^5$$

$$= 5.247 \times 10^5 \text{ N/m}$$

For a weld throat length of (0.707) (9.52×10^{-2})

$$W_1 = 6.73 \times 10^{-3} \text{ m}$$

$$\tau_{shear} = \frac{5.247 \times 10^5}{6.73 \times 10^{-3}}$$

$$= 78 \text{ MPa}$$

Assuming the weld has the same minimum properties as the base material ASTM A36 Sy = 250 MPa, therefore $\tau_{allowable}$ = (0.5) (15) = 125 MPa > 78 MPa.

Stresses due to F_y:

Again for the purposes of analysis conservatively assume gusset plate 'A' only takes the loads due to F_y. Threating the weld as a line, section modules

$$Z_{wA} = \frac{d^2\ (2b + d)}{3\ (b + d)}$$

where d = 0.305 m

b = 0.032 m

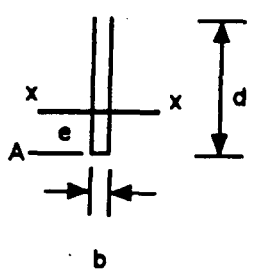

$$Z_{wA} = \frac{(0.305)^2 \; [\; (2)\;(0.032) + 0.305]}{2\;(0.305 + 0.032)}$$

$$= 0.051 \text{ m}^2$$

Centroid

$$e = \frac{d^2}{b + 2d} = \frac{(0.305)^2}{(0.032)+(2)(0.305)} = 0.145 \text{ m}$$

The maximum stresses will occur at the gusset location where the tiedown loads are also transferred to the gusset plates.

Bending Unit Load,

$$f_B = \frac{(F_y)\;(h_y) - (F_{yz})\;(d - e)}{Zw_A}$$

$$f_B = \frac{[\;(17.7 \times 10^3)\;(0.558) + (22.6 \times 10^3)\;(0.305 - 0.145)}{0.051}$$

$$f_B = 2.603 \times 10^5 \text{ N/m}$$

Compression Unit Load,

$$f_c = \frac{F_{yz}}{L}$$

$$= \frac{22.6 \times 10^3}{2(.305)+0.032}$$

$$= 3.502 \times 10^4 \text{ N/m}$$

Shear Unit Load,

$$f_v = \frac{F_y}{L}$$

$$= \frac{17.7 \times 10^3}{2(0.305)+0.032}$$

$$= 2.757 \times 10^4 \text{ N/m}$$

Total Unit Load,

$$f_{TOTAL} = [\;(f_B - f_c)^2 + f_v^2\;]^{1/2}$$

$$= [\;(2.603 - 0.350)^2 + (0.276)^2\;]^{1/2} \times 10^5$$

$$= 2.270 \times 10^5 \text{ N/m}$$

$$\tau_{shear} = \frac{2.270 \times 10^5}{6.73 \times 10^{-3}}$$

$$= 33.73 \text{ MPa}$$

$\tau_{allowable} = (0.5)\ (250) = 125\ MPa > 33.73\ MPa$

(iii) Stresses on Support Beam

Stresses on longitudinal beam due to F_x and F_{zx}

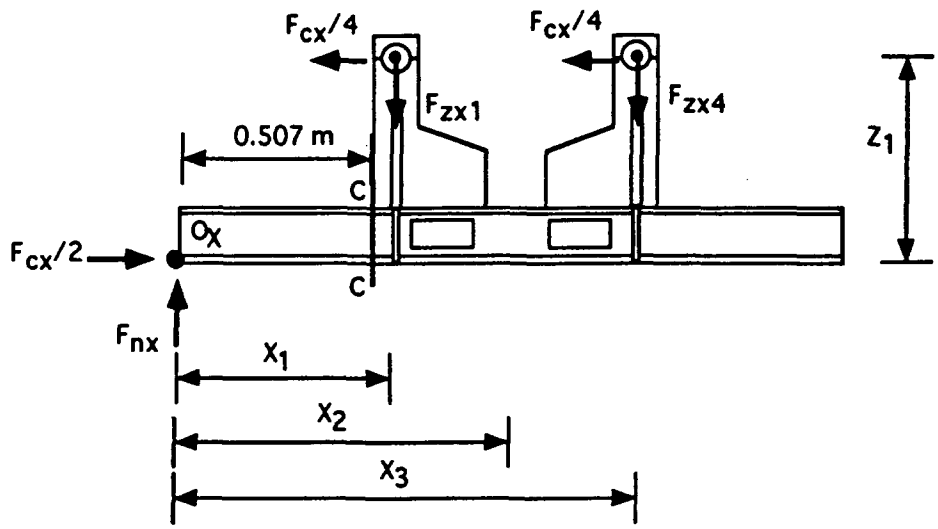

where $x_1 = 0.698m\ (27.5")$

$x_3 = 1.536m\ (60.5")$

$z_1 = 0.761m\ (30")$

$F_{cx} = 580\ kN$

$F_{zx4} = 112.7\ kN$

$$F_{zx1} = \left[\frac{x_1^2 + z_z^2}{x_3^2 + z_1^2} \right]^{1/2} F_{x4}$$

$$= (0.602)\ (112.7)$$

$$= 67.9\ kN$$

$$F_{Nx} = F_{zx4} + F_{zx1} = 180.6\ kN$$

Because the gusset plate will support the cut-out in the beam, the highest bending stresses will occur at location 'C'.

$$\sigma_B = \frac{M}{z} \; ; \; z = 4.96 \times 10^{-4} \text{ for W200 x 46 (W8 x 31) I-beam}$$

$$= \frac{(180.6 \times 10^3)(0.507)}{4.96 \times 10^{-4}}$$

$$= \pm 184.6 \text{ MPa}$$

Compressive Stress

$$\sigma_c = \frac{F_{cx}/2}{A} \; ; \quad A = 5.86 \times 10^{-3} \text{ m}^2$$

$$= \frac{260 \times 10^3}{5.86 \times 10^{-3}}$$

$$= -44.4 \text{ MPa}$$

The maximum stress will occur in compression

$$\sigma_{TOTAL} = -184.6 - 44.4 = 229.2 \text{ MPa}$$

For CSA G40.21 300W, the minimum yield strength is 300 MPa which is greater than the maximum compressive stress.

Stresses on lateral beam due to F_y and F_{zy}

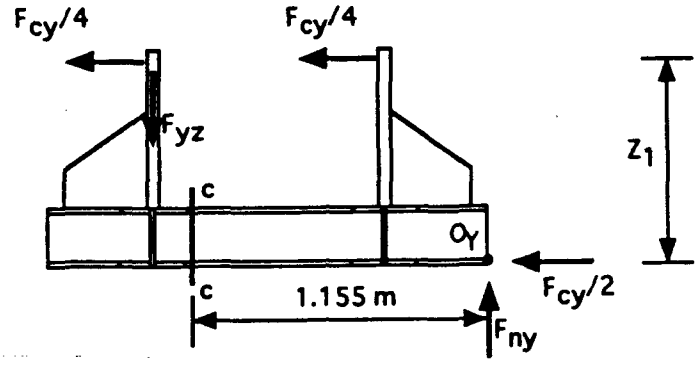

where $F_{cy} = 70.4$ kN

$F_{yz} = F_{Ny} = 22.5$ kN

$z_1 = 0.761$m (30")

Calculating the stresses at location 'C'

$$\sigma_B = \frac{M}{z}$$

$$= \frac{\left[\frac{F_{cy}}{4}\right]\left[z_1\right] - \left[F_{Ny}\right]\left[y_x\right]}{z}$$

$$= \frac{(70.4 \times 10^3)\ (0.761)/4 - (22.5 \times 10^3)\ (1.155)}{4.96 \times 10^{-4}}$$

$$= \pm\ 25.4 \text{ MPa}$$

Compressive Stresses

$$\sigma_c = \frac{F_{cy}/4}{A}$$

$$= \frac{(70.4 \times 10^3)/4}{5.86 \times 10^{-3}}$$

$$= -3.0 \text{ MPa}$$

The maximum stress will occur in compression

$$\sigma_{TOTAL} = -25.4 - 3.0 = -28.4 \text{ MPa}$$

For CSA G40.21 300W, the minimum yield strength is 300 MPa, which is greater than the maximum compressive stress.

A.5.2 Lifting Analysis

A.5.2.1 Trunnion Component Analysis

The package mass is approximately 5.9 Mg (13,000 lbs) and if only two trunnions are used, the lifting force on each trunnion is 29 kN. It is assumed that the safety hoist rings are used for lifting; thereby creating a larger bending moment on the trunnions than if the trunnion are used for lifting.

Design Load: 29 kN

Design Criteria: $\frac{1}{3}$ Sy

Assumptions:

(i) only two trunnions are used for lifting; and

(ii) the safety hoist rings are used for lifting.

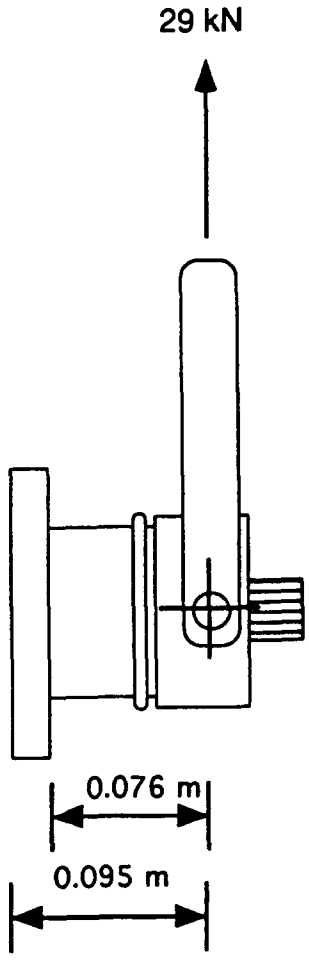

(a) Shear Disc

Shear Area = $\frac{\pi}{4}(0.06)^2 = 0.0028\ m^2$

Average Shear Stress $\tau = \frac{V}{A} = \frac{29 \times 10^3}{0.0028} = 10.4$ MPa

For ASME SA 479 Type XM-19 $S_y = 380$ MPa

Therefore $\tau_{all} = (0.5)\left(\frac{380}{3}\right) = 63.3$ MPa > 10.4 MPa

(b) Trunnions

Bending Stress $S_B = M \cdot \frac{c}{I}$

where, $M = (29000)(0.076) = 2204$ N.m

$c = 0.0445$ m

$I = 3.02 \times 10^{-6}\ m^4$

$S_B = \frac{(2204)(0.0445)}{3.02 \times 10^{-6}} = 32.5$ MPa

Shear Stress $\tau = \frac{V}{A} = \frac{29 \times 10^3}{0.0054} = 5.37$ MPa

Stress Intensity $= [(\frac{S_B}{2})^2 + \tau^2]^{1/2}$

$= \left[\left(\frac{32.5}{2}\right)^2 + (5.37.3)^2\right]^{1/2} = 17.1$ MPa

For SA479 Type XM-19 $S_y = 380$ MPa

Therefore $\tau_{all} = (0.5)\left(\frac{380}{3}\right) = 63.3 > 17.1$ MPa

(c) Cap Screws

The maximum tensile load on the cap screws is,

$$F_B = \frac{M\,[\,L/R + \cos\,(J-1)\,\theta\,]}{NR\,[\,(L/R)^2 + 1/2]}$$

where, $M = (29 \times 10^3)\,(0.0953) = 2764$ N.m

$R = 0.0611$ m

$L = 0.0785$ m

$\theta = 45°$

$N = 8$

$J = 1$

$$F_B = (2764)\,(2.175) = 6012 \quad N$$

$$\text{Tensile Stress} = \frac{6012}{9.14\text{x}10^{-5}} = 65.8 \text{ MPa}$$

For ASME SA 564 Type 630 H1100

$$S_y = 795 \text{ MPa}$$

$$\text{Therefore, } S_{allowable} = \frac{795}{3} = 265 > 65.8 \text{ MPa}$$

A.5.2.2 Safety Hoist Rings

Each safety hoist ring has a rated capacity of 66.7 kN (15,000 lbs) with a factor of safety of five on the ultimate strength of 333.6 kN. This is less than the lifting force of 29 kN.

A.5.2.3 Lifting Bar

The stresses due to lifting in the attachment weld can be given by the following formula from Reference 17:

$$S_u \geq \beta \left[S_1^2 + 3\,(\tau_1^2 + \tau_2^2) \right]^{1/2}$$

where,

S_u = minimum ultimate tensile strength of the base material

β = 0.7 for steels with a yield strength less than 241 kPa

S_1 = normal stress perpendicular to the weld throat

τ_1 = shear stress acting in the throat parallel to the axis of the weld

τ_2 = shear stress acting in the throat transverse to the axis of the weld

The fillet weld specified has a leg size of 9.5 mm and is continuous around the lifting bar which is 1016 mm long. The lifting bar is designed for "two-point" lifting. Therefore at each lift point there will be localized shear and bending forces in addition to the tensile forces in the weldment. The local forces and bending moment for a load of 41.0 kN acting at 45° angle will be as follows:

$P_{tension}$ = 29000 N

P_{shear} = 29000 N

M = (29000) (0.0635)

= 1695 N.m

Assuming an effective weld length of 150 mm on each side of the bar, then

$$S_1 = \tau_1 = \frac{P_T}{tL} + \frac{M}{Z}$$

$$\tau_1 = \frac{29000}{(0.707)(0.0095)(2)(0.15)} + \frac{1841.5}{\frac{(0.0095)(0.707)(2)(0.15)^3}{12\ (0.0762)}}$$

$$= 14.3 + 37.2$$

$$= 51.5 \text{ MPa}$$

$$\tau_2 = \frac{P_s}{tL}$$

$$= \frac{29000}{(0.707)(0.0095)(2)(0.15)}$$

$$= 14.3 \text{ MPa}$$

Therefore,

$$\beta \left[S_1^2 + 3 (\tau_1^2 + \tau_2^2) \right]^{1/2} = 0.7 \, [51.5^2 + 3 \, (51.5^2 + 14.3^2)]^{1/2}$$

$$= 74.2 \text{ MPa}$$

For a 304 stainless steel base material, the ultimate tensile strength is 485 MPa. The factor of safety would exceed seven.

A6 External Pressure Analysis

To satisfy the requirements of water immersion, the following calculations demonstrate that the package containment components can maintain its structural integrity without yielding when subjected to an external gauge pressure of 150 kPa which is equivalent to 15m of water. For conservatism, it assumes the package cavity is not pressurized above atmospheric pressure.

A6.1 Main Flask Body

Treating the main flask body as a thick-walled cylinder, the maximum stresses will occur on the inside diameter when subjected to an external pressure as follows:

Radial Stress $S_r = 0$

Tangential or Hoop Stress $S_t = \dfrac{-2OD^2 \, P_o}{OD^2 - ID^2}$

Axial Stress or Longitudinal $S_a = -\dfrac{\pi}{4} P_o \, (OD^2 - ID^2)$

Substituting the following values,

$P_o = 0.150$

$OD = 0.761$ m

$ID = 0.325$ m

Results in the following stresses,

$S_r = 0$

$S_t = -\ 0.367$ MPa

$S_a = -\ 0.056$ MPa

This is less than the yield strength at 38°C for SA 182 F304 material (205 MPa) as given in Table 6.2.

A.6.2 Rear Cover Plate

Evaluating the plate with a uniform pressure and simply supported at its outer diameter and assuming the plate is not uniformly supported by the rear flange, the maximum bending moment (at the centre of the plate) will be (Reference 9):

$$M_c = \frac{P_o \left[\frac{OD}{2} \right]^2 (3 + \upsilon)}{16}$$

substituting for

$P_o = 0.150$ MPa

$OD = 0.190$ m

$\upsilon = 0.3$

$M_c = 279.2$ N.m/m

the bending stress is given by

$$S_r = S_t = \frac{6\ M_c}{t^2}$$

$$= \frac{(6)\ (279.2)}{(0.022)^2}$$

$$= 3.5 \text{ MPa}$$

This is less than the yield strength of 205 MPa as shown in Table 6.2

A.6.3 Valve Cover Plate

Using the same calculation procedure as for the rear cover plate with an outer diameter of 0.327 m and a thickness of 0.05 m, the bending stress at the centre will be

$$S_r = S_t = \frac{3\ OD^2\ (3 + \upsilon)\ P_o}{32\ t^2}$$

$$= \frac{(3)\ (0.327)^2\ (3.3)\ (0.150)}{32\ (0.05)^2}$$

$$= 2.0 \text{ MPa}$$

which is less than the allowable S_y (205 MPa) at 38°C

A6.4 Rear Flange

For the rear flange where, OD = 0.495 m

$$t(_{min}) = 0.0286 \text{ m}$$

$$S_r = S_t = \frac{3\ OD^2\ (3 + \upsilon)\ P_o}{32\ t^2}$$

$$= \frac{(3)\ (0.495)^2\ (3.3)\ (0.150)}{(32)\ (0.0286)^2}$$

$$= 13.9 \text{ MPa}$$

$$S_m = 138 \text{ MPa} > 13.9 \text{ MPa}$$

A6.5 Front Flange

For the front flange where OD = 0.495 m

$$t(min) = 0.051 \text{ m}$$

$$S_r = S_t = \frac{3\ OD^2\ (3 + \upsilon)\ P_o}{32\ t^2}$$

$$= \frac{(3)\ (0.495)^2\ (3.3)\ (0.150)}{(32)\ (0.051)^2}$$

$$= 4.4 \text{ MPa}$$

$$S_y = 205 \text{ MPa} > 4.4 \text{ MPa}$$

A7 REFERENCES

1. T.K. Hill and W.W. Joseph, "Energy-Absorbing Characteristics of Materials", Sandia Laboratories, SLA-74-0159, 1974 May.

2. AECL Research, "Compression Test Results on Wood Samples for Impact Limiters", Engineering and Design Division Document No. A-13318-TN-2.

3. R.L. Hankinson, "Investigation of Crushing Strength of Spruce at Various Grain Angles of Grain", U.S. Air Service, Air Service Information CIR III (259), 15 pp (1921).

4. Wood Handbook, "Wood as an Engineering Material", Chapter 4, US Department of Agriculture, Forest Service, Agriculture Handbook 72, 1987.

5. Shipping Cask Analysis System (SCANS) Volume 2 - Theory Manual, Impact Analysis, NUREG/CR 4554 (UCID-20674) Volume 2, February 1989.

6. AECL Research, "Irradiated Material Transportation Package - Results of Prototype Testing", Engineering and Design Division Document No. A-13318-TN-4.

7. American Society of Mechanical Engineers Boiler and Pressure Vessel Code Section III, "Rules for Construction of Nuclear Power Plant Components", Division I Appendices, Appendix F, "Rules of Evaluation of Service Loadings with Level D Service Limits", 1992 Edition.

8. American Society of Mechanical Engineers Boiler and Pressure Vessel Code Section III, "Rules for Construction of Nuclear Power Plant", Division 1 - Subsection NB, Article NB-3000 "Design", 1992 Edition.

9. S. Timoshenko and S. Woinowsky - Krieger, "Theory of Plates and Shells", McGraw-Hill, 2nd Edition, 1959.

10. AECL Research, "Irradiated Material Transportation Package Test Specification for Prototype Testing", Engineering and Design Division Document No. A-13318-SP-2.

11. AECL Research, "Irradiated Material Transportation Package Procedure for Prototype Drop Testing", Engineering and Design Division Document No. A-13318-PR-2.

12. AECL Research, "Irradiated Material Transportation Package - Fire Test Plan", Engineering and Design Division Document No. A-13318-PR-2.

13. R. Zane, "Pool Fire Testing of the IMT Package for Atomic Energy of Canada Limited", Ontario Hydro Report B93-11-P, April 23, 1993.

14. International Atomic Energy Agency, Safety Series No. 37, "Advisory Material for the IAEA Regulations for the Safe Transport of Radioactive Material (1985 Edition) Third Edition (As Amended 1990).

15. Welding Research Council Bulletin No. 236, "Determination of Stiffness and Loading in Bolted Joints Having Circular Geometry".

16. Blodgett, O.W., "Design of Welded Structures", The James F. Lincoln Arc Welding Foundation, 1966.

17. S.W.K. Chan, "The Strength of Fillet Welded Joints in Steels Subjected to Static Loading - A Review". Welding Institute Report 379 1988.

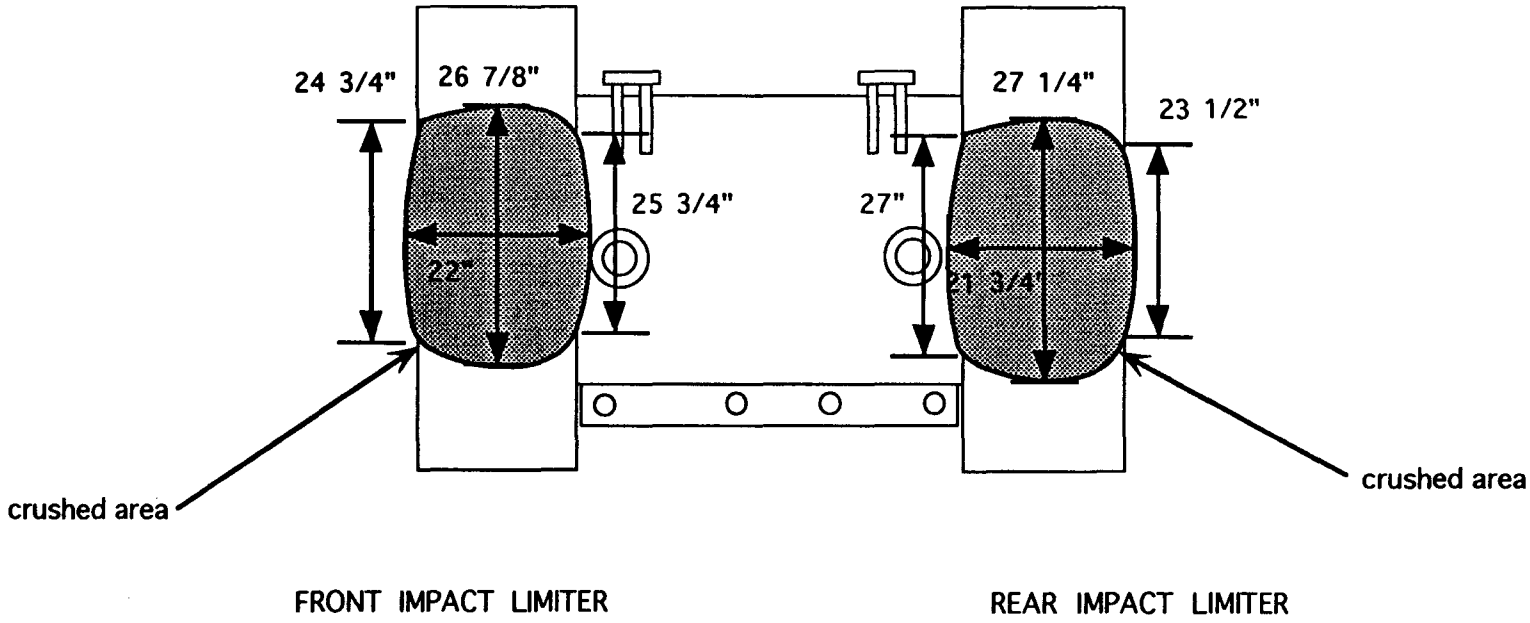

Figure A-4 Configuration of Impact Limiters after 9m Horizontal Side Drop Test

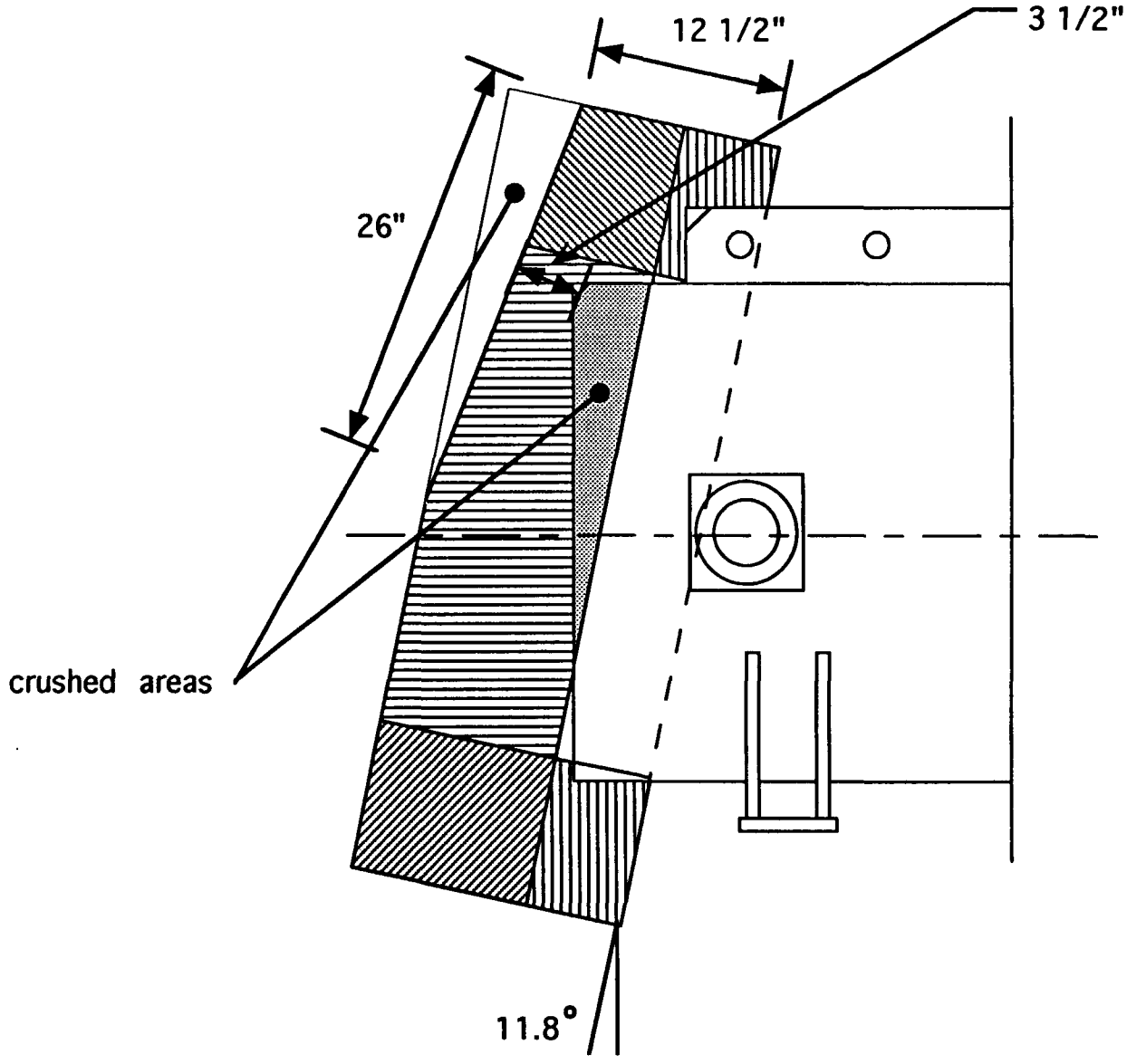

Figure A-5 Configuration of Rear Impact Limiter After 9m Oblique Angle Drop Test

APPENDIX B - THERMAL ANALYSIS

B.1 Normal Condition of Transport

The following analysis estimates the time that would be required for the package to come to thermal equilibrium for an ambient temperature of 38°C and after the package has been loaded with 160 watts of radioactive decay heat. Equation 7.2 in Section 7 gives the heat transfer equation as follows.

Q_t (total) = Q_c (convection) + Q_r (radiation) + Q_a (absorbed)

From Reference 1.*

$Q_c = A_c h_c \ (T_s - T_\infty)$

Where A_c = heat transfer area
= 2.548 m^2
h_c = convection co-efficient
= $1.32 \ [(T_s - T_\infty)/d]^{1/4}$
d = 0.76 m

$\therefore h_c = 1.41 \ (T_s - T\infty)^{1/4}$ watts/m^2K
T_s = package surface temperature K
$T\infty$ = ambient temperature, 311 K

Solving,

$Q_c = 3.59 \ (T_s - 311)^{5/4}$
$Q_r = A_r H_r \ (T_s - T_\infty)$

Where $A_r = A_c$
= 2.548 m^2
$h_r = \sigma EF \ (T_s^2 + T_\infty^2)(T_s + T_\infty)$
G = Stefan-Boltzmann constant
= 5.67×10^{-8} w/m^2k^4
E = emissivity factor
= 0.81 for stainless steel
F = view factor
= 1.0

$\therefore h_r = 4.59 \times 10^{-8} \ (T_s^2 + T_\infty^2)(T_s + T_\infty)$

Solving:

$$Q_r = 11.9 \left[\left(\frac{T_s}{100}\right)^4 - 3.11^4\right]$$

$$Q_z = c \ W \ \frac{\Delta T}{\Delta \theta}$$

* References are listed in Section B.3.

c = specific heat
= 0.036 W.h/kg K for lead
= 0.128 W.h/kg K for steel

W = 670 kg for lead shield insert
= 4271 kg for remaining steel

$\Delta T = T_s^1 - T_s$

T_s^1 = package surface temperature at the end of the time increment, $\Delta\theta$, K

T_s = package surface temperature at the beginning of the time increment $\Delta\theta$, K

$\Delta\theta$ = time increment, hours

Solving:

$$Q_q = 24.12 \frac{\Delta T}{\Delta\theta} \text{ for lead}$$

$$= 546.67 \frac{\Delta T}{\Delta\theta} \text{ for steel}$$

For simplification, consider the lead shield separately. Reference 1 shows that at equilibrium the shield temperature will be 52.2°C, a rise of 14.2°C.

Then $Q_a = \frac{342.5}{\Delta\theta}$

Since the decay heat is 160 watts, then $\Delta\theta \simeq 2$ hours.

So, consider that in the first two hours all the decay heat goes into the lead shield. Then, Q_a need only consider the steel.

Solving:

$$Q_t = 3.59\,(T_s - 311)^{5/4} + 11.9\left[\left(\frac{T_s}{100}\right)^4 - 3.11^4\right] = \frac{546.67}{\Delta\theta}\left[T_s^1 - T_s\right]$$

Substitute Q_t = 160 watts and rearrange.

$$T_s^1 - T_s = \frac{\Delta\theta}{546.67}\left[160 - 3.59\,(T_s - 311)^{5/4} - 11.9\left[\left(\frac{T_s}{100}\right)^4 - 3.11^4\right]\right]$$

Let $\Delta\theta$ = 2 h
T_s = 311K at beginning of $\Delta\theta$

Solving:

T_s^1 = 311.6K at end of $\Delta\theta$

Now, for the next $\Delta\theta = 2$ h
$T_s = 311.6$ K

Solving:

$T_s^1 = 312.1$ K and so on

The following table gives all the results.

Time, h	Lead Liner Temp °C	Steel Temp °C
0	38	38
2	52.2	38
4	52.2	38.6
6	52.2	39.1
8	52.2	39.6
10	52.2	40.1
12	52.2	40.5
14	52.2	40.9
19	52.2	41.8
24	52.2	42.6
29	52.2	43.2
34	52.2	43.7
44	52.2	44.5
54	52.2	45.0

As shown above and plotted in Figure B1, it would take more than 50 hours for the package to reach thermal equilibrium.

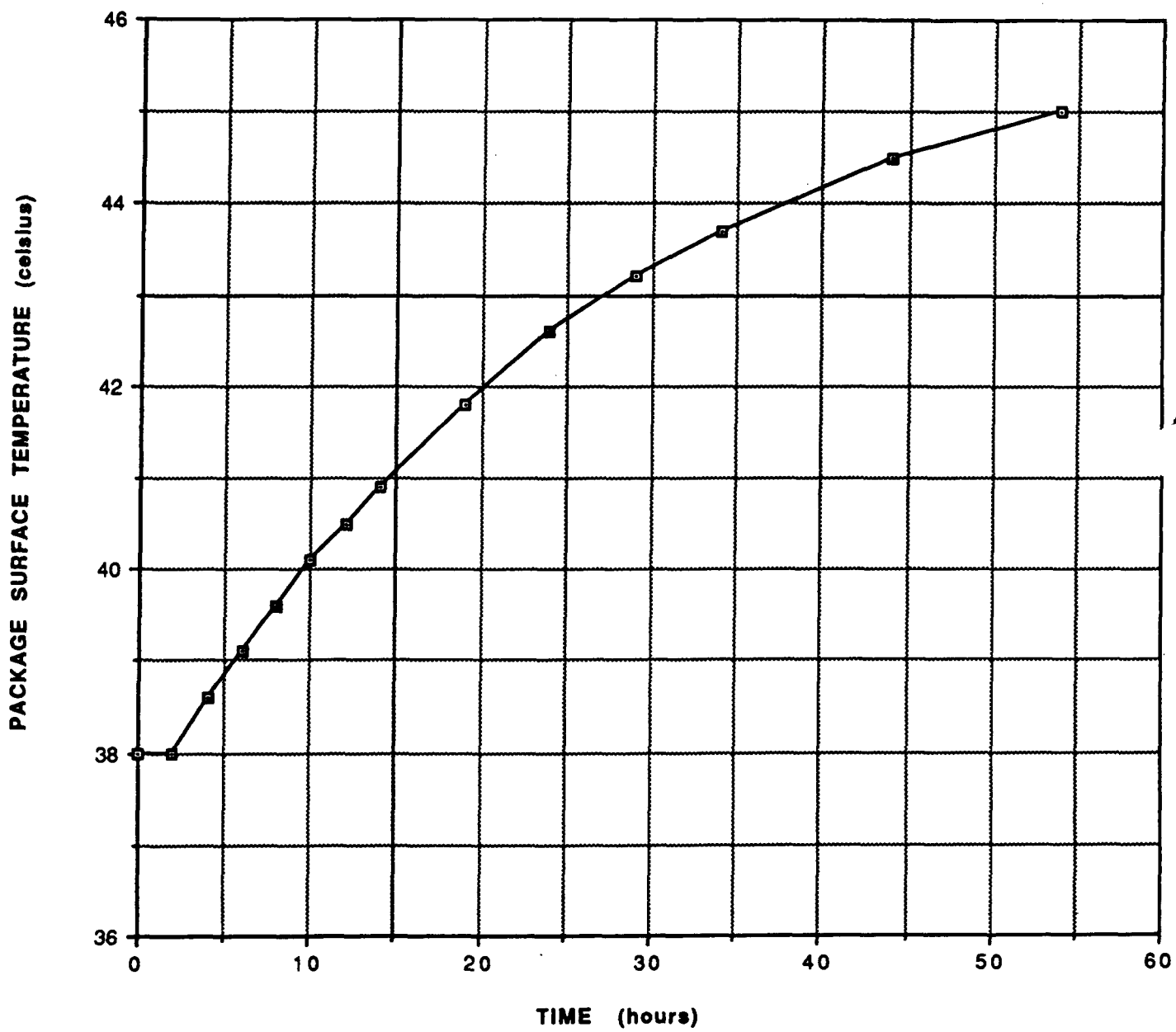

FIGURE B1 PACKAGE SURFACE TEMPERATURES - TIME TO REACH THERMAL EQUILIBRIUM

B.2 Accident Conditions of Transport

During the thermal evaluation of the package it was noted that the actual thermal test that was conducted was not an exact duplication of the regulatory thermal test. On one hand, the regulatory thermal test is 800°C for 30 minutes for the following conditions,

- no solar insolation
- ambient temperature 38°C
- decay heat load 160 watts.

On the other hand, the actual test was 900 to 990°C during the 30 minutes for the following initial conditions,

- no solar insolation
- ambient temperature 4°C
- decay heat load 0 watts.

The higher temperature during the fire test results in additional heat transfer primarily by radiative mechanisms. The ratio of actual radiative heat transfer to the regulatory radiative heat transfer is as follows:

$$\frac{Q_{Actual}}{Q_{Regulatory}} = \frac{[(T_{ACT} + 273)^4 - (T_{AMB} + 274)^4]}{[(800 + 273)^4 - (38 + 273)^4]}$$

$$= \frac{[(900 + 273)^4 - (4 + 273)^4]}{[(800 + 273)^4 - (38 + 273)^4]}$$

$$= 1.43$$

The discrepancies between the regulatory and actual thermal tests off set each other and it was deemed necessary to determine if the measured temperature results for the actual thermal test need to be adjusted. In order to resolve this question, a finite difference computer analysis was completed for the following two cases,

	Case 1	Case 2
Ambient Temperature	38°C	4°C
Solar Insolation	No	No
Decay Heat	160 W	0 W
Package Initial Temperature	47°C	4°C
Environment	800°C	950°C
Test Time	30 minutes	30 minutes

The equations used in the finite difference model were as follows. General equation for conduction in cylindrical coordinates:

$$\frac{1}{r}\frac{\partial}{\partial_r}\left[r\frac{\partial T}{\partial r}\right] + \frac{1}{r^2}\frac{\partial^2 T}{\partial \phi^2} + \frac{\partial^2 T}{\partial z^2} + \frac{q}{k} = \frac{1}{\alpha}\frac{\partial T}{\partial t}$$

For one-dimensional heat transfer in the radial direction

$$\frac{\partial T}{\partial \phi} = 0$$

$$\frac{\partial T}{\partial z} = 0$$

Therefore,

$$\frac{1}{r}\frac{\partial}{\partial r}\left[r\frac{\partial r}{\partial r}\right] + \frac{q}{k} = \frac{1}{\alpha}\frac{\partial T}{\partial t}$$

Expanding,

$$\frac{1}{r}\frac{\partial T}{\partial r} + \frac{\partial^2 T}{\partial r^2} + \frac{q}{k} = \frac{1}{\alpha}\frac{\partial T}{\partial t}$$

Where, r = radial coordinate

T = temperature

t = time

α = thermal diffusivity coefficient

Using finite difference methods for internal nodes:

$$\frac{\partial T}{\partial r} = \frac{T^i_{n+1} - T^i_{n-1}}{2\Delta r}$$

$$\frac{\partial^2 T}{\partial r^2} = \frac{T^i_{n+1} + T^i_{n-1} - 2T^i_n}{\Delta r^2}$$

$$\frac{\partial T}{\partial t} = \frac{T_n^{\,i+1} - T_n^{\,i}}{\Delta t}$$

where n - is a node

i - is a time step

substituting into the above general equation and re-arranging terms, the temperature at an internal node at a point in time is as follows:

$$T_n^{i+1} = T_n^i + \frac{\alpha \Delta T}{\Delta r^2}\left[T_{n+1}^i\left(1 + \frac{\Delta r}{2r}\right) + T_{n-1}^i\left(1 - \frac{\Delta r}{2r}\right) - 2T_n^i\right] \quad \text{Equation (B1)}$$

Apply the boundary conditions for the inside surface of a cylinder with internal heat generation,

$$V\, c_p\, \rho \frac{\partial T}{\partial t} = k \frac{\partial T}{\partial r} + q$$

and substituting the forward finite-differences equations,

$$c_p \frac{\Delta r}{2\Delta t}\left(T_n^{i+1} - T_n^i\right) = k\left(T_{n+1}^i - T_n^i\right) + q$$

Re-arranging terms, the temperature at the inside node of a hollow cylinder would be,

$$T_n^{i+1} = T_n^i + \frac{2\alpha\Delta t}{\Delta r^2}\left(T_{n+1}^i - T_n^i\right) + 2\alpha q \Delta t \quad \text{Equation (B2)}$$

Apply the boundary conditions for the outside surface of the package subject to radiative environment.

$$V\, \rho\, c_p \frac{\partial T}{\partial t} = -k \frac{\partial T}{\partial r} + h(T_a - T_i) + \sigma F\,(T_a^4 - T_i^4)$$

Again using finite difference equation and re-arranging terms, the temperature at the outside node would be,

$$T_n^{i+1} = T_n^i - 2\left[\frac{k}{\Delta r} C\,(T_{n+1}^i - T_n^i) + Ch\,(T_a - T_n^i)\right]$$

$$+ \sigma\, FC\,(T_a^4 - T_n^{i\,4}) \quad \text{Equation (B3)}$$

where , $C = \dfrac{k\Delta t}{\rho\, c_p\, \Delta r^2}$

Using equations B1, B2 and B3, with the appropriate time step, and node size, the temperatures for a cylinder can be calculated for transient conditions. The results as shown in Figure B2 and B3 are given for stainless steel cylinder with an inner radius of 0.15 m and an outer radius of 0.38 m. The regulatory thermal test calculations shown in Figure B2 are in good agreement with the two-dimensional finite-element code (TOPAZ) given in SCANS (Reference 2).

The maximum temperature for Case 1 and Case 2 are as follows.

	Case 1	Case 2
Outer Surface	396.0°C	554.6°C
Inner Surface (at 1.7 hours)	183.2°C	218.4°C

Because Case 2 gives the more severe results it was concluded that the measured temperature results are valid without adjustment. A comparison between Case 2 and the actual test results for the outer surface temperature are given in Figure B4.

B.3 References

1. Y. Liner et al., "Temperature Analysis of Irradiated Material Transportation Package" CRL Thermalhydraulics Development Branch Report ARD-TD-318 COG-92-03, 1992 January.

2. Shipping Cask Analysis System - A Microcomputer Based Analysis System for Shipping Cask Design Review, NUREG/CR-4554 UCID-20674 Vol. 1.

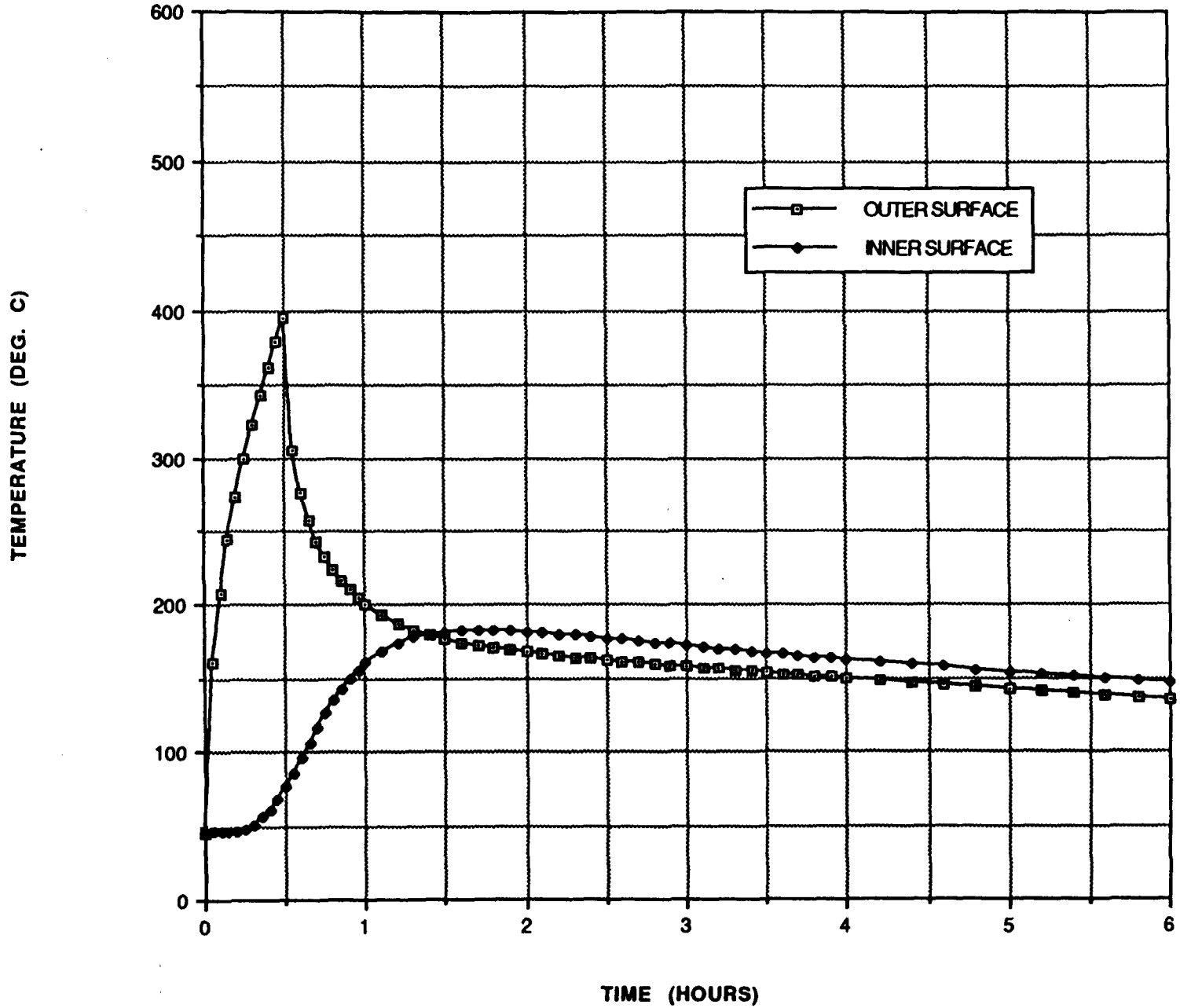

FIGURE B2 REGULATORY THERMAL TEST CALCULATION RESULTS

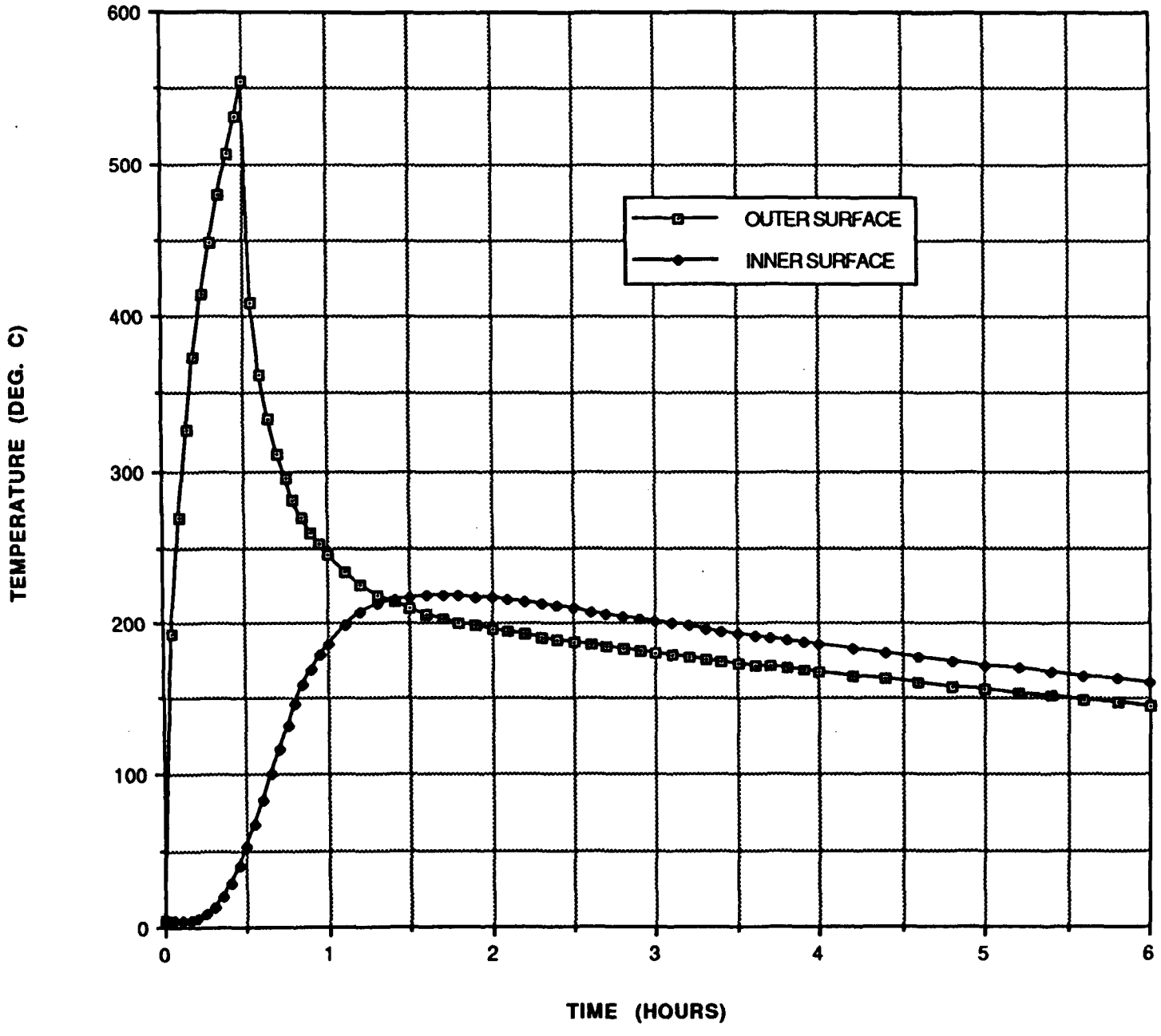

FIGURE B3 ACTUAL THE[illegible] TEST CALCULATION RESULTS

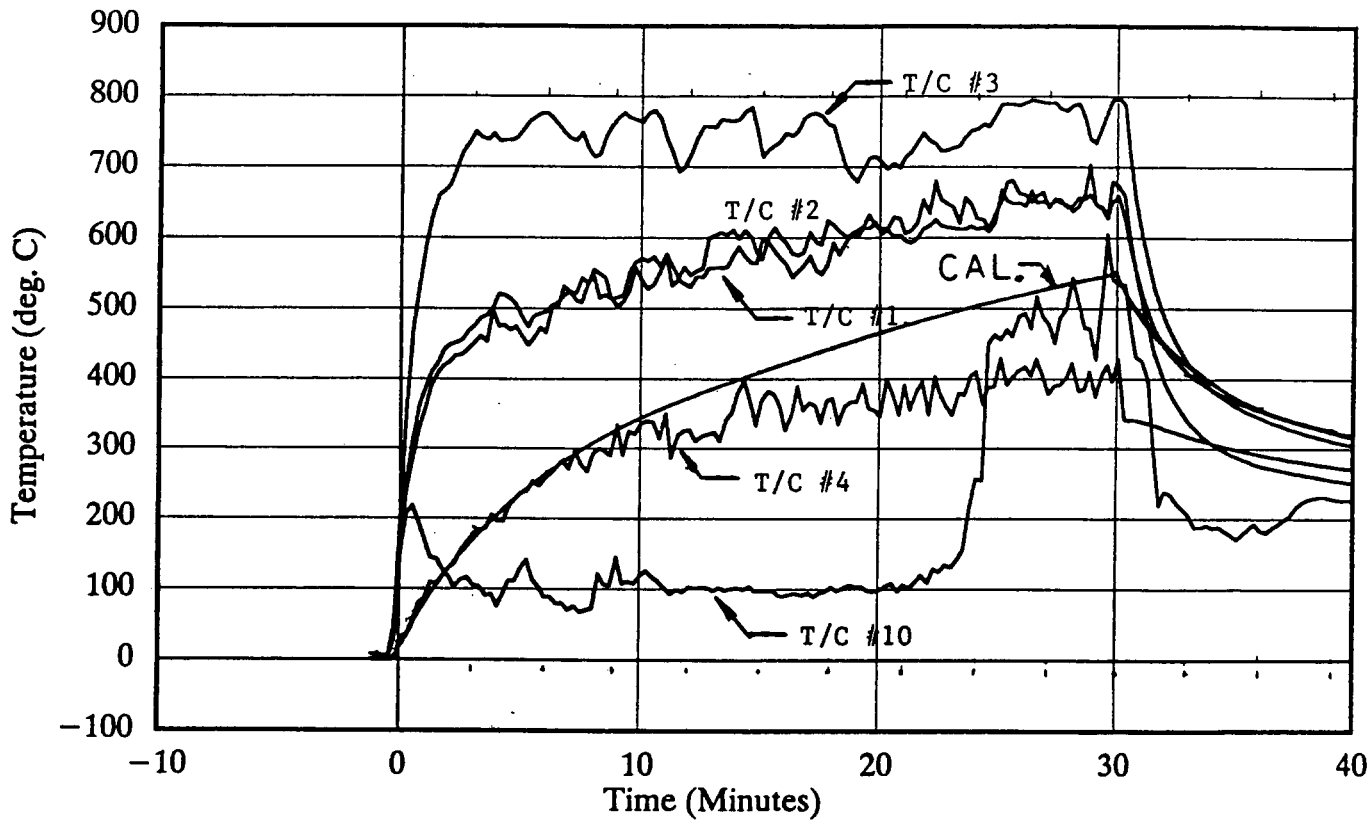

T/C#1 - Flask Top
T/C#2 - Flask Side
T/C#3 - Flask Bottom
T/C#4 - Flask Side (½" Below Surface)
T/C#10 - Flask Corner

FIGURE B4 COMPARISON BETWEEN ACTUAL TEST RESULTS AND ANALYTICAL RESULTS FOR OUTER PACKAGE SURFACE TEMPERATURES

APPENDIX C - CONTAINMENT ANALYSES

C.1 Introduction

The design requirements for both normal and accident conditions of transport will be based on the concept of "leaktight", that is, 1×10^{-8} Pa.m^3/s, as given in Reference 1*. This rate, which is based on dry air at 25°C and for a pressure differential of 101.3 kPa against a vacuum of 1 kPa or less, is considered to satisfy the regulatory containment requirements that are specified in terms of activity per unit time. The preshipment requirement will be 1×10^{-4} Pa.m^3/s which is also given in Reference 1.

Two analyses are given below, one that represents shipments of irradiated power reactor channel tube sections and irradiated test specimens and one that represents irradiated fuel bundles and elements. The analytical method follows that which is described in Figure 1 of Reference 2. In this method the numerical results depend on the choice of release fraction values. The data on release fraction values are quite limited and variable and so, the numerical results can range over 1 or 2 orders of magnitude. Consequently, the purpose of these analyses is to:

a) demonstrate that 1×10^{-8} Pa.m^3/s is an acceptable specification for the design requirements;

b) calculate the range for the gas leakage rates, based on the available choice of release fraction values; and

c) estimate <u>realistic</u> gas leakage rates for the purpose of comparing these rates to the preshipment requirements of 10^{-4} Pa.m^3/s.

Certain air flow rates, called reference rates, have the following practical significance, as stated in paragraphs A-548.8 and A-548.9 of Reference 3:

1) 1×10^{-2} Pa.m^3/s indicates a moderately large leak and is an upper limit for gas leakage testing;

2) 1×10^{-6} Pa.m^3/s indicates a small leak and, in practice, even the smallest particle size powder would not be expected to escape; and

3) 1×10^{-8} Pa.m^3/s indicates a very small leak that, in practice, is considered to be leaktight, regardless of the form of the radioactive material.

The above values are based on a pressure difference of 10^5 Pa across a leak and are given here for establishing the significance of the calculated results.

* References are listed in Section C.5.

C.2 Containment Analysis for Tube Sections and Test Specimens

C.2.1 Calculation

This analysis will follow the method that is given in Figure 1 of Reference 2. Because the radioactive material is in solid form, only Steps 1, 2, 3, 8, and 9 will be completed.

Step 1. Consider a package that has been loaded at a hot cell and contains a pressure tube section which is made of Zr-2.5 wt% Nb metal. A 0.5 m long tube section has a nominal outside diameter of 0.112 m, a nominal inside diameter of 0.103 m and a mass of 4565 grams. Although the typical activity of the tube section is 150 TBq, assume the maximum permissible activity of 3000 A_2. The predominant radionuclide is Zr-95 (A_2 = 0.9 Tbq) but some Nb-95 (A_2 = 1.0 Tbq) is present. Because the A_2 values are similar, consider that the total activity is 2700 Tbq and only Zr-95 need be considered. Although the component is in solid form, particulates may be present.

The specific activity of the calculation model is,

$$\text{Specific Activity} = \frac{2700}{4565}$$

$$= 0.591 \text{ TBq/g}$$

[Note: That the specific activity of Zr-95 is 794.2 TBq/g, Table A-III-1 of Reference 3].

The specific activity is based on 2700 TBq rather than 150 TBq to include an adequate degree of conservation to account for the fact that not all particles may be uniformly radioactive.

It should also be noted that some residual contamination may be on the tube section surfaces. This contamination might arise from the hot cell or the package cavity from some previous shipment. This source of releaseable radioactive material is considered to be of secondary significance and need not be evaluated.

Step 2. In this step, four release fractions must be determined, two for normal conditions of transport and two for accident conditions of transport. The release fractions FC_{iN} and FC_{iA} refer the release from the radioactive contents to the package containment system or cavity. These values are easily determined and are both equal to 1.0, the maximum possible value. The release fractions FE_{iN} and FE_{iA} refer to the fraction of Zr-95 which is released from the containment system to the environment. These fractions are difficult to establish because, the spectrum of particle sizes has not been determined. Evidence indicates that only 10% of the

particles released into the cavity may remain air borne and available for release to the environment, Reference 4. For the time being these fractions will be left undetermined.

Step 3. The regulatory containment criteria are,

a) $A_2 \times 10^{-6}$ per hour for normal conditions of transport, and,

b) A_2 in a period of one week for accident conditions of transport.

For Zr-95, A_2 = 0.9 TBq and therefore,
$R_N = 0.9 \times 10^{-6}$ TBq per hour, and
R_A = 0.9 TBq in a period of one week.

Because the specific activity is 0.591 TBq/g, the containment criteria in mass terms are,
$R_N = 1.52 \times 10^{-6}$ g per hour, and
R_A = 1.52 g in a period of one week.

The density of zirconium is 6.43×10^6 g/m^3 and so in volume terms,
$R_N = 2.36 \times 10^{-13}$ m^3 per hour, and
$R_A = 2.36 \times 10^{-7}$ m^3 in a period of one week.

For the purposes of this analysis, the time periods will be averaged in seconds.

Thus,

$$L_N = \frac{R_N}{3600}$$

$$= 6.56 \times 10^{-17} \text{ m}^3/\text{s and,}$$

$$L_A = \frac{R_A}{3600 \times 168}$$

$$= 3.90 \times 10^{-13} \text{ m}^3/\text{s.}$$

Step 8. The spectrum of particulate sizes that would be released from the radioactive components as a result of normal and accident impact conditions of transport has not been established. Therefore, a limiting diameter for a leak that is based on the physical characteristics of the particulates cannot be established. As an alternative, the range of leak diameters that should be considered will be estimated.

For normal conditions of transport, this range will be determined by,

a) calculating the particle size for a single particle that is released in one hour, and,

b) calculating the particle size for a continuous flow of uniform sized particles during a one second period.

Consider a spherical particle whose volume is,

$$V = \frac{\pi}{6} D^3$$

For $R_N = 2.36 \times 10^{-13}$ m^3 per hour

Then

$$\frac{\pi}{6} D^3 = 2.36 \times 10^{-3}$$

$$\therefore D_N = 7.66 \times 10^{-5} \text{ m}$$

For $L_N = 6.56 \times 10^{-17}$ m^3/s

$$\frac{\pi}{6} D_N^3 = 6.56 \times 10^{-17}$$

$$\therefore D_N = 5.00 \times 10^{-6} \text{ m}$$

The last calculation means that the regulatory containment requirements will be satisfied provided that a flow rate of one particle per second, for a time period of one hour, is not exceeded when the particle diameter is 5.00×10^{-6} m or smaller. From these two calculations, the pertinent leak diameter ranges from about 5 to 80 microns. For comparison, if the particles were 100% Zr-95, the pertinent leak diameter range would be about one order of magnitude smaller.

For accident conditions of transport, consider only the case where D_A is based on $L_A = 3.90 \times 10^{-13}$ m^3/s. Then, $D_A = 9.1 \times 10^{-5}$ m or abour 90 microns.

Step 9. The values of $D_N = 5 \times 10^{-6}$ m and $D_N = 7.66 \times 10^{-5}$ m will be used in Equation B1 of Reference 2 to determine the range of Q_{NSLR}. Similarly $D_A = 9.1 \times 10^{-5}$ m will be used to determine Q_{ASLR}

Thus,

$$Q_{NSLR} = 0.0123 \frac{D_N^4}{\mu a} (Pu^2 - Pd^2)$$

$$+ 1.204 \frac{D_N^3}{a} \sqrt{\frac{T}{M}} (Pu - Pd)$$

where Q_N is given in terms of $Pa.m^3/s$ for dry air, and

$Pu = 1.013 \times 10^5$ Pa

$Pd = 0$ Pa

$\mu = 1.85 \times 10^{-5}$ Pa.s at 25°C

a = O-ring seal diameter

$= 5 \times 10^{-3}$ m

T = 298 K

M = 0.029 kg/mol

T = 298 k

M = 0.029 kg/mol

For $D_N = 5 \times 10^{-6}$ m,

$Q_{NSLR} = 8.53 \times 10^{-7} + 3.09 \times 10^{-7}$

$= 1.16 \times 10^{-6}$ $Pa.m^3/s$

For $D_N = 7.66 \times 10^{-5}$ m,

$Q_{NSLR} = 4.70 \times 10^{-2} + 1.11 \times 10^{-3}$

$= 4.81 \times 10^{-2}$ $Pa.m^3/s$

For $D_A = 9.1 \times 10^{-5}$ m,

$Q_{ASLR} = 9.36 \times 10^{-2} + 1.86 \times 10^{-3}$

$= 9.54 \times 10^{-2}$ $Pa.m^3/s$

C.2.2 Discussion

In Step 2 above, the release fractions FE_{iN} and FE_{iA} were not determined. This issue will be addressed here, beginning with accident conditions of transport. The equivalent air flow rate of 9.54×10^{-2} Pa.m³/s is relatively large and is easy to achieve in the package design. It also refers to a continuous flow of particles on a one second time basis but for a period of one week, i.e. about 600,000 particles. It is inconceivable that enough particles will be generated (about ten times the permissible number of particles that can be released) so that the regulatory containment requirements will be exceeded. Because a design verification leakage test of 9.54×10^{-2} Pa.m³/s is beyond the upper limit for gas leakage testing it becomes unnecessary to actually determine FE_{iA}. It may be simply assumed that $FE_{iA} = 1.0$, the maximum value.

For normal conditions of transport two extremes have been determined for Q_{NSLR}, 1.16×10^{-6} and 4.81×10^{-2} Pa.m³/s. As in the case for accident conditions of transport, if a design verification leakage test of 4.81×10^{-2} Pa.m³/s were specified, it may be simply assumed that $FE_{iN} = 1.0$ and it becomes unnecessary to determine the actual value.

If the design verification leakage test were specified as 1.16×10^{-6} Pa.m³/s then some 36000 particles of 5 micron size would have to be generated and some 3600 of these would have to be released within one hour before the regulatory containment requirements would be exceeded. A release of this magnitude is considered to be unrealistic. However, a design verification leakage test of 1×10^{-6} Pa.m³/s is achievable and is acceptable. This decision obviates the need to determine an actual value of FE_{iN}. For the purposes of discussion, a realistic value of Q_{NSLR} is considered to be midway value between the two extremes or about 1×10^{-4} Pa.m³/s.

C.3 Containment Analysis for Irradiated Fuel

C.3.1 Calculation

Consider a Pickering fuel bundle with a burnup of 1150 GJ/kg of initial uranium (19.86 kg) and a storage time of 0.5 years that has been loaded in a storage pool. The analysis is complex because there are four potential sources of radioactive material release and there are many release fractions to take into account. The four sources of release are:

a) the residual contamination from the storage pool which is considered to be of secondary significance and will not be evaluated here;

b) the fuel element zirconium alloy sheaths;

c) "crud" which includes such things as corrosion and activation products from the reactor coolant system which adhere to the fuel element surfaces; and,

d) the irradiated uranium which is a source of fission products and actinides.

Because the analysis is complex, the four sources of release will be considered separately.

C.3.1.1 Zirconium Alloy Fuel Sheaths

The total mass of zircalloy that encapsulates the uranium fuel is 2039 grams which is about 45% of the material that was assessed in Section C.2.1. The results of that analysis showed that the containment of irradiated zirconium particulates would be satisfied if

$Q_{NSLR} = 1 \times 10^{-4}$ Pa.m³/s (realistic value), and

$Q_{ASLR} = 9.54 \times 10^{-2}$ Pa.m³/s.

In this assessment, the contribution from the fuel sheaths to the releasable radioactive material will be assumed to be the same.

C.3.1.2 Crud

The contribution from crud to the releasable radioactive material is based primarily on work that was completed in the USA, Reference 5.

However, Reference 6 does contain some information that can be used to compare crud formation on CANDU fuel. Reference 5 is particularly useful because it assesses the contribution of crud in relation to package gas leakage testing, i.e. Reference 1. Reference 5 assesses five year cooled PWR and BWR fuel and the pertinent findings are:

a) $L_N = 1 \times 10^{-3}$ to 1×10^{-4} cm³/s
($Q_{NSLR} = 1 \times 10^{-4}$ to 1×10^{-5} Pa.m³/s, approximately)
L_A (or Q_{ASLR}) is several orders of magnitude higher than L_N (or Q_{NSLR});

b) the major radionuclides are Cr-51, Mn-54, Co-58, Fe-59, Co-60, Zn-65 and Zr-95;

c) because the fuel has been cooled for five years, Co-60 predominates the crud activity at the time of shipment; and

d) the particles have a mean diameter of 3×10^{-6} m and 99% of the particles have a diameter of 10×10^{-6} m or less.

For CANDU fuel, Reference 6 lists the major radionuclides as Fe, Ni, Cu, Cr, Mn and Co with Fe as the most predominant radionuclide. For heavy water reactor designs the crud deposit ranges from 0.03 to 0.05 grams per bundle.

Because the CANDU fuel will be stored for 180 days before shipment, the predominant radionuclides will be Fe-59 and Co-60 due to the relatively short half-lives of the other radionuclides.

Because both the USA and Canadian research have identified the same major radionuclides, it seems reasonable to assume that the particle sizes and the permissible gas leakage rates that were identified in the USA assessment would be applicable to CANDU fuel.

C.3.1.3 Irradiated Uranium

This analysis will follow the method that is given in Figure 1 of Reference 2 and so, Steps 1 through 9 will be completed.

In this analysis the data for the radionuclide inventory has been extracted from Reference 7. References 6, 8 and 9 will be used for selecting release fractions. The tabulation of all the pertinent data will follow the format of Reference 8.

Step 1. Columns 1 and 2 of Tables C1 and C2 list the predominant radionuclides in the CANDU fuel bundle.

Step 2. Columns 3 and 4 of Tables C1 and C2 list the release fractions FC_{iN}, FC_{iA}, FE_{iN} and FE_{iA}. These fractions require discussion. The factor 0.03 in Table C1 represents the fraction of fuel elements that could fail as a result of normal conditions of transport. This factor has been found acceptable for U.S. fuel and is considered to be conservative. There is little data for the failure rate of CANDU fuel for these conditions. In the prototype tests that were completed, simulated CANDU fuel bundles were included, but no failures were detected. In Table C2, it has been assumed that all fuel elements fail. In Column 3 of both Tables, the factor 2×10^{-4} refers to the release fraction of volatile radionuclides that escapes from the fuel cladding and the factor 2×10^{-5} refers to the release fraction of particles or "fines" that escape with the radioactive gases from the fuel cladding.

Although only the radioactive material in the interconnecting void spaces within the fuel cladding is available for release, the release fractions are based on the total radioactivity for each radionuclide. A review of the literature shows that the data on release fractions is limited and the following examples illustrate the uncertainty of these values.

	H-3	Kr-85	Cs-134, Cs-137	I-131
Reference C6	1×10^{-4}	2×10^{-1}	5×10^{-2}	2.5×10^{-1}
Reference C8	--	3×10^{-1}	2×10^{-4}	--
Reference C9	1×10^{-2}	1×10^{-1}	7×10^{-6}	--

In Column 4 of both Tables, the factor 1.0 refers to gases or volatile radionuclides and indicates that 100% of those released to the cavity remain airborne and available for release to the environment. The factor 0.1 refers to the fines and indicates that only 10% of those released to the cavity remain airborne and available for release to the environment.

Column 5 in both Tables gives the releaseable activities either RI_{iN} or RI_{iA}.

Step 3 Column 6 in the Tables lists the A_2 values for each radionuclide. Because a mixture of radionuclides is present it is necessary to determine equivalent A_2 values. This can be done as follows,

$$A_2 \text{ for mixture} = \frac{\Sigma_i \, RI_{iN}}{\Sigma_i \, (RI_{iN}/A_{2i})} \text{ and}$$

$$= \frac{\Sigma_i \, RI_{iA}}{\Sigma_i \, (RI_{iA}/A_{2i})}$$

Column 7 gives the values for either RI_{iN}/A_{2i} or RI_{iA}/A_{2i}.

Then, the equivalent A_2 values are

A_2 = 0.907 TBq for normal conditions of transport, and

A_2 = 0.234 TBq for accident conditions of transport

For accident conditions of transport, Kr-85 is evaluated separately by comparing it to the release limit of 10 A_2 or 100 TBq. In this case Kr-85 becomes insignificant because less than 1 TBq is available for release.

For normal conditions of transport, the permissible activity release rate is $A_2 \times 10^{-6}$ per hour, or, when time averaged in seconds,

$$R_N = \frac{0.907 \times 10^{-6}}{3600}$$

$$= 2.52 \times 10^{-10} \text{ TBq/s.}$$

For accident conditions of transport the permissible activity release rate is A_2 in a period of one week. The calculation above gives $A_2 = 0.234$ TBq and from Table C.2 the total releasable activity is 2.25×10^{-2} TBq or less than the permissible release. Therefore, the regulatory requirements will be satisfied. Nonetheless, for completeness, the calculations will be completed on a time averaged basis of one second.

$$R_A = \frac{0.234}{168 \times 3600}$$

$$= 3.87 \times 10^{-7} \text{ TBq/s}$$

Step 4. The activity release of H-3 by permeation need not be evaluated because the permissible release is 4×10^{-5} TBq/hour and 40 TBq/week for normal and accident conditions of transport respectively but the H-3 activity available for release is only 6×10^{-7} TBq.

In the case of Kr-85 the activity available for release is 2.16×10^{-3} TBq. The permissible release is 100 TBq/week for accident conditions of transport and this can not be exceeded. For normal conditions of transport the permissible release is 1×10^{-5} TBq/hour and so release by permeation must be assessed. Worked example D5 of Reference 2 and Reference 10 provide useful information for the calculation.

For steady state, the release is given by,

$$Q_p = P_m L \Delta P$$

where,

Q_p is the release rate, $Pa.m^3/s$
P_m is the permeation coefficient, m^2/s
L is the O-ring length, m
ΔP is the partial pressure difference across the O-ring, Pa.

For ethylene-propylene, $P = 1 \times 10^{-9}$ m^2/s approximately as estimated by extrapolating the data in Figure 4 of Reference C10 at a temperature of 150°C. There are two O-rings, one at each end of the cavity, and both are 0.36m in diameter. Therefore $L = 2\pi D = 2.26$ m.

The partial pressure of Kr-85 shall be determined as follows from the releaseable activity, 2.16×10^{-3} TBq.

The specific activity of Kr-85 is 1.23×10^3 TBq/mole, Worked example D5, Reference C.10. The number of mols of Kr-85 in the cavity is

$$n = \frac{2.16 \times 10^{-3}}{1.23 \times 10^3}$$

$$= 1.76 \times 10^{-6} \text{ mols}$$

The partial pressure is determined from the ideal gas equation

$$p = \frac{nR_oT}{V}$$

where, R_o = the universal gas constant
= 8.31 J/mol K

T = cavity bulk air temperature
= 150 + 273
= 423 K

V = cavity free air volume
= 0.01 m^3

Solving,

$$p = \frac{1.76 \times 10^{-6} \times 8.31 \times 423}{0.01}$$

$$= 0.62 \text{ Pa}$$

Assume that the partial pressure downstream of the O-ring is zero

$$\therefore \Delta P = 0.62 \text{ Pa}$$

Then,

$$Q_p = 1 \times 10^{-9} \times 2.26 \times 0.6$$

$$= 1.4 \times 10^{-9} \text{ Pa.m}^3/\text{s}$$

This gas flow rate by permeation will be compared to the regulatory containment requirements as follows.

First, convert Q_p, a quasi-mass term, to a volumetric term at standard conditions

$$Q_p = PL$$

where,

P is the standard atmospheric pressure
$= 1.013 \times 10^5$ Pa, and

L is the volumetric flow rate, m^3/s

$$\therefore L = \frac{1.4 \times 10^{-9}}{1.013 \times 10^5}$$

$$= 1.38 \times 10^{-14} \text{ m}^3/\text{s} \quad \text{at STP}$$

$$= 4.98 \times 10^{-11} \text{ m}^3/\text{hour}$$

The permissible release rate for Kr-85 is 1×10^{-5} TBq/hour. From worked example D5, Reference 10, the specific activity of Kr-85 is 5.1×10^{10} Bq/cm^3 or 5.1×10^4 TBq/m^3. Therefore, the permissible release rate in volumetric terms is

$$L = \frac{1 \times 10^{-5}}{5.1 \times 10^4}$$

$$= 1.96 \times 10^{-10} \text{ m}^3/\text{hour}$$

So, the calculated release of Kr-85 is about 25% of the permissible release.

Step 5. Strictly speaking, one should deduct the release rate due to permeation before the remainder of the analysis is completed. This will not be done because this degree of precision is not deemed appropriate for this analysis. (If the reduction were to be made, the values of Kr-85 in Table C1 and C2 would also have to be reduced by 25%).

Step 6. The releaseable activity that is listed in Tables C1 and C2 is considered to be a mixture of radioactive gases and fine suspended particles in the cover gas within the package cavity, that is, an aerosol. This aerosol is considered to be the "medium" which will leak like a gas. The free gas volume within the cavity is 0.01 m^3 for both normal and accident conditions of transport.

$$\therefore C_N = \frac{RI_{TN}}{V_N}$$

$$= \frac{2.83 \times 10^{-3}}{0.01}$$

$$= 2.83 \times 10^{-1} \text{ TBq/m}^3\text{, and}$$

$$C_A = \frac{RI_{TA}}{V_A}$$

$$= \frac{2.25 \times 10^{-2}}{0.01}$$

$$= 2.25 \text{ TBq/m}^3$$

Step 7. From Step 3, $R_N = 2.52 \times 10^{-10}$ TBq/s

$$L_N = \frac{R_N}{C_N}$$

$$= \frac{2.52 \times 10^{-10}}{2.83 \times 10^{-1}}$$

$$= 8.90 \times 10^{-10} \text{ m}^3\text{/s}$$

From Step 3, $R_A = 3.85 \times 10^{-7}$ TBq/s

$$L_A = \frac{R_A}{C_A}$$

$$= \frac{3.85 \times 10^{-7}}{2.25}$$

$$= 1.71 \times 10^{-7} \text{ m}^3\text{/s}$$

Step 8. Assuming that the package cavity has been vacuum dried and contains no residual moisture, Sections 7.4.3 and 7.5.5 give the following bulk gas operating conditions

$P_N = 1.5 \times 10^5$ Pa at 150°C and

$P_A = 2.0 \times 10^5$ Pa at 265°C

$Q_N = L_N P_N$

$= 8.90 \times 10^{-10} \times 1.5 \times 10^5$

$= 1.34 \times 10^{-4}$ Pa.m.^{3}/s at 150°C

$Q_A = L_A P_A$

$= 1.71 \times 10^{-7} \times 2 \times 10^{-5}$

$= 3.42 \times 10^{-2}$ Pa.m^3/s at 265°C

Step 9. To convert Q_N to Q_{NSLR}, first correct Q_N to account for the differences in P_u and P_d. Use Equation B2 of Reference C2 since the flow is in the laminar range.

For Q_N,

$P_u = 1.50 \times 10^5$ Pa

$P_d = 2.50 \times 10^4$ Pa (Para. 534, Reference C3)

$\mu = 2.30 \times 10^{-5}$ Pa.s (air at 150°C)

For Q_{NSLR},

$P_u = 1.013 \times 10^5$ Pa

$P_d = 0$ Pa

$\mu = 1.85 \times 10^{-5}$ Pa.s (air at 25°C)

$$Q'_{NSLR} = 1.34 \times 10^{-4} \times \frac{2.3 \times 10^{-5}}{1.85 \times 10^{-5}} \left[\frac{(1.013 \times 10^5)^2}{(1.5\times10^5)^2-(0.25\times10^5)^2} \right]$$

$= 7.8 \times 10^{-5}$ Pa.m^3/s at 150°C

Finally, correct Q'_{NSLR} to 25°C

$$\therefore Q_{NSLR} = 7.8 \times 10^{-5} \frac{293}{423}$$

$$= 5.4 \times 10^{-5} \text{ Pa.m}^3/\text{s}$$

Similarly, for Q_A,

$P_u = 2.0 \times 10^5$ Pa

$P_d = 2.5 \times 10^4$ Pa

$\mu = 2.75 \times 10^{-5}$ Pa/s (air at 265°C)

$Q'_{ASLR} = 1.32 \times 10^{-2}$ Pa.m³/s at 265°C

and

$Q_{ASLR} = 7.2 \times 10^{-3}$ Pa.m³/s at 25°C

For the unusual situation that some residual moisture remains in the package cavity, the resultant pressure, as given in Section 7.4.3, would be 6.12×10^5 Pa for normal conditions of transport. With this value for P_u the reworked calculations give

$Q_{NSLR} = 3.2 \times 10^{-6}$ Pa.m³/s at 25°C

For accident conditions of transport, see Section 7.5.5, the resultant pressure was calculated to be 5.37×10^8 Pa. A similar analysis would give a very low value of Q_{ASLR} but the result is not meaningful because, from Table C2, the total calculated releaseable activity is less than the regulatory permissible release. The conclusions that should be drawn from this assessment are,

a) ensure that the package closure design has been designed for the possibility of a pressure of 5.37×10^8 Pa, and

b) ensure that the package cavity is vacuum dried whenever it has been loaded in a storage pool.

C.4 Conclusions

Conclusions of the containment analyses for both the tube sections and the irradiated fuel are as follows.

1. The typical value of Q_{NSLR} is between 1×10^{-4} and 1×10^{-5} Pa.m³/s. Under the most pessimistic assumptions, the minimum value of Q_{NSLR} is about 1×10^{-6} Pa.m³/s.

2. The value of Q_{ASLR} is in the order of 1×10^{-2} Pa.m³/s.

3. The data on release fractions is limited and variable.

4. For normal conditions of transport, the release of Kr-85 through the ethylene proplylene O-rings by permeation is about 25% of the regulatory permissible release value.

5. In general, the leakage of radioactive gases is not very significant. The releaseable amounts of H-3 are less than the regulatory permissible values. The same is true for Kr-85 for accident conditions of transport. If for normal conditions of transport Kr-85 were the only radionuclide to be considered, calculations give Q_{NSLR} = 7.8×10^{-4} Pa.m³/s.

6. Regardless of the failure rate of the fuel elements or the activity release rate values, there will always be some releaseable activity due to crud. Consequently, the maximum value for Q_{NSLR} for irradiated fuel shipments is between 1×10^{-4} and 1×10^{-5} Pa.m³/s.

7. The analyses show that a specification of 1×10^{-8} Pa.m³/s as a design verification requirement is acceptable.

8. The analyses show that a realistic design verification requirement is about 1×10^{-5} Pa.m³/s. For these analyses, the results are based on a single O-ring seal. However, the actual closure designs use double O-ring seals. It is reasonable to specify a preshipment requirement of 10^{-4} Pa.m³/s which is applied to both seals.

C.5 References

1. American National Standard "For Radioactive Materials - Leakage Tests on Packages for Shipment", ANSI N14.5-1987.

2. International Organization for Standardization, "ISO Standard - Leakage Testing on Packages for the Safe Transport of Radioactive Materials", DRAFT N, ISO/TC 85/SC5/WG10, 30th March 1993.

3. International Atomic Energy Agency Safety Series No. 37, "Advisory Material for the IAEA Regulations for the Safe Transport of Radioactive Material (1985 Edition)", Third Edition, Vienna 1987.

4. T.L. Sanders et al, "An Estimate of the Contribution of Spent Fuel Products to the Releasable Source Term in Spent Fuel Transport Casks", Patram '89 Proceedings, Washington, D.C. June 1989, pages 179-185.

5. H. Jordon et al, "An Estimate of the Contribution of "Crud" to the Radioactivity Source Term of a Spent Fuel Transport Cask", Patram '89 Proceedings, Washington, D.C., June 1989, pages 171 - 178.

6. J.L. Crosthwaite, "CANDU Irradiated - Fuel Handbook," Atomic Energy of Canada Limited, WNRE-371, 1979 January.

7. L.J. Clegg and J.R. Coady, "Radioactive Decay Properties of CANDU Fuel Volume 1: The Natural Uranium Fuel Cycle", Atomic Energy of Canada Limited, AECL-4436/1, January 1977.

8. L.E. Fischer, "Method of Calculating Test Leakage Rate for a Spent Fuel Cask", UCRL-JC-10422 Preprint, June 13, 1990.

9. H. Kowalewsky, "Criteria for and Proof of Leaktightness Concerning Casks for Dry Transport and Intermediate Storage of Spent LWR-Fuel Elements", Patram '83 Proceedings, New Orleans, Louisiana, May 15-20, 1983, pages 638-645.

10. K. Brehm et al, "Permeation through Elastomeric O-ring Seals," Patram '86 Proceedings, Davos Switzerland, IAEA-SM-286/44P, June 16-20, 1986, pages 359-367.

TABLE C1 RELEASEABLE RADIOACTIVE MATERIAL FOR ONE SIX MONTH COOLED CANDU FUEL BUNDLE. NORMAL CONDITIONS OF TRANSPORT

(1)	(2)	(3)	(4)	(5) [(2)x(3)x(4)]	(6)	(7) [(5) ÷ (6)]
Radioisotope	Radioactivity TBq	Release Fraction to Cavity	Airborne Fraction	Releaseable Activity RI_{iM} TBq	A_{2i} TBq	RI_{iM}/A_{2i}
H-3	0.2	$1 \times 10^{-4} \times 0.03$	1.0	6.00×10^{-7}	40	1.50×10^{-8}
Kr-85	2.4	$3 \times 10^{-1} \times 0.03$	1.0	2.16×10^{-3}	10	2.16×10^{-4}
Sr-89	19.0	$2 \times 10^{-4} \times 0.03$	1.0	1.14×10^{-4}	0.5	2.28×10^{-4}
Sr-90	17.2	$2 \times 10^{-4} \times 0.03$	1.0	1.03×10^{-4}	0.1	1.03×10^{-3}
Nb-95	148.7	$2 \times 10^{-5} \times 0.03$	0.1	8.92×10^{-6}	1.0	8.92×10^{-6}
Zr-95	76.6	$2 \times 10^{-5} \times 0.03$	0.1	4.60×10^{-6}	0.9	5.11×10^{-6}
Ru-106	177.2	$2 \times 10^{-5} \times 0.03$	1.0	1.06×10^{-4}	0.2	5.30×10^{-4}
I-131	5.5×10^{-5}	$3 \times 10^{-1} \times 0.03$	1.0	4.95×10^{-9}	0.5	9.90×10^{-9}
Cs-134	24.2	$2 \times 10^{-4} \times 0.03$	1.0	1.46×10^{-4}	0.5	2.92×10^{-4}
Cs-137	29.3	$2 \times 10^{-4} \times 0.03$	1.0	1.76×10^{-4}	0.5	3.52×10^{-4}
Ce-144	242.9	$2 \times 10^{-5} \times 0.03$	0.1	1.46×10^{-5}	0.2	7.30×10^{-5}
Pu-238	0.17	$2 \times 10^{-5} \times 0.03$	0.1	1.02×10^{-8}	2×10^{-4}	5.10×10^{-5}
Pu-239	0.13	$2 \times 10^{-5} \times 0.03$	0.1	7.80×10^{-9}	2×10^{-4}	3.90×10^{-5}
Pu-240	0.28	$2 \times 10^{-5} \times 0.03$	0.1	1.68×10^{-8}	2×10^{-4}	8.40×10^{-5}
Pu-241	26.68	$2 \times 10^{-5} \times 0.03$	0.1	1.60×10^{-6}	1×10^{-2}	1.60×10^{-4}
Cm-242	3.33	$2 \times 10^{-5} \times 0.03$	0.1	2.00×10^{-7}	1×10^{-2}	2.00×10^{-5}
Cm-244	0.11	$2 \times 10^{-5} \times 0.03$	0.1	6.60×10^{-9}	4×10^{-4}	1.65×10^{-5}
				2.83×10^{-3}		3.12×10^{-3}

TABLE C2 RELEASEABLE RADIOACTIVE MATERIAL FOR ONE SIX MONTH COOLED CANDU FUEL BUNDLE. ACCIDENT CONDITIONS OF TRANSPORT

(1)	(2)	(3)	(4)	(5) [(2)x(3)x(4)]	(6)	(7) [(5) ÷ (6)]
Radioisotope	Radioactivity TBq	Release Fraction to Cavity	Airborne Fraction	Releaseable Activity RI_{iA} TBq	A_{2i} TBq	RI_{iA}/A_{2i}
H-3	0.2	1×10^{-4}	1.0	2.00×10^{-5}	40	5.00×10^{-7}
Kr-85	2.4	3×10^{-1}	1.0	7.20×10^{-1}	10	7.20×10^{-2}
Sr-89	19.0	2×10^{-4}	1.0	3.80×10^{-3}	0.5	7.60×10^{-3}
Sr-90	17.2	2×10^{-4}	1.0	3.44×10^{-3}	0.11	3.44×10^{-2}
Nb-95	148.7	2×10^{-5}	0.1	2.97×10^{-4}	1.0	2.97×10^{-4}
Zr-95	76.6	2×10^{-5}	0.1	1.53×10^{-4}	0.9	1.70×10^{-4}
Ru-106	177.2	2×10^{-5}	1.0	3.54×10^{-3}	0.2	1.77×10^{-2}
I-131	5.5×10^{-5}	3×10^{-1}	1.0	1.65×10^{-6}	0.5	3.30×10^{-6}
Cs-134	24.2	2×10^{-4}	1.0	4.84×10^{-3}	0.5	9.68×10^{-3}
Cs-137	29.3	2×10^{-4}	1.0	5.86×10^{-3}	0.5	1.17×10^{-2}
Ce-144	242.9	2×10^{-5}	0.1	4.86×10^{-4}	0.2	2.43×10^{-3}
Pu-238	0.17	2×10^{-5}	0.1	3.40×10^{-7}	2×10^{-4}	1.70×10^{-3}
Pu-239	0.13	2×10^{-5}	0.1	2.60×10^{-7}	2×10^{-4}	1.30×10^{-3}
Pu-240	0.28	2×10^{-5}	0.1	5.60×10^{-7}	2×10^{-4}	2.80×10^{-3}
Pu-241	26.68	2×10^{-5}	0.1	5.34×10^{-5}	1×10^{-2}	5.34×10^{-3}
Cm-242	3.33	2×10^{-5}	0.1	6.66×10^{-6}	1×10^{-2}	6.66×10^{-4}
Cm-244	0.11	2×10^{-5}	0.1	2.20×10^{-7}	4×10^{-4}	5.50×10^{-4}
				2.25×10^{-2} Excluding Kr-85		9.63×10^{-2} Exclud. Kr-85